DP Jack up SIMOPS Operations Dynamic Position Risk Identification

ニチン, ダモダル, ターカー

DP Jack up SIMOPS Operations Dynamic Position Risk Identification

DEPARTMENT OF MARINE SYSTEMS ENGINEERING

GRADUATE SCHOOL OF ENGINEERING

KYUSHU UNIVERSITY

YEAR – 2021

NITIN DAMODHAR THULKAR

CONTENTS

1 INTRODUCTION

1.1 BACKGROUND OF RESEARCH

The jack-up vessel [4][24][43][44] may be either a barge or a ship shaped vessel and have three or more legs that can be mechanically extended to the seabed to lift the vessel above the sea surface. However, whatever the shape of the vessel, when it is in DP [29][31][41][28] operation with the legs in the raised position the centre of gravity of the vessel is much higher than when the legs are in the lowered position. This alters the vessel's stability, affects its motion behaviour and changes the DP performance.

The leg jacking speed of the vessel should be well documented and should be taken into consideration. This can help determine how long the vessel will be in the transition phase between DP operation and leg touchdown to soft pinning during DP and jacking simultaneous operation (SIMOPS) [34].

During leg deployment there will be changing environmental forces that influence the vessel's position [35] and consequently the DP system will respond by applying more or less thrust. When the legs are above the seabed the DP system should be given a settling time to ensure that the DP computer model has acquired these new forces and that vessel position is steady [31] [32][34][38].

Leg designs can be either trussed type with three or four chords or cylindrical type. The trussed type legs are popular for Jacking system having pinion. The pinion climbs on the rack of each chord. The cylindrical legs design varies too. There are three type of jacking system associated with cylindrical leg. In one design, the rack fixed on cylinder surface at outer side for movement of hull using pinion type jacking system. The second cylindrical leg design comprises of hole on the outer surface to facilitates pin engagement when hydraulic jacking system cylinders used to move the hull or leg. The 3rd type of jacking system associated with cylinder leg is gripper type, which does not need holes or rack. The gripper holds the leg by friction. This is non-positive engagement type jacking system.

In DP vessels, the leg design does impact the thruster sizing due to drag coefficient and area of the leg spudcan. When environmental forces act on them the forces various a lot among trussed type and cylindrical type legs [30]. However, it is possible both leg designs might have similar type of spudcan [45] design.

The vessel's DP capability plots should identify the maximum environmental operating conditions under which vessel position can still be maintained when operating. The worst-case failure should be identified for the vessel using failure mode effect analysis (FMEA). The suitability of vessel operations must be considered for worst case failure (WCF). The WCF will have limited thrusters, engine power. In DP jack up vessel under intact (all thrusters working) and WCF (loss of maximum thrusters due to single fault) the position of leg and spudcan can reduce the environmental capability (e.g. wind, current, wave height and wave period) during simultaneous operation. The vessel shall be operated so that it will not lose position in event of worst-case failure [11].

A DP system interfaces with the vessel's propulsion systems to hold the vessel in position against external forces that are acting to move the vessel [29].

Jack-up legs can be very large structures that can significantly contribute to the overall wind forces that are imposed on a vessel [31][44]. Wind forces on the vessel may change as the legs are lowered or raised. When in DP mode and lowering of the legs commences, the DP system should recognise this gradual wind force change and compensate the heading and vessel position accordingly [43].

As the legs are continually extended below the hull the current has more area upon which to act. This current force increases with leg lowering [29]. The DP system should recognise this gradual current change and compensate the heading and vessel position accordingly [2][3].

For DP vessels with jack-up capability – when a vessel moves into position on DP but intends to undertake the work on location as a jack-up vessel [1]. There can potentially be excessive stresses induced into the legs during the transitional period from being on DP to leg touchdown to soft pinning of the legs [43][44]. The first leg contact with the seabed will restrict the vessel's motion which may indicate a position error to the DP system. This could then lead to an increase of thrust of the vessel's positioning propulsion systems and consequently may impart these excessive stresses on the legs [14].

When the vessel's legs penetrate the seabed, the vessel is then effectively moored on the legs. As soon as it becomes obvious that the DP system is not required anymore for position keeping, the Dynamic Positioning Operator (DPO) can select manual joystick mode keeping all thruster propulsion at zero thrust. At this stage it is important the DP system keeps the DP model; in case the vessel has to transfer back to full DP mode during the initial stage of soft pinning of the legs.

The DP Jack up vessels currently use two popular designs of legs, i.e., cylindrical leg type and trussed type (i.e. rack & chord lattices). Although such design of legs is popular since inception of jack up in 1950. Leon B. Delong for Magnolia Petroleum platform design with cylindrical type legs and in 1955 by R.G. Letourneau by developing Jack up drilling rig [4][9] Scorpio Zapata with triangular truss type leg with Rack and pin concept. The reference is cited under web link http://www.energyglobalnews.com/offshore-rig-51-first-jackup-drilling-rig-2/.Non-self-propelled jack up needs tugs to move to the location. This is time consuming exercise and additional cost. Also, some locations are critical with regards to environmental weather window for installation of jack ups. In 1960 EBI cited under weblink Liftboat - Elevating Boats LLC. (ebi-inc.com) has design Self Propelled Self Elevated Crane Barge with a brand name of liftboat. The Dynamic position system which was assisting marine vessel for automatic position is then developed by Howard Shatto cited in Marine Technology Services (MTS) Howard Shatto – 1924-2018 (dynamic-positioning.com). The DP system developed by Shatto, was then installed on vessel Eureka in 1961. The DP system development started [5][7][12][13][25][26][27][28][33][36][37][40][41] and improved over last 6 decades with advancement in the technology.

Dynamic positioning system acts as a facilitator to maintain the position in offshore marine environment and helped to do the offshore activities such as drilling, heavy lifting, cable lay, pipe lay operations etc. Many of these activities are performed in simultaneous operational mode (e.g., DP and Crane, DP + Drilling, DP + Cable Lay, DP +Pipe Lay etc.). During simultaneous operation interface of both/all system is important. The DP system is matured and highly automated with less work to the DP operator, while other system such as Drilling, Jacking, Pipe or Cable lay, Heavy lift etc. needs continues operators input [10][11][18][35].

During author carrier of DP trials on liftboat, seen both DPO and Barge master involvement and engagement in the simultaneous operation. Both operates exchange information by talking with each other. The operations usually carried out very closed to assets. The wrong operator action can lead to assets collision. A dynamic positioning control system [2][5][8][14][22][29] requires minimum 23~30 minutes for the mathematical model [5][7][17][24][29][38] to learn the vessel's hydrodynamic behaviour. The mathematical model then helps to account forces not calculated by DP system via a function of residual current. Although when moving between location, DP Jack-up vessels provide time for the DP model to learn hydrodynamic behaviour, the spudcan that holds the vessel position and headings does not allow the mathematical model to learn. The residual current remains constant until the spudcan is in the seabed. As a result, the DP mathematical model-building process does

not help the DP system to estimate the additional forces in the form of residual current. Soon after the spudcan detaches from the seabed, the vessel drift occurs because the vessel thruster's response needs a rapid response of thrust and azimuth (directions). The DP system manufacturers currently use a sensor-less approach to account for the hydrodynamic forces on the legs and spudcan to build a factor into the mathematical model. The jack-up DP system addresses two simultaneous forces on the legs. The leg element in the air is subject to aerodynamic effects and the leg and spudcan elements in the water are subject to hydrodynamic effects. DP systems currently use drag coefficients (Cd) to compute drag forces, however the hydrodynamic force variations during the complete lowering and raising processes are never completely considered. This weak link in the overall operation leads to positional error and is generally unrecognized by the vessel operators. The risk falls to DP officer and the jacking master to handle. The DP and jacking simultaneous operations mode (SIMOPS) may easily last between 15 and 90 minutes, depending on jacking speed, operational water depth and field procedures, on approach to the asset. The area of operation is close to the asset, which increases the risk of collision with the asset. Most of the studies on jack-up vessels focus on impact force acting on the leg during touch down or penetrations such as Elkadi et al. (2014) [15] and Kreuzer et al. (2014) [30].

Deguhee (2012) [8] published a paper in Marine Technology Services (MTS) DP Positioning on dynamic positioning control augmentation for jack-up vessels, showing that the positional deviation is quite high during heading change and during bottom touchdown and lift off. Hoes (2012) [24] of Delft University, recommended an increased vertical drag force on the skirted spudcan in his paper Liebert (2019) [34] published a paper on Dynamic position of windfarm jack-up vessel, in which the author has used a Morison approach to calculate the hydrodynamic forces on the cylindrical legs. Yao (2019) [44] has performed the analysis of the wave load of jack-up offshore wind turbine installation vessels during dynamic positioning.

Many makers have produces liftboats design due to high demand in both offshore oil and wind market. [8] However, no one knows the risk of vessel drifting limits. My research will bring new era in offshore and wind industry to understand the risk, behaviour of hydrodynamic forces on leg and spudcan, which can influence station keeping performance and how industry can cope up with this to safeguard their assets.

1.2 OBJECTIVE OF RESEARCH

The main objective of my research is to help oil majors and offshore wind farm industry to understand the risk of collision due to the station keeping when jacking and DP simultaneous

operation performed. The position excursion can lead to collision, and this brings extreme risk to both jack up and offshore assets. Since liftboats differs from each other in many ways such as leg design, spudcan design, shapes, thrusters, engines, power generation and distributions, jacking system, different preloading and jacking procedure etc. The common solutions cannot be applied to all the liftboats. However, method of analyzing the risk can be universally applied. The DP designers including industry DP pioneer company is start working on the solution to limit the drifting of Jack up vessel. However, offshore testing proves the applied solution is not matured yet despite DP is matured system from last four decades. The DP system measure excursion from the set centre of rotations of the vessel usually set as midship. The position excursion from mid ship and other points such as DGPS antenna may not be identical when change in heading and position occurs. The following Figure 1-1 issues,

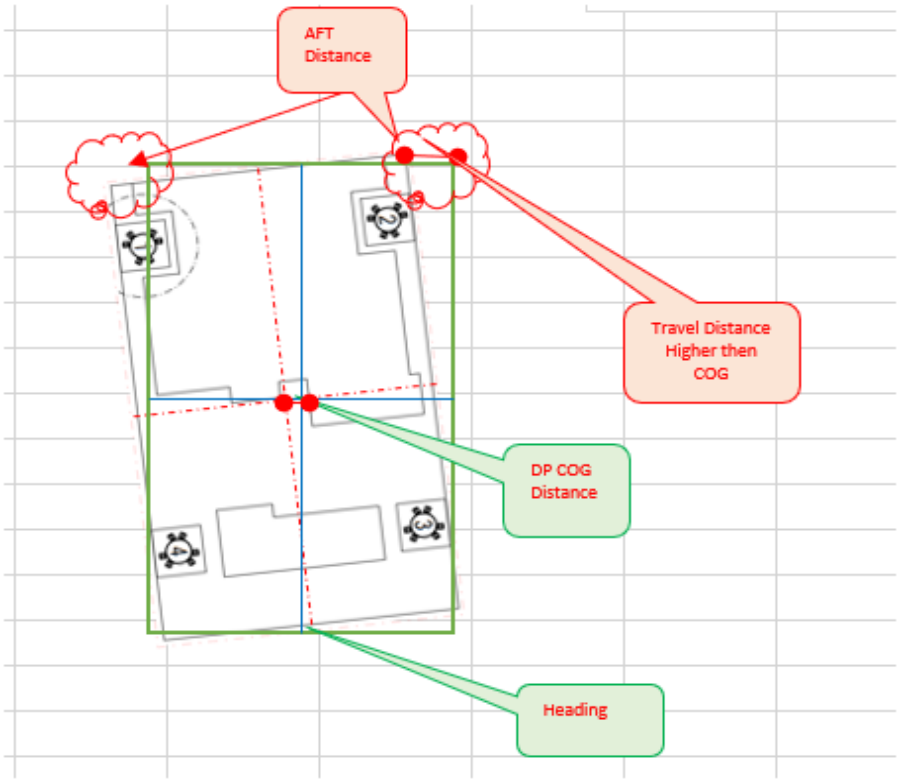

Figure 1-1 Position excursion issue of DP Jack ups boundaries

During the offshore experiment, we observed the DP vendor was using Morison equations to calculate the hydrodynamic forces. Since the jack up leg cylinder diameter is relatively large compared to the wavelength this calculation method is not valid. The Morrison equation (Eq. 1-1) has limitation and typically applied when D (diameter of cylinder) / Wavelength (λ) < 0.2.

$$F_T = C_m \rho \dot{V} V_{vol} + \frac{1}{2} \rho C_d A_p V_c^2 \quad \text{(Eq. 1-1)}$$

The liftboats involve two simultaneous (i.e., DP + Jacking) operations, when approaching to the assets for work and moving away from the assets after the work. These two critical operations are different when compare with leg spudcan movement and direction. The spudcan shapes different at top and bottom. The near field effect of the seabed can impact the hydrodynamics force. The variable sea current at different depth can also impact the hydrodynamic forces.

Currently industry is working with a risk handle by peoples as when where and how much vessel will drift during DP Jack up simultaneous operation is not known to the dynamic position operators.

The DP system has proven track records for assisting offshore marine industry with reliable position keeping performance, however International Marine Contractors Association (IMCA) every year reports DP accidents in their public bulletin, which are reported to them after the incidence for industry information. The lesson learnt used by industry to minimize recurring damage.

DP vendor well understand the risk of mathematical models, which will not updated when spudcan in seabed. The residual current measurement, which provide assistance to correct DP mathematical model to compensate against non-accounted hydrodynamic force will not help in DP Jack up vessel. The DP system designer must build some additional filters and high gain factors in surge, sway and yaw direction to provide rapid response to thrusters to maintain the position soon after spudcan detached from the seabed. The steering angle response of the thrusters in the correct direction to prevent loss of position and heading is also important, when operating in a very tight position limits in the offshore marine environment.

The maker of DP system can use this research work to define the Jacking Leg and spudcan interface with DP system. They can define gain factors for short time to take into account dynamics of leg and spudcan when approaching and moving away from the locations. The near seabed effects due to spudcan on the hydrodynamic forces is paramount important and our intension through this research to make them aware of these drastic changes, which can impact station keeping during most critical operational phase.

1.3 OUTLINE

This thesis consists of six chapters.

In Chapter 1 entitled “Introduction”, the background and purposes of this research are introduced.

In Chapter 2 entitled “History of current DP Jack up usages”, the chapter describes how self-elevated self-propelled vessel progressing to dynamic positioning and issues associated with station keeping reported by previous researchers.

In Chapter 3 entitled “ DP Jack up model and fundamentals of DP control system”, the chapter describe DP Jack up model used for research and fundamental of DP control system, role of Kalman filters and DP sensors in the station keeping.

In Chapter 4 entitled “Evaluate Hydrodynamic Behaviours of Leg spudcan”, the chapter describe Computation Fluid Dynamics (CFD) cases describing various cases, impact of drag coefficient, drag forces, lift forces are validated using tank experiments. The peculiar response of drag and lift forces when spudcan near seabed also studied in CFD and using tank experiment. The CFD analysis further used to see the transient response for both leg lowering and lifting cases. The values are compared with static results. The spudcan top and bottom pressure behaviours during leg spudcan lowering and lifting also analyse. The data provide critical information to the DP software engineers and help them in identifying focused area, when considering gain factors application for better station keeping performance.

In Chapter 5 entitled “Offshore experiment on DP Jack ups and learning”, the chapter describe details of offshore experiments and current risk to the offshore work, which has very tight operational limits for position.

In Chapter 6 entitled “Conclusions”, The CFD results show some interesting facts about the behaviour of the hydrodynamic forces (i.e., drag force Fx and lift force Fy) during the touchdown approach and lift off of a jack up spudcan. The cyclic force behaviour (i.e., increase, decrease, and then increase) due to seabed vicinity is visible when operating near seabed. Large impacts on station-keeping, when the jack up vessel’s legs and spudcan detach from the seabed are evident during offshore experiments. The CFD analysis, the tank experiments and offshore experiment provide interesting facts about hydrodynamic forces when near the seabed. The oil majors, offshore wind industries and vessel owners need to know the maximum overshoot of position in real operating conditions for both lowering and lifting operations. The CFD and tank experiments risk applied to the live projects and demonstrated the excursion issue to the industry DP pioneer company.

2 HISTORY OF CURRENT DP JACK UPS USAGES

2.1 EVALUATION OF JACK-UPS VESSELS

The jack-ups vessels [1][4][30][42][44][45] are categories as non-self-propelled and self-propelled type. The self-propelled jack ups vessel is also called lift boat. These self-propelled and self-elevated jack ups are associated with thruster for propulsion purpose and jacking system to lift the vessel at working height for workover. They are primary build for limited water depth operation in offshore industries. Historical reference of various jack up design and their operating water depth can be found below in Table 2-1.

Table 2-1 Courtesy Mobile Rig Register for 2000 and Offshore Data Services for 2001/02

TABLE 14.1—NOTABLE JACKUP DESIGNS AND THEIR GENERAL CHARACTERISTICS

Designer (No. Built)	Type	Model or Class	Years Built	Initial Cost (M$)	Max. Water Depth (ft)	Hull Size (ft)	Leg Length (ft)	Drilling VDL (Tons)	Cantilever			Comments
									Long (ft)	Pt/Stb (+/- ft)	Load Rating (lb)	
Baker Marine (26)	3 I,M,S,C	BMC	1978–1983	21–32	148–250	191×132×16	162–336	1,621–1,975	40	15	1,000,000	Includes BMC- 150, 200 & 250 Models. Many of these models are still being used successfully at relatively inexpensive rates.
Bethlehem (30)	3 M, I	JU	1979–1982	32–35	100–200	157×132×18	162–269	1,339–2,150	25–45	10	200,000–1,000,000	Includes JU-100, 150 and 200 models. Attractive unit when spud can holes are not wanted.
Bethlehem (29)	3 M, S	JU	1974–1982	10–42	250–270	166×132×16	312	2,250	NA	NA	NA	Workhorse unit of the 1970s and 1980s and many are still in operation.
Friede – Goldman (34)	3 I, C	L-780	1981–1983	30–52	250–300	180×175×25	251–417	1,766–2,277	40	15	1,000,000	Includes L-780 and L-780 Mod II models. Still a very attractive independent leg unit.
Friede – Goldman (7)	3 I, C	Mod V B	1986–Present	62–150	350–400	228×222×31	496–540	3,707–4,166	52–70	15	1,500,000–2,500,000	Also includes KFELS Mod V B, which are upscale, enhanced units for the 2000s. Mod V A units are designed for North Sea operations.
Le Tourneau (31)	3 I, C	82	1978–1985	20–41	250	207×176×20	360	1621–1725	34–40	15	1,000,000	Includes Models 82, 82SD both slot and cantilever. Good unit for shallow water, especially in as shallow as 14 ft.
Le Tourneau (56)	3 I, S, C	116	1973–1983	9.3–43	243–350	243×200×26	410–477	2,200–2855	40–57	15	1,087,000–1,250,000	Includes Models 84, 116S and 116C. Many of the early 84S and 116S have been converted to 116C. Highly desirable and very common unit.
Le Tourneau (8)	3 I, C	Gorilla	1984–Present	85–212	328–450	306×300×36	504–605	2,594–8,125	52–75	20	1,875,000	Le Tourneau's largest, most capable and expensive unit. There are a number of different sizes for this class.
Livingston (21)	3 I, C, S	111	1971–1987	10.5–56	231–300	200×186×23	339–418	1,570–2,590	35–50	15	1,000,000–1,600,000	Some rigs have been converted to skid off units. Shipyard is out of business.
Mitsui (10)	3 I, C	300C	1981–1983	25–35	220–400	220×190×26	408–505	1,610–1,984	45	12	1,250,000–1,390,000	Few in number but a capable unit.
Offshore Co. (13)	4 I, S	Orion	1976–1988	10–50	200–307	172×134×21	305–400	2,006–2,080	NA	NA	NA	One of the older designs that is still being used in the industry. However, many have been lost, scrapped, or converted to production units.
MSC (2)	3 I, C	C370-150 MC	2003–Present	200+	492–625	291×336×39	673	10,000	90	32.8	3,080,000	In 2003 this was the world's largest jackup, built primarily for North Sea operations.

1. The above characteristics are general. Since types are grouped, variance on listed statistics will occur.
2. Type includes independent leg (I), mat (M), slot (S), and/or cantilever (C).
3. Within designs, variations are the rule rather than the exception. When designs are grouped, the largest hull is emphasized.
4. There are many more designs that are not listed. The above listings are representative of all the designs that are available.
5. Source: Mobile Rig Register for 2000 and Offshore Data Services for 2001/02.

The jack up vessels with 3 legs, 4 legs,6 legs,8 legs and10 legs were built since inception. The leg design varies from square plate type, cylindrical type, and truss type legs. The vessel seajacks vessel of NG2500X GustoMSC working on oil and gas platform shown below in Figure 2-1.

Figure 2-1 Seajacks Kraken Four Leg Jack Up (Courtesy: SEAJACKS

The Jack up vessels were primary built for drilling operations. However, their operations were limited to shallow water.

2.2 DYNAMIC POSITIONING PENETRATION IN OFFSHORE INDUSTRY

The Dynamic positioning vessels primary build for deep water application. As time progress these vessels slowly pushed to operate in shallow water. However, industry come across limitation of using DP Vessel in shallow water. The vessel draft, shallow water waves and thruster dynamic interaction with seabed are main elements contributing to the limitation in Shallow water. The shallow water offshore and windfarm industries are getting dense day by day. Due to closed proximity of platforms / offshore windfarms, the approach of Jack up vessel for installation for maintenance and installation become critical operation. To tackle this critical operation, vessel designer decided to upgrade the self-propelled vessel self-elevating jack up vessel with Dynamic positioning system.

2.3 INTRODUCTION OF DP IN JACK-UP VESSEL

2.3.1 The latest trend shows, high demand of DP Jack up vessels in offshore and windfarm industries. There are three type of DP class notations for vessels,

1) Ships with class notation IMO DP 1 are able to keep their position at least in automatic mode and joystick mode. However, the single fault can lead to loss of position.

2) Ship with class notation IMO DP2 are able to keep their position even after single failure in an active component. However, the fire and flood can jeopardize and defeat worst failure design intend of the vessel.

3) Ship with class notation IMO DP3 are able to keep their position and able to keep their position even after single failure in an active component as well as static components even in fire and flood condition.

DP2 vessels are taking maximum share among DP vessels as it provides redundancy against single fault as fire and flooding of the compartment are rare in comparison to other failure. It also offers cost economic balance. The use of DP Jack ups in renewable industry for installation of Wind turbine, piles and maintenance of turbine industrial mission work dominated by DP2 jack up vessel. The Wind carrier shows below in Figure 2-2.

Figure 2-2 Jack Up Vessel Wind Turbine Installation Vessel (Courtesy: Gusto MSc)

2.3.2 The Jack-ups approach to the installation in DP2 mode (i.e., Intact mode- All thrusters are active and working) with following three (3) installations operation.

1. Vessel moves toward installation with leg lowering operation.
2. Leg already pre-lowered condition with approximately 5~10m above seabed and approach to the installation.
3. Leg lowered for soft pining before DP2 mode stops.

4. The SIMOPS operation of DP and Jacking system ends. The barge master continues with Jacking operation. The DP system stops to prevent unnecessary thrust actions after soft pining achieve by leg spudcan of jack up vessel.

2.3.3 The Jack-ups leave the installation in DP2 mode with following three (3) installations operation.

1. Lowered the hull in water, use bouncy to release spudcan from the seabed. Start thrusters and vessel engage DP system.
2. After 30 mins of time, the Barge master and Dynamic position operator analyses the spudcan extraction and routes to move vessel from the location.
3. The Dynamic Position Operator (DPO) set DP system in joystick mode and barge master keep alerting DPO on leg extraction process, once leg extracted from seabed DPO try to limit the extraction using joystick control and redirect vessel on route. The barge master continues his work of leg moving away from seabed to the park position. SIMOPS of DP and Jacking stops when leg fully retracted. The DPO continues with his DP operations for taking vessel out from field.

The simultaneous operation (SIMOPS) of DP2 and Jacking system carried out with variable leg speed during lowering, lifting and near seabed operational phase. The DP2 system currently depends on mathematical model to provide good station keeping performance. The dynamic positioning system estimates the new position based on the acting environment. The available thruster generates required thrust in the direction as per thruster allocation algorithm. The heading and position reference (i.e., sensor gyro & position reference system) compare time to time with estimated position in all the process. The current mathematical model also helps to maintained position in dead reckoning condition which vessel witness during loss of all available position reference on the vessel. The DP station keeping stability achieved by accurate mathematical model. The wind and current area of the vessel is important in the force calculation process.

The mathematical model calculates forces acting on the vessel but without considering jack up legs. Some DP jack up has interface of jacking system leg distance and leg speed interface with DP controller. The drag force calculated using Morison equations. However, this approach did not help DP Jack ups owners for guaranteed station keeping performance. The dependency on DPO and barge master skills become paramount important for safe work. In high current conditions the leg and spudcan of jack ups, which moves either in Up/Down at different speed, could lead to very large hydrodynamic forces. The leg spudcan, when moves near to the seabed as claim in Hoes (2012), hydrodynamic coefficient of spudcan in proximity

of seabed during Jack up installation increases, when it is half of spudcan diameter near to seabed. Since, it is evident from current practise, the weak link in DP interface with Jacking system. The dynamic positioning mathematical model is not aware of the hydrodynamic forces of jack up leg and spudcan.

The paper published in MTS DP Positioning by Deguhee (2012) [8] on dynamic positioning control augmentation for Jack-up vessels, shows the position deviation is quite high during heading change and also during bottom touchdown and lift off operation. Both vessels' Seajacks Kraken and Bold Tern Wind carrier shown above in Figure 2-1 and Figure 2-2 respectively dealt by author in design of electrical and control engineering activities performed during the shipbuilding of vessels in Lamprell Shipyard, Dubai, UAE. Since the author was also involved in DP Dept. for plan approval and Noble Denton for Failure Mode Effect Analysis (FMEA) studies on DP, the issue picked up to study in depth on how currently this risk is managed. During visit to various oil majors, found that DP Jack up vessels has been asked to remove thrusters or disable DP functions when charting jack up vessel with DP. These are the same charters who has DP2 requirement to operate within 500 m zone. This trigger author to do research in this area.

During DP2 jack up move, when hull lowered to water, the DP2 mode activated with legs and spudcan in seabed. The DP vessel always provided time for mathematical model building, while extracting the leg from the seabed. However, since the position remain same until spudcan in seabed. The mathematical model never updates with situation of spudcan detach from the seabed. As a result, even when DP joystick mode used, the vessel drift soon after spudcan detached from seabed, until the azimuth and thrust counter these situations.

3 DP JACKUP MODEL AND FUNDAMENTALS OF DP CONTROL SYSTEM

3.1 VESSEL MODEL CHARACTERISTICS

There are two popular designs predominating in Self Elevating Jack Up Dynamic Position Controlled vessel. The vessel model considered for study the response is cylindrical leg and Rack & Chord lattice leg design. The effect of hydrodynamic forces studies and found the most domination leg among these two leg designs is a cylindrical leg. The focused of study is then shifted mainly on cylindrical leg design. This vessel mainly used for wind farm installation, offshore well intervention unit, platform maintenance vessel etc. All though the vessel mainly does its industrial mission work in jack up condition. The approach to the vessel is always via dynamic positioning system. The outline of the Jack up cylindrical leg is shown in Figure 3-1

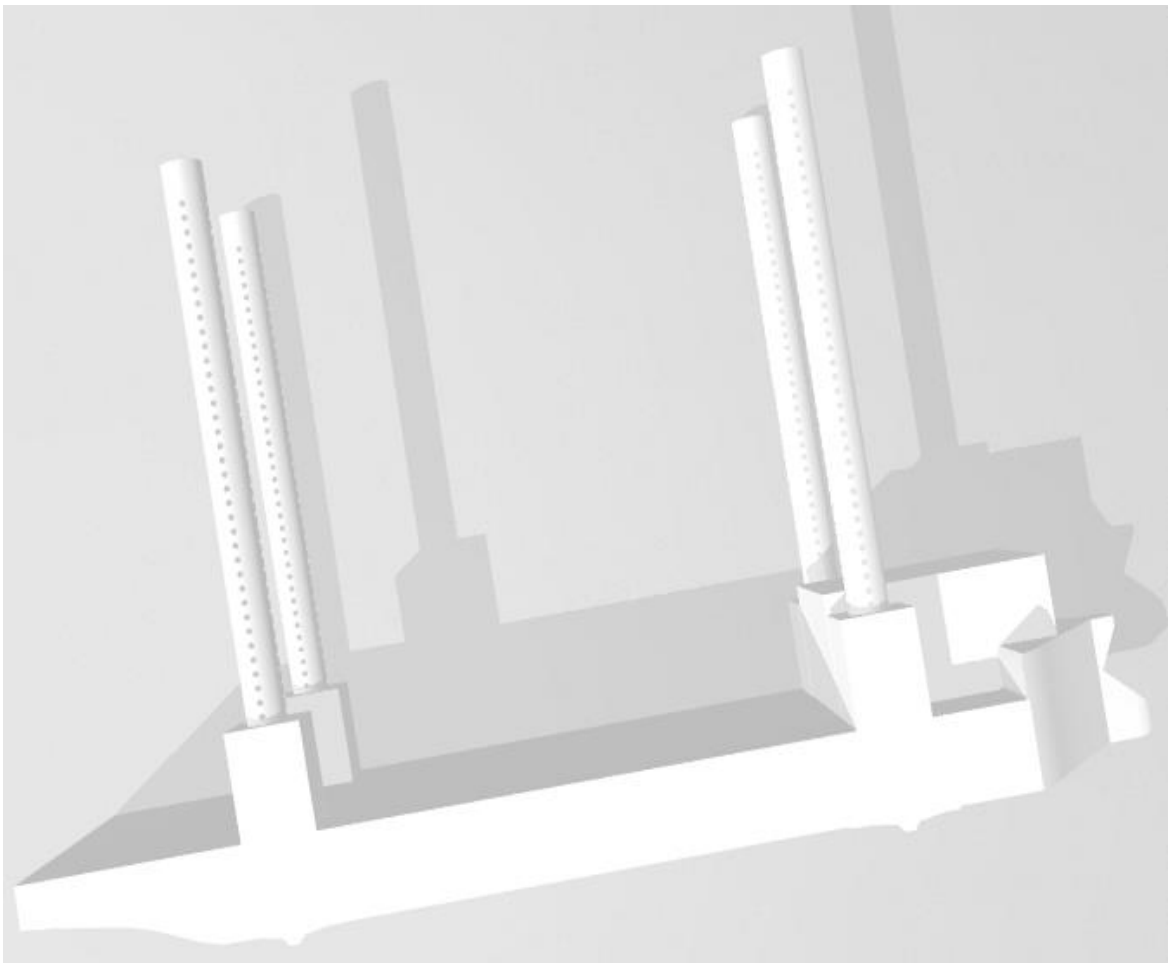

Figure 3-1 Jack Up DP Vessel (Cylindrical leg)

This jack up vessel in transit mode of operation, works with leg fully extracted. The spudcan is design such that it flush with hull to reduce the resistance during transit. The approach to the installation depends on the company procedure and project specific procedure. The DP Jack Up vessel approaches to the installation position from 500 m with leg lowered but kept gap of approximately 2 to 5 m above seabed.

The typical vessel particulars shown below in Table 3-1

Table 3-1 Vessel Particular for Study

Length	125 mtr
Width	42 mtr
Hull Depth	7.5 mtr
Draft	5.0 mtr
Leg Design	Cylindrical Type
Diameter	4.5 mtr
Leg Length	75 mtr
Operating Water Depth	50 mtr
Jacking Speed	Slow – 0.5 mtr/ min
	Medium – 1.0 mtr/ min
	Fast – 2.0 mtr/ min

The spudcan attached to the bottom of the leg to support the jack up when operating in elevated mode. Spudcan also has functionality to assist in smooth penetration in the seabed, which is achieved by conical design at the bottom end of spudcan as shown below in Figure 3-2. The spudcan structural arrangement is complex physically very strong and varies from

different leg designs. The spudcan also has jetting system with nozzle arrangements at upper and bottom plate. The jetting and nozzle system helps in removing spudcan from the seabed. There are two types of spudcan design floodable and non-floodable type. The new design of spudcan approach detailed in Zheng (2015) paper [45], showing sharp conical solid tip.

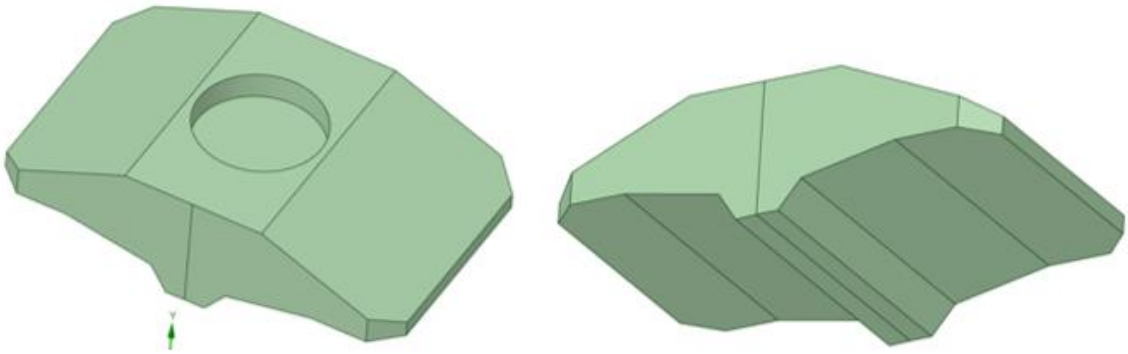

Figure 3-2 Spudcan Typical design

3.2 DP HISTORY AND DEVELOPMENT

The concept of DP system is not new to the world, Conceptual idea of DP published in 1895 in the non-fiction novel of “Jules Verne”. The “Propeller Island”, Evans (2005) [16], String quartet traveling from San Francisco to San Diego, Ended up on the floating Standard-Island. The propellers kept position (steady as an island), which was too deep for mooring.

The DP system developed in 1960 by continental union Shell and superior oil consortium for drilling vessel. The vessel Sedco 445, Dillard S (1972) [9] builds for drilling at approximately3500 m. The station keeping was maintained using four azimuth thrusters, manual control by visual observation and sonar tracking.

The Eureka is a first DP vessel built in 1961 for the purpose of drilling [9]. The concept of automatic position and heading maintained implemented using mostly analogue sensors. The concept of redundancy was not thought in any of the systems.

The DP goes digital in 1967, with the development of dynamic positioning system for Glomar Challenger. The control logic function for DP Station keeping implemented and shown below in Figure 3-4 which was not using position sensor. The set point enters in the DP system considering vessel along ship and athwartship line from centre point. The set point distance measured considering vessel geometry in longitudinal and lateral direction. The heading was calculated of this set point and vessel alongside as shown below in Figure 3-3.

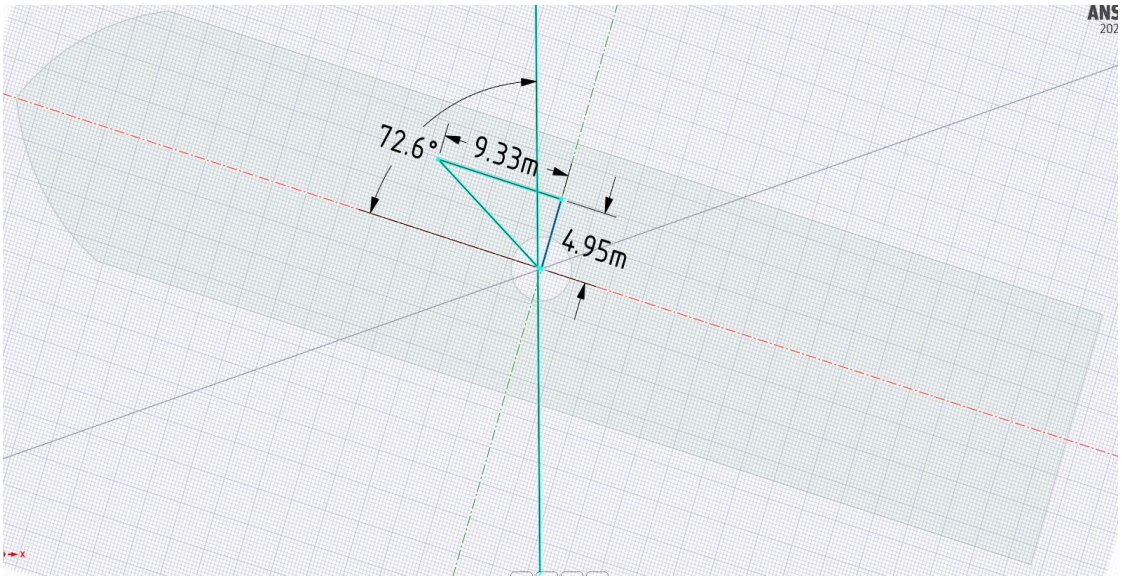

Figure 3-3 Position (alongside and athwartship) and heading setpoint

The first DP model was developed without any consideration to *external position reference*. The relative position reference sensor was under development, but vessel was keeping the position based on lateral and longitudinal position on the vessel. The heading reference was calculated by measuring the angle between along ship axis and position point on the vessel. The basic DP control system without position sensor shown below in Figure 3-4.

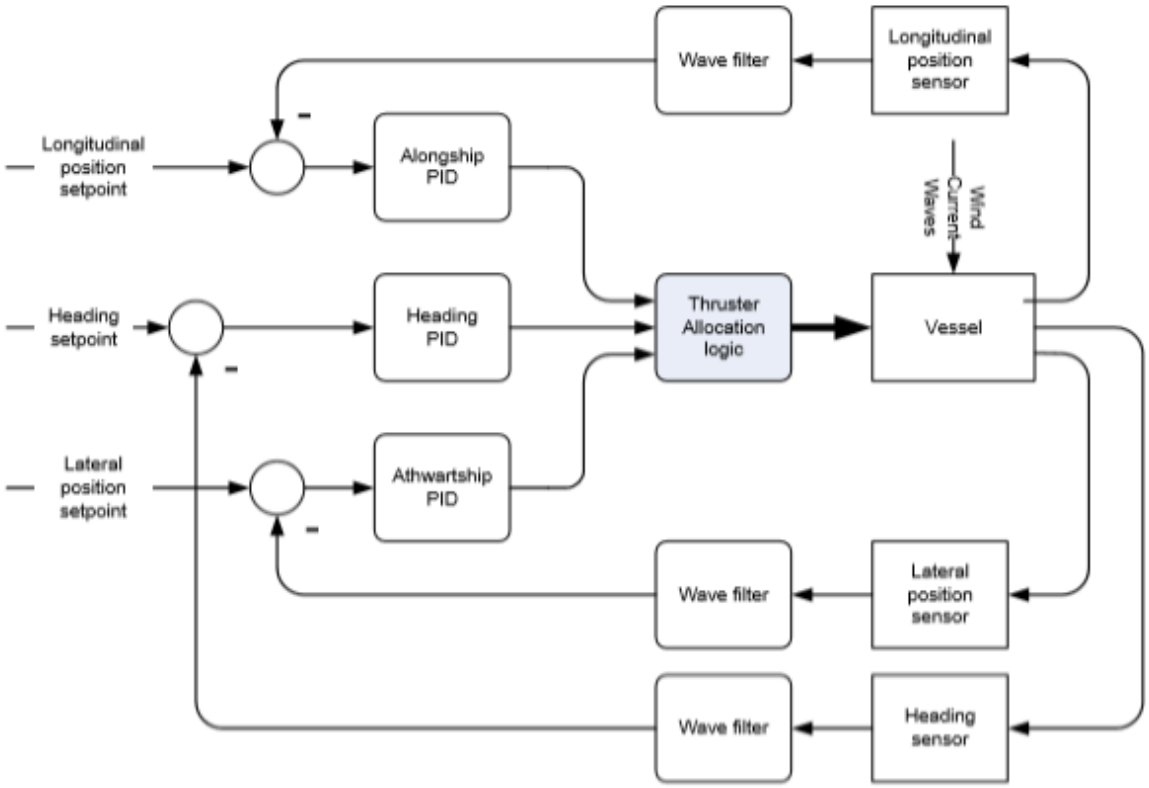

Figure 3-4 Basic DP control system (no position sensor- Courtesy KM)

In 1971, the DP system goes more robust by building, redundant system for drilling vessel SEDCO 445 [9]. The DP system build with computer redundancy and position reference system sensor redundancy as shown below in Figure 3-5.The first ever position reference system was developed exclusively to provide position reference from the nearest fixed reference for DP vessel. The acoustic position reference works on the principal of transceiver which is fixed below the vessel hull emits the signal at known frequency and transponder installed on the seabed reflect this signal back to the transceiver. Based on the time measurement of signal sending and receiving the distance and angle is calculated. The reference used as relative position reference. The taut wire is a mechanical type of position reference system. Its purpose is to provide accurate data of a surface vessel's movements with respect to the position of a depressor weight on the sea floor.

A wire is maintained at a constant tension by means of a depressor weight on the seabed and a pneumatic and electric servo-assisted "mooring" system. Any movement of the vessel will cause the tensioned wire to deviate from its initial inclination. This movement activates

potentiometers mounted in the gimbal (sensor) head and produces changes of analogue signals directly proportional to the deviation in inclination.

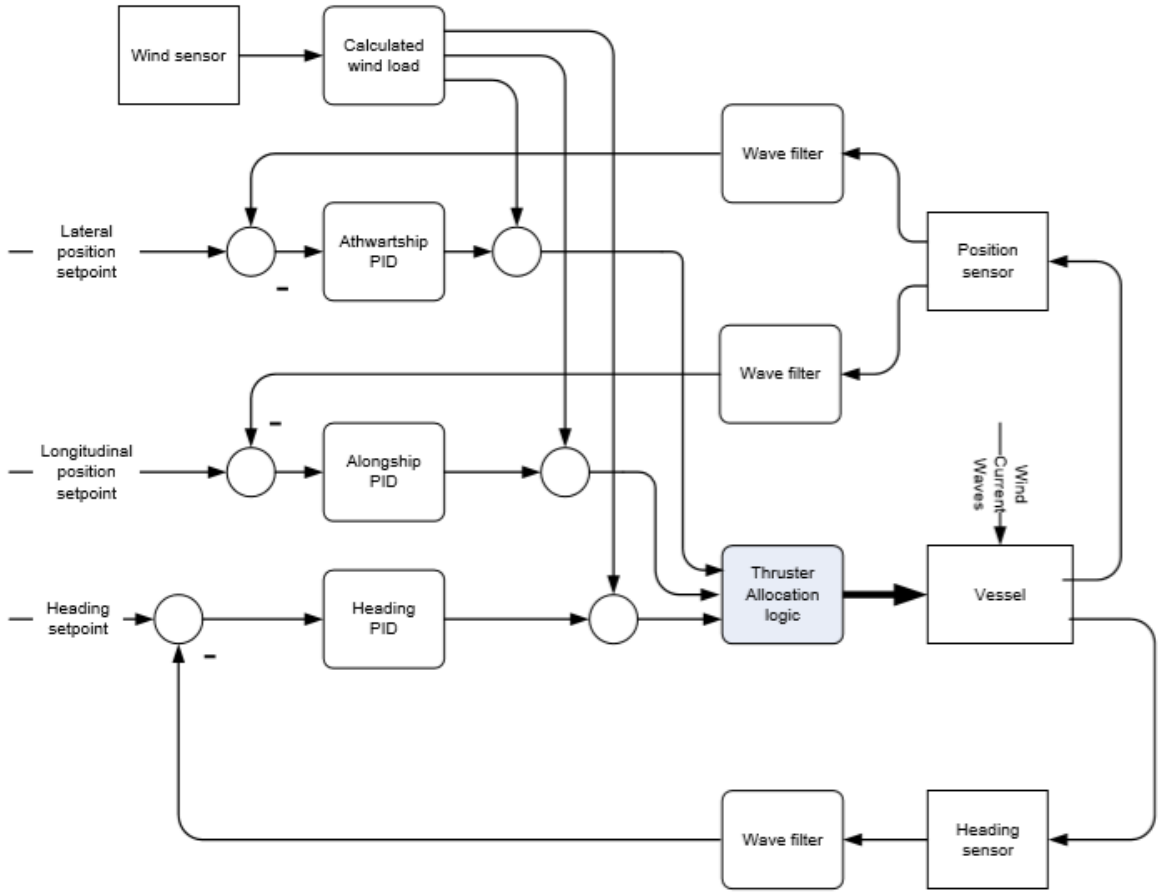

Figure 3-5 DP control system with Position sensor (No voting rejection-Courtesy KM)

The DP system development continues in Norway. In 1970 Balchen [5] (NTNU) started working on modern control theory to develop a dynamic position system. The state of the vessel consists of position (x, y), heading and velocities (in surge, sway and yaw) as well as steady-state current (Cx, Cy, Cz).

The most modern Dynamic position system developed in 1975 has model-based approach. Each DP vessel has hydrodynamic model build for DP force calculation estimation based on wind input. The system used vessel motion (VRU) or Motion Reference Unit (MRU), sensor information to compensate position sensor error and avoid vessel misunderstanding on moving due to roll, pitch and heave motion acting on the vessel.

The Kalman filter [7][17][38] with adaptive wave filtering implemented so that DP system automatically reject not performing sensors based on voting when available (i.e out of 3

sensors,1 sensor is not showing correct information) or the sensor inputs out of range due to noise etc.

The DP system calculates estimated position (i.e, Transvers and Longitudinal) of the vessel and heading and compares with the real sensor data. The position excursion, heading, wind and current error are feedback to the Kalman filter [7][17][38] to calculate the Kalman gain factor based on true sensor readings. As the process is iterative, the difference between estimation and actual will reduces as a result Kalman gain factor reduces. The DP Controller generate thrust and azimuth command to each individual thruster by thruster allocation logic. The DP system also monitors feedback from each thruster and feeds to mathematical model. The wind sensor input is fed to both controller and mathematical model.

The wind gust compensation is directly taken care by controller and then preciously generated thrust command to the thrusters, while non wind gust situation is taken care by DP mathematical model to provide better station keeping stabilities. In DP, mathematical model updates when model sees large difference between estimated and sensor data Kalman gain factor increases to reduce the gap between estimate and actual. The residual currents which account all non-sensor-based forces updates DP estimation systems, so the position error reduces quicker to smallest possible values. In DP system residual current fluctuating characteristics indicates model is not tunned and it needs more time before start of offshore activity. The steady residual current or slight difference between previous readings confirm the DP model learning is completed and vessel can now deploy for offshore activity.

3.3 ROLE OF MATHEMATICAL MODEL IN DP

The mathematical model is nothing but the estimator of position and heading. This is done simply by directing the sensor information of wind and also feeding information for current position heading and feedback of thruster. The estimator/equations in the mathematical model then calculates how the vessel will reacts or moves as a function of the forces acting upon it. The model is a hydrodynamic description, i.e., it involves the vessel's characteristics such as mass and drag. The design criterion for the model is an as accurate as possible description of the vessel's motions and reaction to any external forces. The mathematical model does affect as vessel has six degrees of freedom, while mathematical model usually deals with only linear parameters such as surge, sway and yaw movement of the vessel. Moreover, it also calculates equivalent current and estimate waves as a function of wind.

The vessel velocity in surge and sway and rate of turn defined as $\upsilon_x, \upsilon_y, r$ respectively and shown below in Figure 3-6.

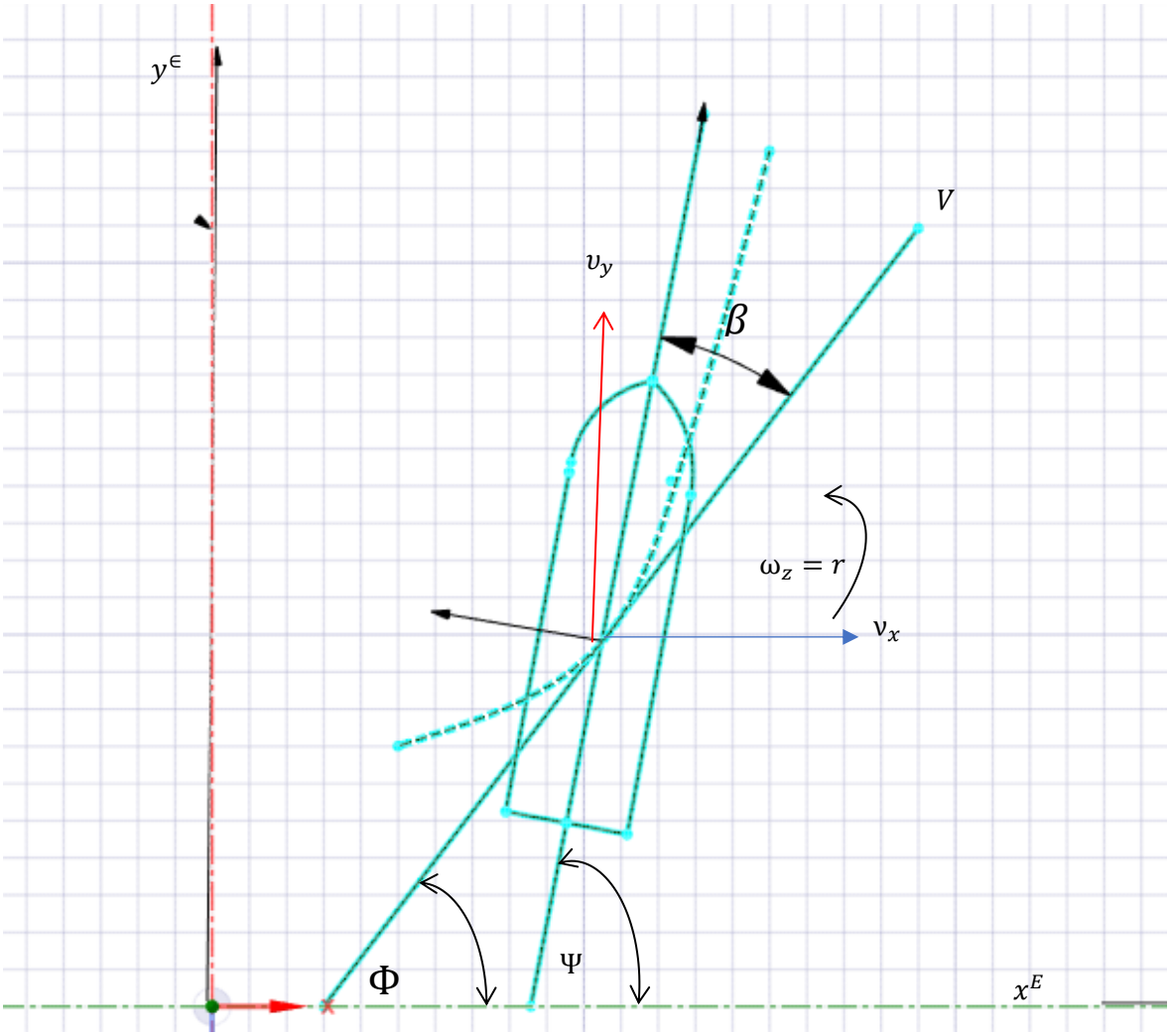

Figure 3-6 Ship co-ordinate system for motion equations

The vessel position defines in north (Latitude) and east (Longitude) define as $x^{\in}, y^{\in}$

The vessel heading defined as Ψ

The kinematics to find new position of vessel in latitude direction using (Eq. 3-1)

$$\chi^{\epsilon} = \upsilon_x . cos\Psi - \upsilon_y . sin\Psi \quad \text{(Eq. 3-1)}$$

The kinematics to find new position of vessel in longitude direction using (Eq. 3-2)

$$y^{\epsilon} = \upsilon_y . cos\Psi + \upsilon_x . sin\Psi \quad \text{(Eq. 3-2)}$$

$\psi = r$

r = Rate of Turn = $\omega_z = \frac{d\psi}{dt}$

$m = Ship\ Mass$

$m_x =$ added mass due to inertia of the water when accelerating in x − direction

$m_y =$ added mass due to inertia of the water when accelerating in y − direction

The equation of the motion read as follows,

Longitudinal Forces calculated using equation shown below in (Eq. 3-3)

$$F_{x=} (m + m_x)\ \frac{dv_x}{dt} - (m + m_y).v_y.\omega_z \quad \text{(Eq. 3-3)}$$

Latitude Forces calculated using equation shown below in (Eq. 3-4)

$$F_{y=} (m + m_y)\ \frac{dv_y}{dt} + (m + m_x).v_x.\omega_z \quad \text{(Eq. 3-4)}$$

Yawing moments calculated using equation shown below in (Eq. 3-5)

$$M_{z=} (I + I_z)\ \frac{dw_z}{dt} + (m_y - m_x).v_x.v_y \quad \text{(Eq. 3-5)}$$

The velocity component can then be calculated using (Eq. 3-6) sets of equations of motion,

$$v_x' = \frac{m+m_y}{m+m_x}.v_y\ .\omega_z + \frac{F_x}{(m+m_x)}$$

$$v_y' = -\frac{m+m_x}{m+m_y}.v_x\ .\omega_z + \frac{F_y}{(m+m_y)} \quad \text{(Eq. 3-6)}$$

$$\omega_z' = \frac{M_z}{(I+I_z)} - \frac{(m_y-m_x).v_x.v_y}{(I+I_z)}$$

The new heading and position coordinates are necessary for Dynamic position system. Mathematically they can be calculated using (Eq. 3-7)

$$\psi' = \omega_z = r \quad \text{(Eq. 3-7)}$$

The vessel course angle can be calculated using (Eq. 3-8)

$$\text{Course } \phi = \psi - \beta \quad \text{(Eq. 3-8)}$$

Course = $\psi - \arcsin({}^{v_y}/_{V})$

whereas $V = \sqrt{(v_x^2 + v_y^2)}$ and $v_y = -V\ sin\beta$

The new position latitude (x) and longitude (y) -direction of vessel can be calculated using equation (Eq. 3-9)

$$x_r' = \sqrt{(v_x^2 + v_y^2)} * cos\phi$$

(Eq. 3-9)

$$y_r' = \sqrt{(v_x^2 + v_y^2)} * sin\phi$$

The wind forces are calculated as a function of measured wind speed and direction, while thruster forces are calculated as a function of thruster/propeller pitch/rpm and direction. The system incorporates algorithms for the estimation of sea current and waves, and the forces caused by these. The mathematical model then estimates new vessel position and heading of the vessels. These estimations then are input to the main DP controller, who compares output with desired position and heading. The main outputs from the mathematical model are filtered estimates of the vessel's heading, position, and speed in each of the three degrees of freedom - surge, sway and yaw. The mathematical model itself is never a 100% accurate representation of the real vessel.

The Kalman filtering technique [5][7][17] is a game changer in model-based DP system as shown in Figure 3-7 and helps in continuously correcting model process. The vessel's heading and position are measured using the gyrocompasses and position reference sensors and are used as the input data to the DP control system.

This data is compared to the predicted or estimated data produced by the mathematical model, and the differences are calculated. These differences are then used to update the mathematical model to the actual situation.

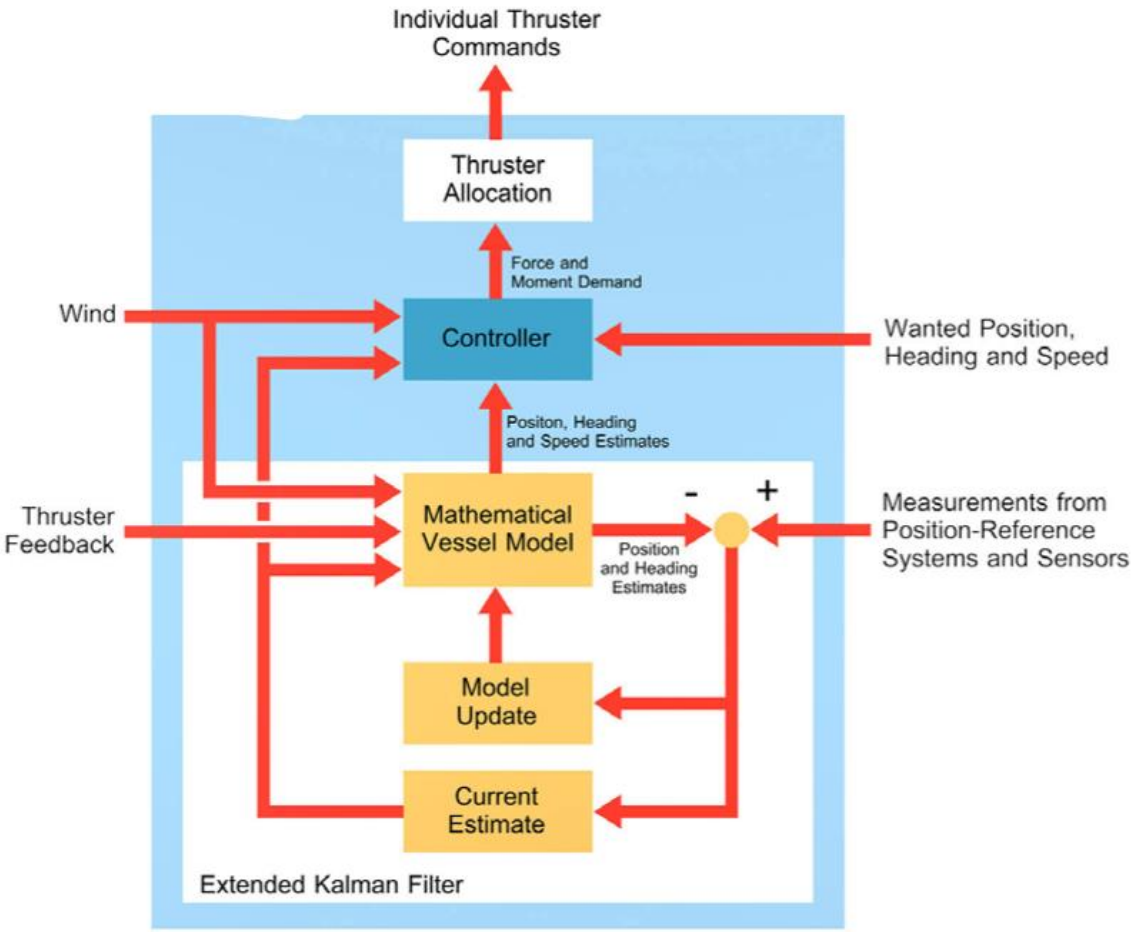

Figure 3-7 Modern DP Control System with Extended Kalman Filter (Courtesy: KM)

The vessel's mathematical model and the Kalman filtering technique provide advantages such as,

1) Ignore data out of range and filter heading and position measurements.
2) The DP2/DP3 vessels needs minimum 3 position reference system (PRS), two of them must be work on different operating principles. The DGPS are satellite-based position system with correction signals while, one of them must be from relative position reference system such as CyScan, Radius, HiPAP, Tautwire, RadaScan, Fanbeam, Spotbeam etc. It is certain to expect each system provide a position-reference system and it will be differed from other PRS. The mathematical role then assigns the different weighting on their measurements according to each system's individual quality (accuracy, stability, repeatability). The median criteria (e.g., within 3m) chosen by operator will decide, which PRS should be consider and which one should be ignore, when providing resultant position of the vessel.

3) The model provides an accurate position keeping for at least first 5 min even when DP system all position reference sensors lost. This is called "dead-reckoning" mode. This means that the system can perform accurate positioning for several minutes without position updates from any position-reference systems.

3.4 CHALLENGE OF JACKING LEG INTERFACE WITH DP

Leg placement and removal are the two most critical operational modes for dynamically positioned jack-ups when working close to an offshore asset. Any positional deviation may lead to collision and damage to the asset. Industry operates with a weak link between the dynamic positioning (DP) system and the jacking system. Current DP systems operate without any sensors identifying the hydrodynamic force variations on the legs and spudcan, which vary between different leg and spudcan designs. When the spudcan is near to the sea bottom, the hydrodynamic force must be reported to avoid large positional deviations driven by the DP system [12][13][25][26][27][33][36][37][40][41].

A jack-up's dynamic positioning control system requires minimum 23~30 minutes for the mathematical model to learn the vessel's hydrodynamic behaviour and response to the environment. Although when moving between location, DP Jack-up vessels provide time for the DP model to learn hydrodynamic behaviour, the spudcan that holds the vessel position and headings does not allow the mathematical model to learn. The residual current remains constant until the spudcan is in the seabed. As a result, the DP mathematical model-building process does not help the DP system to estimate the additional forces in the form of residual current. Soon after the spudcan detaches from the seabed, the vessel drift occurs because the vessel thruster's response needs a rapid response of thrust and azimuth (directions).

The storyboard indicating vessel jack up legs transition to seabed are shown in below,

1) Figure 3-8-Indicates Jack up Leg completely raised and spudcan recessed in the Hull.
2) Figure 3-9 Indicates Jack up Leg Lowering to Seabed.
3) Figure 3-10 Indicates Jack up Leg spudcan ready for soft pining with seabed. Near Seabed effect on station keeping. Change of CG and forces acting on the leg.
4) Figure 3-11 Indicates Jack up Leg spudcan in the seabed. The fixed position due to spudcan in seabed does not allow mathematical DP model to learn vessel motion as both heading and position remain unchanged. However, soon after spudcan detached from seabed, the vessel will drift, and DP system need special function to prevent drifting of Jack up vessel.

The co-ordinate system shown below in the story board followed for CFD analysis. The fluid flow applied in X-direction. The drag force measured along x-axis, while lift force measured along y-axis.

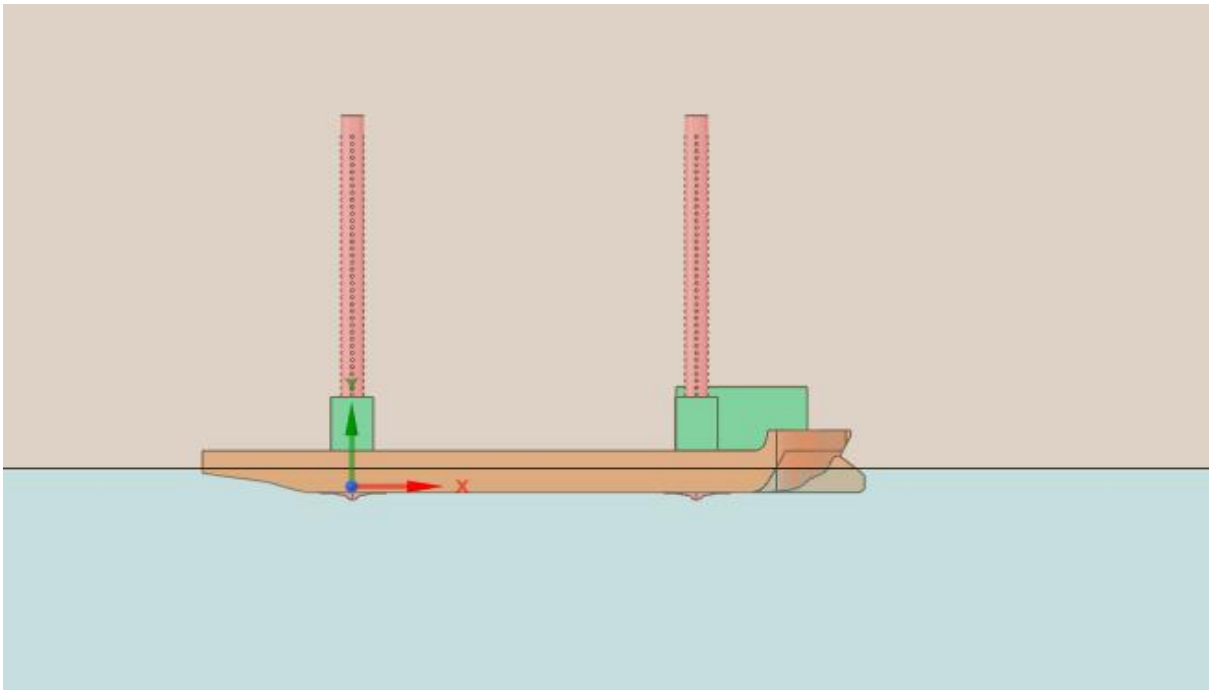

Figure 3-8 Storyboard 1- Jack-up Leg completely raised – Arrival at Location

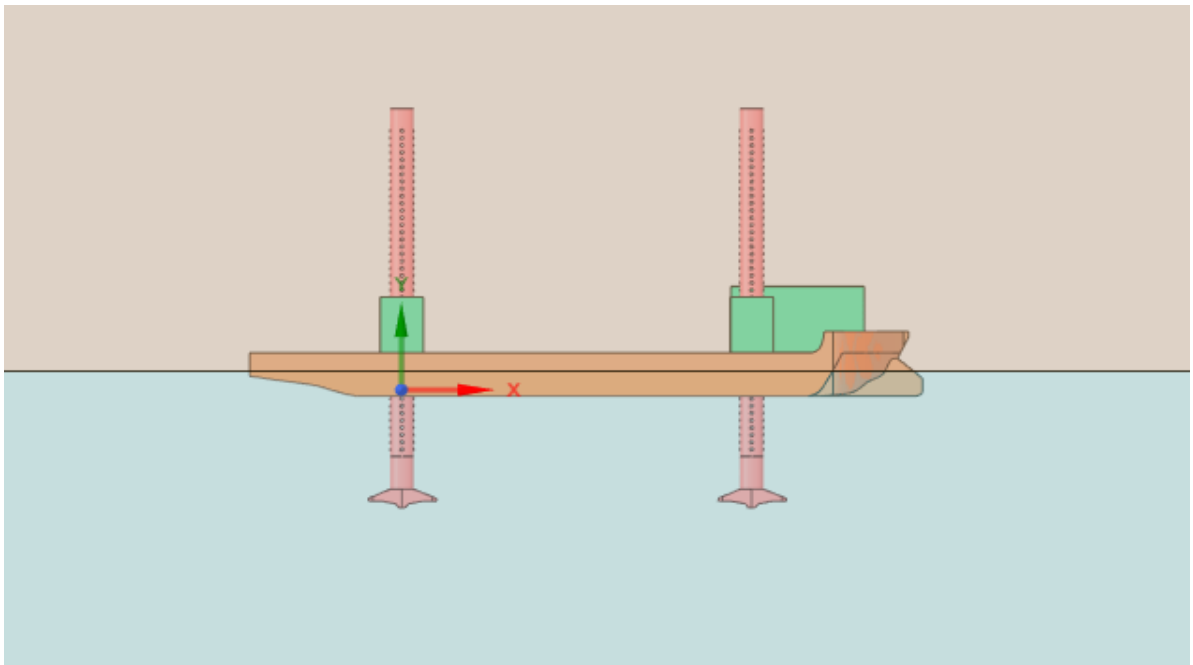

Figure 3-9 Storyboard 2 -Jack up Leg lowering

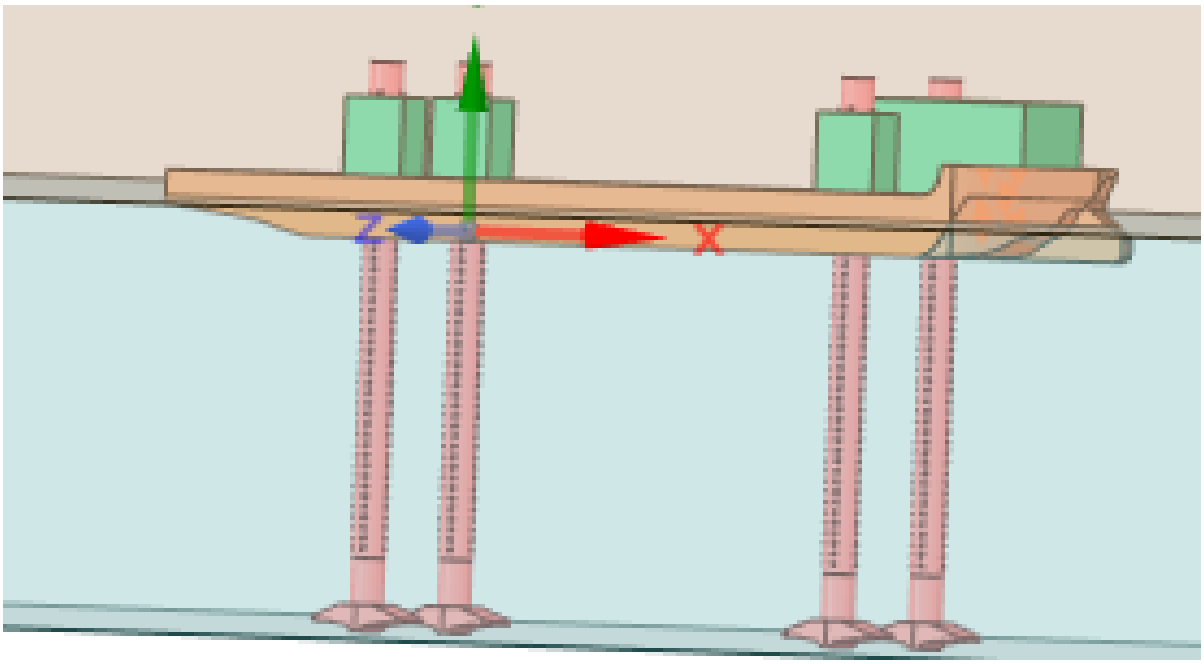

Figure 3-10 Storyboard 3- Leg near Seabed for Spudcan soft pining

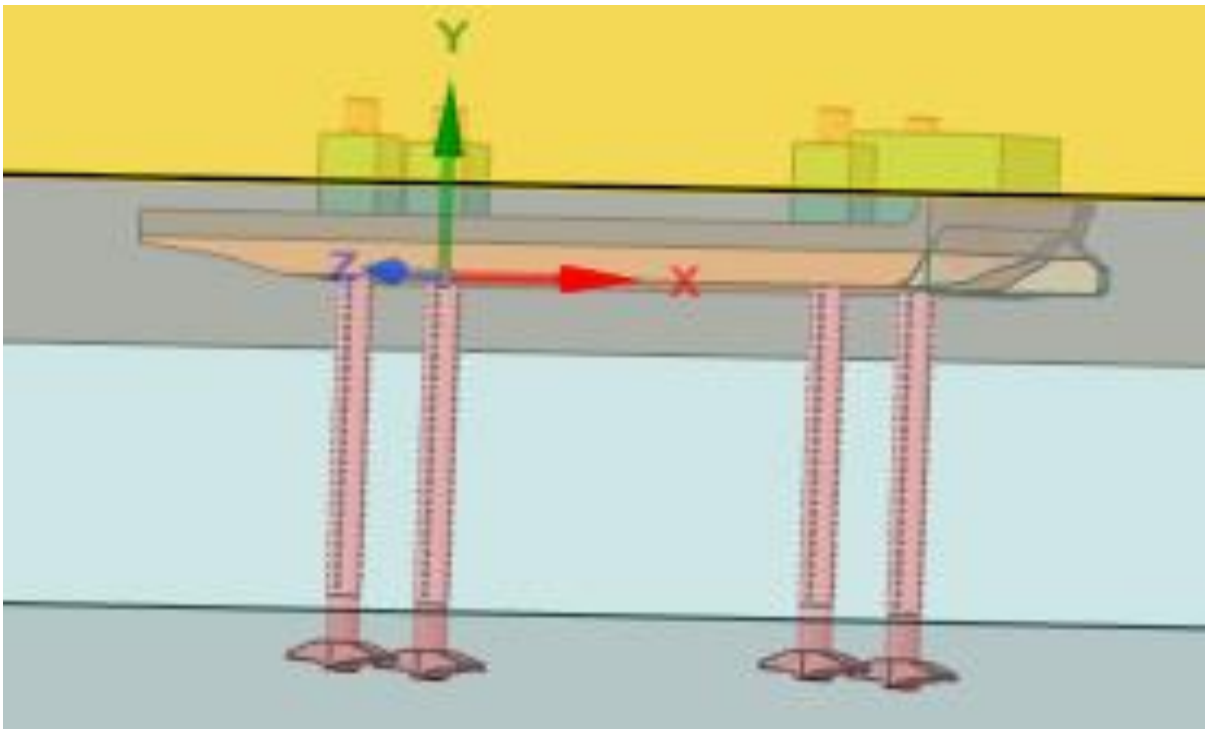

Figure 3-11 Storyboard 4 – Spudcan in the seabed (DP OFF)

3.4.1 Deguhee (2012) [8] published a paper in MTS DP Positioning on dynamic positioning control augmentation for jack-up vessels, showing that the positional deviation is quite high when spudcan lift off. The time response in Figure 3-12 clearly shows position deviation before it

comes to acceptable position excursion limit in approximately 8 to 10 min in most of the cases. The compensation gain factor challenge applied to DP model of the vessel during lift off when current acting on the DP jack-up vessel of1 knot, 1.5 knot, 1.7 knot and 1.9 knot however since the gain factors were not tuned for each current case. As a result, the position error various a lot during lift off. The results clearly indicate gap of DP control system in providing required position accuracy for carrying out offshore work safely.

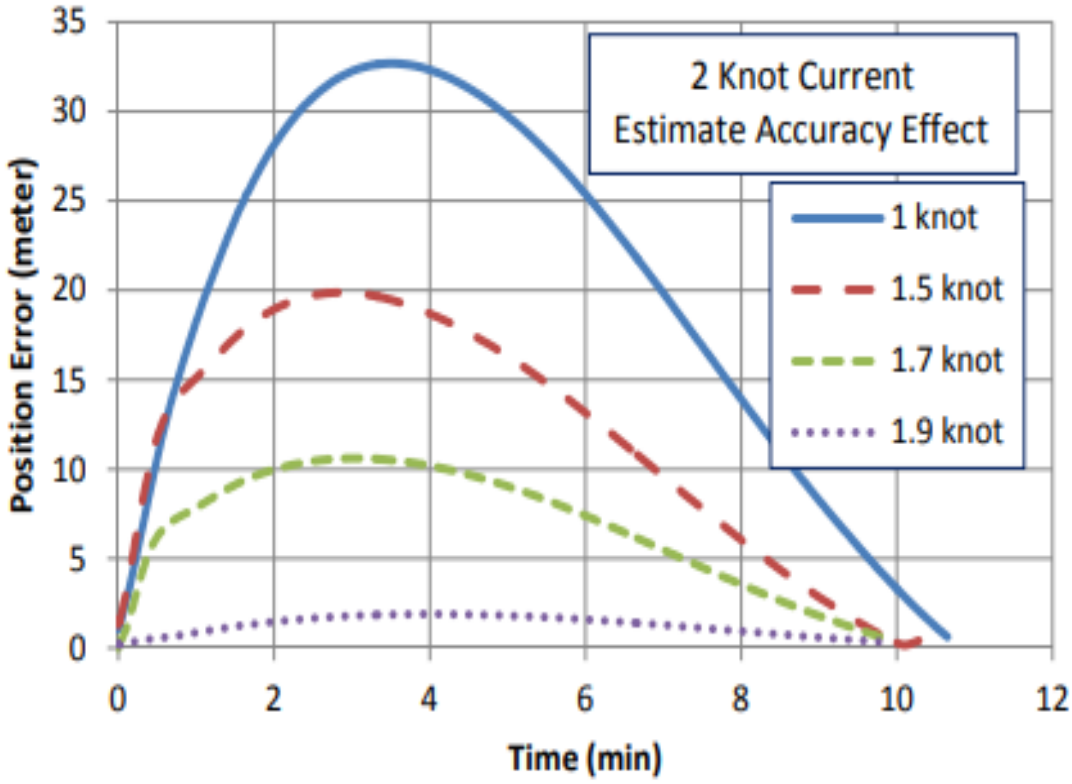

Figure 3-12 Position Deviation Vs Time (even with current compensation – Deguhee 2012)

3.4.2 The control system principal of DP system clearly re-direct us to following questions,

Q1. How is the current DP system of Jack ups taking into account Jacking Simultaneous operation?

Q2. What mathematical model DP Jack-ups vessel uses, in absence of sensors to account leg forces, while approaching and leaving the installation sites?

Q3. How variable leg speed lowering, and lifting are taken into account in hydrodynamic force calculation?

Q4. How DP system accounts, seabed effects which can affect hydrodynamic force?

Q5. How DP model building process helps to account for hydrodynamic forces of Jack ups when position, heading of the vessels remain the same till spudcan detach from the seabed?

Q6. How will thrusters align in the direction of demand thrust forces soon after spudcan detached from the seabed?

Q7. Do DP vendors know drifting distance and direction, soon after spudcan detach from the seabed?

Q8. Do DP mathematical models use an additional set of gain factors in surge, sway and yaw directions for tight position and heading controls? How do they calculate and apply?

Q9. How variable current acting on the leg at different depth level taken into accounts?

Q10. How DP jack ups vessel different leg and spudcan design accounted in DP software?

Q11. What best DP vendor can do to improve station keeping in SIMOPS operational mode?

4 EVALUATE HYDRODYNAMIC BEHAVIORS OF LEG SPUDCAN

4.1 BACKGROUND

The chapter deals with evaluating current response of the leg under various operational condition. It was noted, DP mathematical model approach may not provide accurate station keeping and leg can influence jack up vessel drag, the CFD analysis and Tank experiments carried out.

4.2 DEFINE CASES FOR EVALUATION OF HYDRODYNAMIC FORCE

The DP jack ups/lift-boats [8] has thrusters for self-propelled operation and jacking system for self-elevated functionality. The experiment and CFD cases are considered based on offshore activates and real vessel application in the offshore and renewable energy industries as shown in Figure 4-1

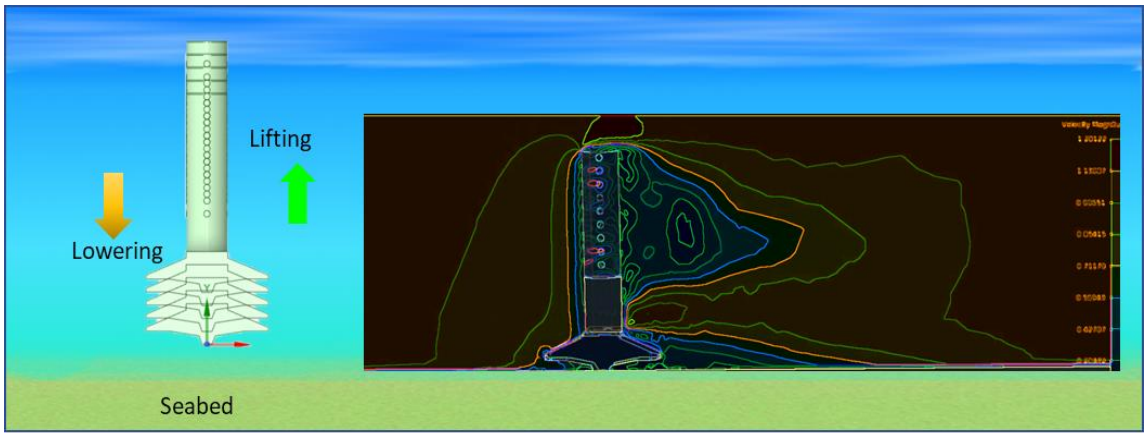

Figure 4-1 Overview of Leg spudcan movement of Jack-up vessel

To begin with hydrodynamic drag forces calculations, the author intends to find the composite body drag coefficient. There are various experiments conducted in the past to evaluate the drag coefficient and drag force of such leg designs, but they are only available in a steady state condition. To evaluate the drag force in both the steady state CFD cases as well as transient case for leg lowering and lifting conditions, first set of CFD simulation carried out. The tank experiment conducted as well to validate the results. Both the cases of drag coefficient simulated away from the seabed approximately 20 m. Since intention of study is to evaluate and compare the drag force in steady condition of leg and transit condition of leg. To start with investigate micro level impact of leg & spudcan with respect to environment under different combination of variable current and leg-spudcan speed.

The DP system designer use dynamic coefficient (Cd) [24] to compute drag forces, However, the hydrodynamic forces variation during complete process never completely considered by DP Vendors. This provides weak link in the overall operation. It should be noted that no vessel /charter is really aware about the position error which can result due to above dynamics in the real operation. The risk is left with DPO and Jack master to handle. The overall DP and jacking simultaneous operations (SIMOPS) mode could easily last from 15 min to 90 min, depending on jacking speed, operational water depth and procedures on approach to the assets. The area of operation is closed to the assets, which increases risk of collision with assets. The paper published in MTS DP Positioning by Deguhee [8] on Dynamic positioning control augmentation for jack-up vessels, shows the position deviation is quite high during heading change and also during bottom touchdown and lift off operation.

Mr. Hose [24] of Delf University has also recommended work of increased vertical drag force on the skirted spudcan, in his paper of “Analysis of Hydrodynamic coefficient of spudcan in proximity of seabed during Jack-up installation” In this research our intention is to evaluate the hydrodynamic forces behaviours on leg spudcan, operating during DP in all phased.

To proceed with research work, the author decided first to evaluate independently hydrodynamics behaviour on leg and spudcan. After reviewing the two popular leg design and its operational speed of leg lowering and lifting, its impact on hydrodynamic forces are evaluated using CFD and validated using tank model.

1) CFD simulation of cylindrical legs and lattices leg moving at a speed of 0.5 m/min,1 m/min and 2 m/min. Direction UP / DN. The reasons of selecting these leg speeds based on jacking system design for handling the leg movement in UP/DN direction.
2) Tank experimental validation of CFD Simulation.
3) CFD simulation of the seabed touchdown effect on cylindrical legs spudcan UP / DN.
4) Behaviour of spudcan top and bottom plate pressure.
5) Behaviour of lift forces.
6) Behaviour of drag forces.
7) Time domain analysis of leg UP / DN.
8) Tank experiment for validation for touch down cases.

In total, 42 CFD cases were studied to identify, how is the behaviour of hydrodynamic force, when the leg spudcan is moving downwards towards seabed and moving upward (lifting off)

from seabed and steady state case. Placement of jack up condition and removing spudcan results showed different behaviour.

4.3 CHARACTERSITCS

In order to capture the behaviour of the forces on the jack up leg, the author decided to study the complex physics in computational fluid dynamics (CFD) on leg and spud can geometry cylindrical and lattice types of legs. Firstly, CFD evaluations completed on cylindrical legs, followed by prototype tank experiment to validate the results. Once, the validation process completed. A full scale CFD model simulation carried out both on cylindrical leg model and later lattices leg model. The first two steps are mainly for validation purpose as both CFD, and tank testing results harmonize each other. In total 42 test cases were studied during the tank experiments.

The CFD simulations were also done for a small piece of rack and chord type lattices legs-spudcan. The purpose of this analysis is to find out the behaviour of the hydrodynamic force in both up and down direction. As CFD results shows peculiar behaviour, when operating near seabed. Also, this moment is critical during DP station keeping for jack up DP vessel. The seabed bottom effect is also analysed in CFD and validated using tank experiments.

4.4 CFD ANALYSIS SETUP FOR CASES ABOVE SEABED (>10M)

4.4.1 Geometry Modelling

The 3D geometry of the prototype model is constructed using space claim design modular Ansys software for design. Due to file size limitation in the software, it is decided to build a model with similar shape of leg and spudcan but small in length as shown in Figure 4-2. The full scale CFD model has a scale factor of 27 times. The 3D prototype model is made for cylindrical leg with holes for jacking hydraulic pin. The leg diameter is approximately 165 mm, leg length 808 mm with top plate sealed and sealed spud can. The holes of 25mm diameter at 90 degrees around 360 degrees made for hydraulic pin and placed at an interval of 75mm.

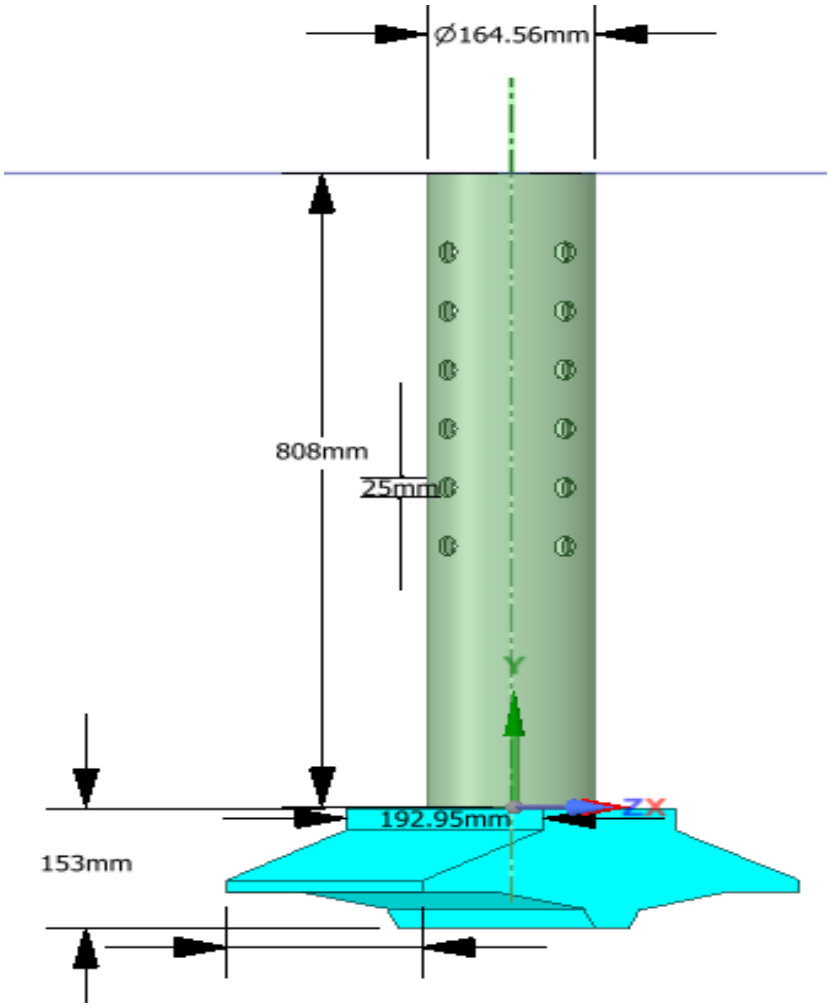

Figure 4-2 Leg-Spudcan 3D prototype model

4.5 CFD DOMAIN

The computational domain was made large in order to overcome any wall boundary effects. The current applied on leg & spud can from one direction is as shown in Figure 4-3 and velocity (current) of fluid for different simulation cases varies among 0.5/1/1.75/2 knots respectively. The reasons for selecting sea current are based on jack up operating area reported seabed current. The jack up operates in shallow water and some of them in shelter areas. No pressure gradient is considered at the outlet. There are mainly two types of walls defined in CFD model one for sides, top and bottom with no slips and one exclusively for leg-spudcan composite body. The leg-spudcan wall was considered to move up/down at a speed of 0.5m/min, 1 m/min and 2 m/min for each simulation case. The reasons for selecting these leg speeds are based on jacking system design for handling the leg movement in UP/DN direction. The leg wall

surface is considered smooth to avoid any corrosion effects. The effect of corrosion also studies to see an increase in drag coefficient based on uniform marine growth.

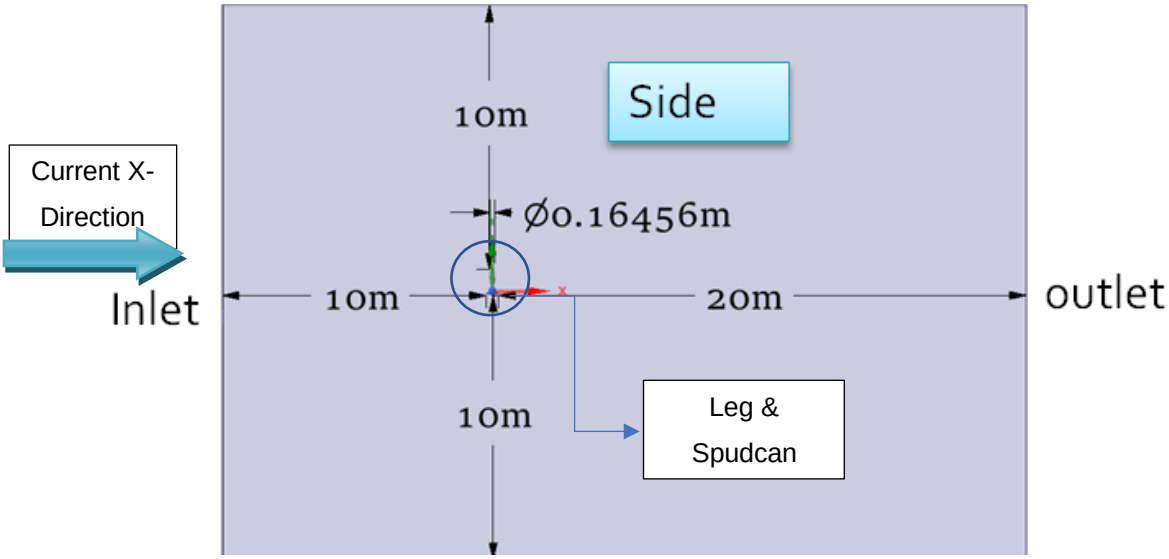

Figure 4-3 CFD simulation domain side view

4.6 MESHING

The polyhedral mesh for the CFD model is presented in Figure 4-4. The advantages of the polyhedral mesh over other mesh types, they used less computing power, less elements and fast convergence. The number of cells of unstructured polyhedral meshing counted to 256880 and nodes 573030 creating fine mesh around holes, legs, and simulation domains.

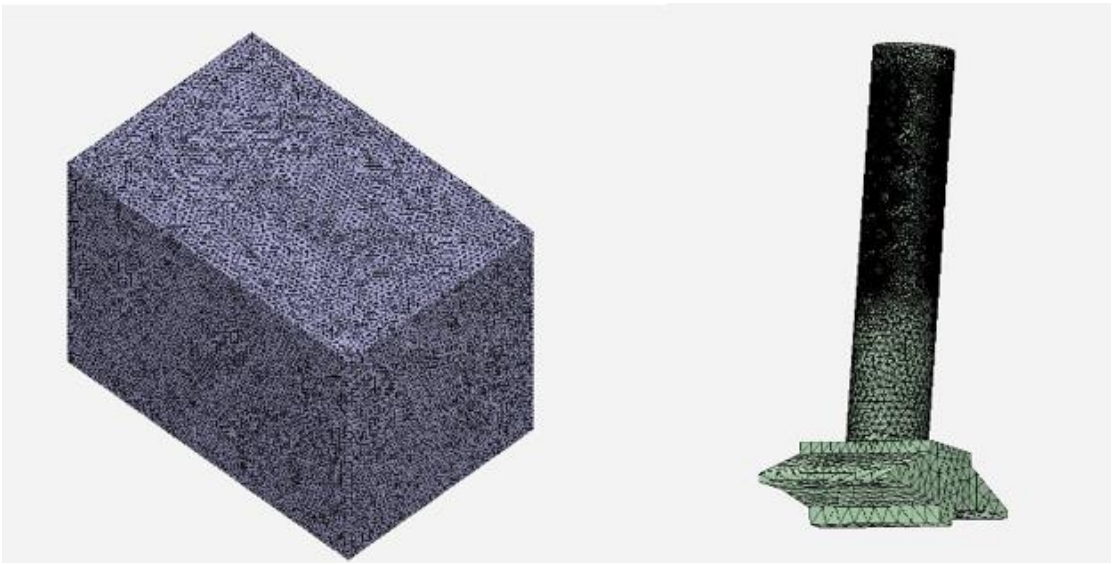

Figure 4-4 Polyhedral meshing of CFD model

4.7 PHYSICS SOLVER

The CFD calculations are performed in fresh water, to assess the same domain with respect to density and viscosity as for the tank experiments. Since the spudcan is submerged for all phases, the buoyancy effect neglected during the CFD analysis. The standard Menter [46] k-ω SST turbulence model is applied that uses two differential equations, which serve as a closure for the Reynolds-Averaged Navier-stokes equations (RANS). The first equation (Eq. 4-1) represents turbulence kinetic energy (k) whereas the second equation (Eq. 4-2) represents frequency dissipation.

$$\frac{\delta(\rho k)}{\delta t} + \frac{\delta(\rho \mu_j k)}{\delta x_j} = P_k - \beta^* \rho \omega k + \frac{\delta}{\delta x_j}\left[\left(\mu + \frac{\mu_t}{\sigma_k}\right)\frac{\delta k}{\delta x_j}\right] \quad \text{(Eq. 4-1)}$$

$$\frac{\partial(\rho\omega)}{\partial t} + \frac{\partial(\rho u_j \omega)}{\partial x_j} = \frac{\gamma_1}{v_t} P_\omega - \beta_1 \rho \omega^2 + \frac{\partial}{\partial x_j}\left[\left(\mu + \frac{\mu_t}{\sigma_\omega}\right)\frac{\partial \omega}{\partial x_j}\right] + 2(1 - F_i)\frac{\rho \sigma_{\omega 2}}{\omega}\frac{\delta k}{\delta x_j}\frac{\delta \omega}{\delta x_j} \quad \text{(Eq. 4-2)}$$

Where as

$k =$ represent turbulent kinetic energy

$\mu_t = eddy\ viscosity$

$\frac{\delta(\rho k)}{\delta t} =$ represents rate of change of k

$\frac{\delta(\rho \mu_j k)}{\delta x_j} =$ represent transport of $k\ by\ convection$

$P_k =$ represent rate of production of k

$\beta^* \rho \omega k =$ represent rate of dissipation of k

$\frac{\delta}{\delta x_j}\left[(\mu + \rho_k \mu_t)\frac{\delta k}{\delta x_j}\right] =$ represent transport of k by turbulent diffusion

$\omega =$ represent turbulance frequency

$\frac{\partial(\rho\omega)}{\partial t} =$ represents rate of change of turbulance frequency ω

$\frac{\delta(\rho \mu_j \omega)}{\delta x_j} =$ represent transport of $\omega\ by\ convection.$

$\frac{\gamma}{v_t} P_\omega =$ represent rate of production of ω

$\beta_1 \rho \omega^2 =$ represent rate of dissipation of ω

$\frac{\delta}{\delta x_j}\left[(\mu + \rho_\omega \mu_t)\frac{\delta \omega}{\delta x_j}\right] =$ represent transport of ω by turbulent diffusion

$2(1 - F_i)\frac{\rho \sigma_{\omega 2}}{\omega}\frac{\delta k}{\delta x_j}\frac{\delta \omega}{\delta x_j} =$ represent cross diffusion between k and ω

Model constants

$\sigma_k = \sigma_\omega = 2.0,\ \gamma 1 = 0.553\ \beta_1 = 0.075, \beta^* = 0.09$

4.8 TURBULENCE MODEL

The k-ω SST turbulence model provides an accurate representation of the near wall boundary region and is preferred when high accuracy is required for a wide range of Reynolds numbers. The steady state evaluation of the two equation RANS turbulence model for high Reynolds number in a hydrodynamic flow uses the k-ω SST turbulence model for incompressible flow around a large cylinder. The k-ω SST turbulence model has been proven to be effective by Ghezelbashan and D'Mello (2018) [20] for turbulence calculations, and by Andries et. al (2017) [1] for the calculation of the hydrodynamic forces on jack-up legs. One of the advantages of the k-ω formulation is the near wall treatment for low-Reynolds number computations where the model is more accurate and more robust. The k- ω based SST model accounts for the transport of the turbulent shear stress and gives highly accurate predictions of the onset and the amount of flow separation under adverse pressure gradients.

4.9 CONVERGENCE

The analysis is performed by changing the mesh fidelity in Ansys AIM. In total 5,000 iterations have been performed. As shown in Figure 4-5, the typical convergence criterion of E-0.5 could not be satisfied for residual velocities. However, a convergence criterion of E-0.3 is achieve. This convergence issue for CFD simulations performed on jack-up legs is also reported by Andries *et al* (2017) [1]. The reason why the residual velocity convergence criterion is not satisfied due to leg and spudcan disturb the steady flow and create turbulence.

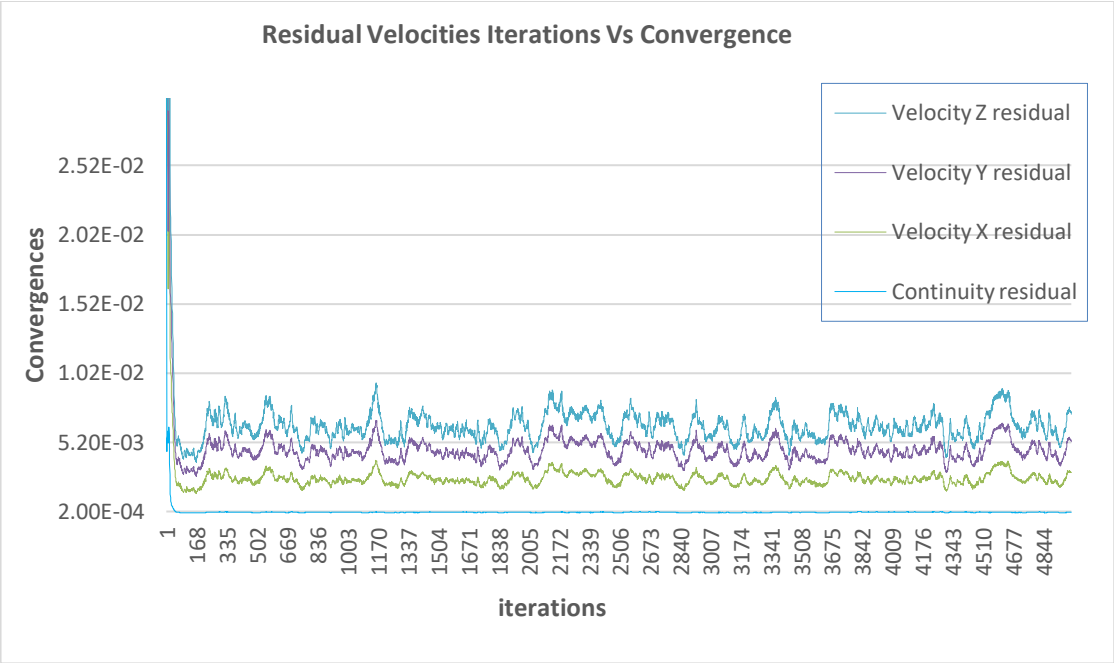

Figure 4-5 Iteration convergence problem of Model CFD results

The flow turbulence also affects the drag force (Fx) in X-direction and vertical forces (Fy). Three convergence cases are studied on the CFD model, representing the cases used during the tank experiments for validation. The CFD analysis is perform for the case with 2 knots of current acting on the leg and spudcan in the x direction. For the tank experiments, the projected area of the leg and spudcan model is 0.1768m2 in the direction of acting flow. The CFD results obtained for mesh convergence are shown in Table 4-1. The case one shows the lowest mesh fidelity, while case three shows the highest mesh fidelity setup. The second case shows middle fidelity results. The drag forces (Fx) for all three cases are very close to each other. These results are also validated using the empirical formula of drag forces shown below in (Eq. 4-3)

$$Drag\ Force\ (F_x) = \frac{1}{2} C_d \rho v_c^2 A \qquad \text{(Eq. 4-3)}$$

Whereas:

Cd – Drag Coefficient -

Density of water (ρ) - 997.05 kg/m^3

Current (v_c)– 1.0289 m/s

Projected area (A) – 0.1768 m^2

The CFD drag forces calculated for the model leg and spudcan in varying mesh fidelity are compared with this empirical figure in Table 4-1

Table 4-1 Mesh Fidelity effect on Drag Force Vs Calculated Results using Formula

Fidelity No.	Mesh Nodes	Mesh Elements	Fx (N)	% Error Force for model
1	86811	307307	62.4	3.1%
2	120756	428932	61.5	4.6%
3	181060	427049	60.4	6.5%

The Cd values also measured in the CFD analysis and noted as 0.6891. The drag forces calculated using equation (Eq. 4-3) as **64.3N**. Based on the above results mesh size (2) is expected to bring optimize results and for this reason chosen for the CFD calculations here.

4.10 TANK TESTING FOR LEGSPUDCAN ABOVE SEABED (>20M)

The experiments were performed to investigate the steady state condition behaviour of drag force on leg-spudcan at Kyushu University as shown in Figure 4-6. The tank dimension is 38.8m long, 24.4m wide and 2.0 m deep. Since, the depth of the basin is quite small, the leg-spudcan model is mounted differently. The facility has computerized planar motion carriage (CPMC) which can move in x-y direction.

Figure 4-6 Launch of experiment model

4.11 EXPERIMENTAL METHODOLOGY

In order to study the effect of the lowering of the leg-spudcan, as occurs in the CFD analyses, the computerize motion carriage X-Y movement is used. The experimental setup for each case is computed by considering current (m/s) on X axis and Leg-spudcan velocity (m/s) on a Y-axis as shown in Figure 4-7 below

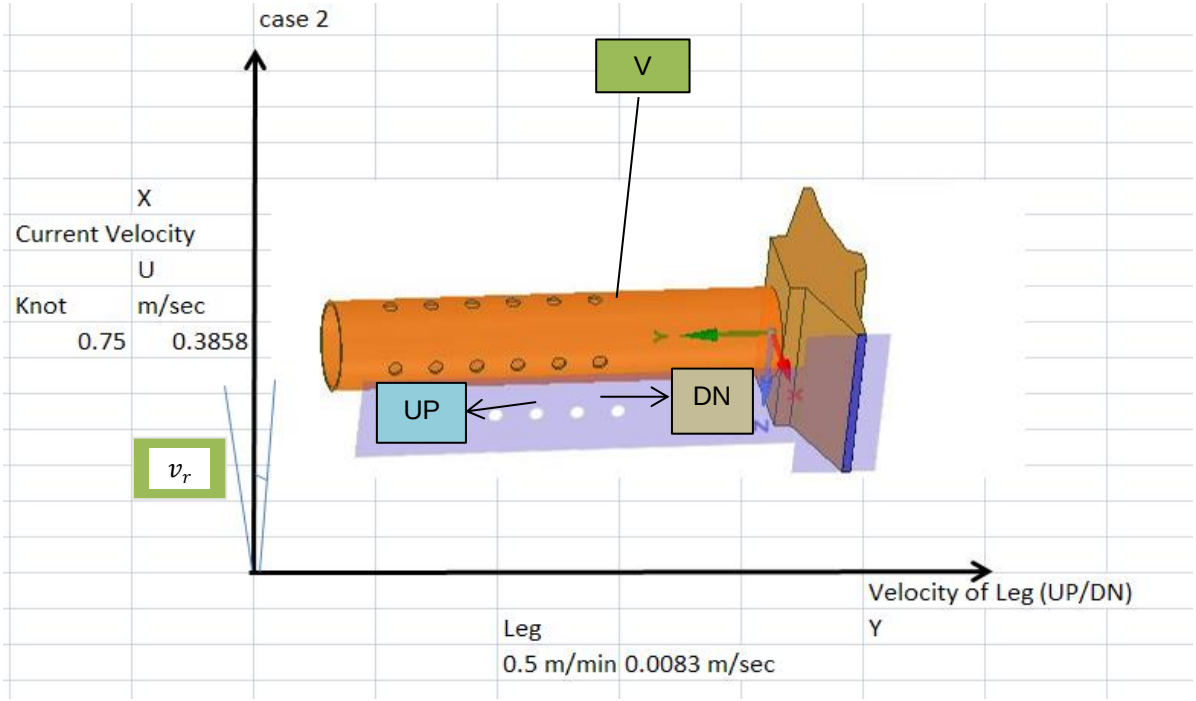

Figure 4-7 Planview of X-Y plane for CPMC input computation

The resultant velocity is calculated for CPMC as shown in Figure 4-8 using the following simple equation (Eq. 4-4).

$$\text{Resultant Velocity } (v_r) = \sqrt{U^2 + V^2} \quad \text{(Eq. 4-4)}$$

Whereas U = Current (m/sec) and V= (Leg Speed)

Similarly resultant angle is calculated provided to the CPMC as shown in Figure 4-8 using the following simple equation (Eq. 4-5).

$$Resultant\ angle\ (\emptyset\ in\ Deg) = \tan^{-1}\left(\frac{V}{U}\right) \times \frac{180}{\pi} + offset\ if any \quad \text{(Eq. 4-5)}$$

Figure 4-8 CPCM Control Room

Once the resultant velocity and angle input are entered to the CPMC, carriage moves, and the load cells start to measure the drag force (Fx) and transverse force (Fy). The shows the measurement graph of load cell with respect to time.

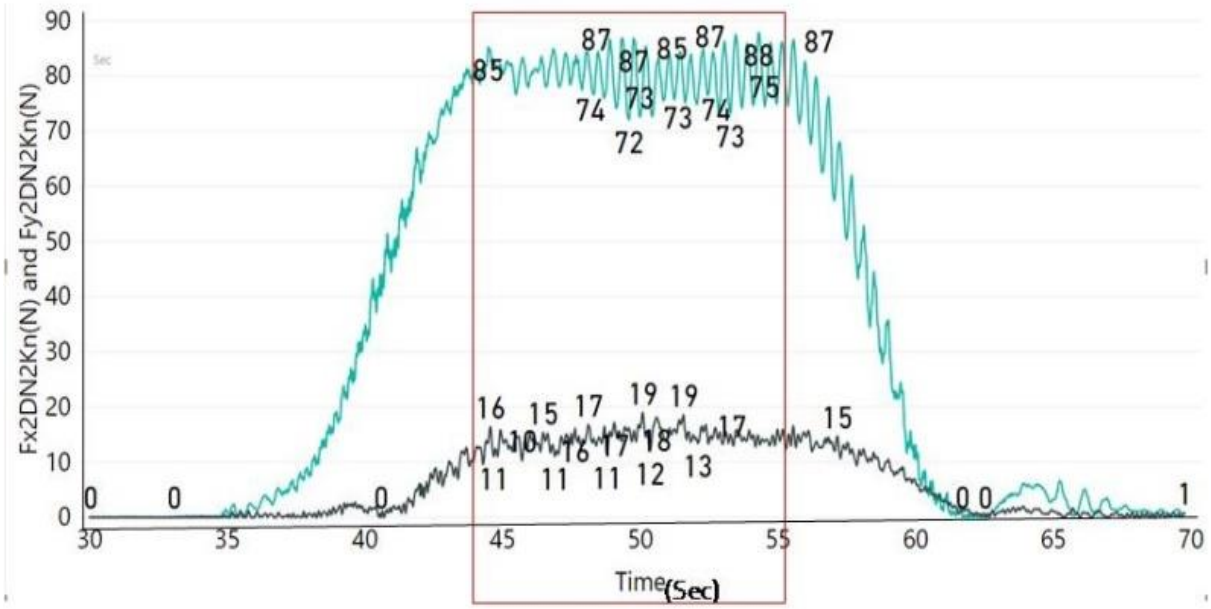

Figure 4-9 Load cell measurement for Case 42

Since the carriage require sometime to reach the steady state speed, the average results of hydrodynamic forces are calculated by averaging over a period of steady state as marked in Figure 4-9. The non-steady Fx and Fy can also be observed in Figure 4-10 below,

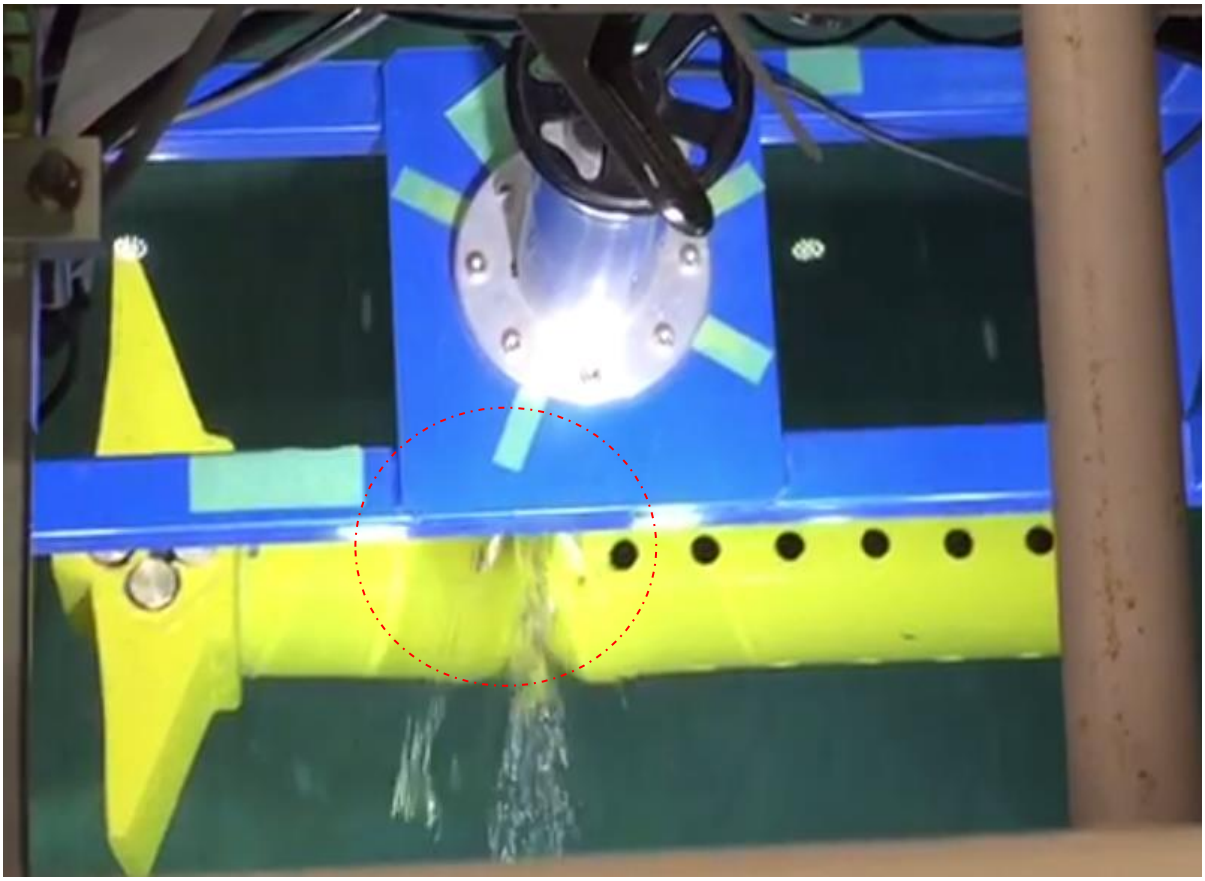

Figure 4-10 Turbulence Flow around leg during tank testing

4.12 DETAILS OF TEST CASES FOR LEG-SPUDCAN ABOVE SEABED (>10M)

In total 42 cases were studied during the tank experiment. Different current velocity and leg speed are studied for all cases. In the remainder, the leg speed will be indicated as + ve and -ve signed for DN and UP direction respectively. Table 4-2 shows the combination of current and leg speed.

Table 4-2 Experimental cases matrix

Case No.	Leg Speed (m/min)	Current (knot)	Direction
1.	0	1	steady

Case No.	Leg Speed (m/min)	Current (knot)	Direction
2.	-0.5	1	up
3.	0.5	1	down
4.	-1	1	up
5.	1	1	down
6.	-2	1	up
7.	2	1	down
8.	0	1.25	steady
9.	-0.5	1.25	up
10.	0.5	1.25	down
11.	-1	1.25	up
12.	1	1.25	down
13.	-2	1.25	up
14.	2	1.25	down
15.	0	0.5	steady
16.	-0.5	0.5	up
17.	0.5	0.5	down
18.	-1	0.5	up
19.	1	0.5	down

Case No.	Leg Speed (m/min)	Current (knot)	Direction
20.	-2	0.5	up
21.	2	0.5	down
22.	0	1.5	steady
23.	-0.5	1.5	up
24.	0.5	1.5	down
25.	-1	1.5	up
26.	1	1.5	down
27.	-2	1.5	up
28.	2	1.5	down
29.	0	1.75	steady
30.	-0.5	1.75	up
31.	0.5	1.75	down
32.	-1	1.75	up
33.	1	1.75	down
34.	-2	1.75	up
35.	2	1.75	down
36.	0	2	steady
37.	-0.5	2	up

Case No.	Leg Speed (m/min)	Current (knot)	Direction
38.	0.5	2	down
39.	-1	2	up
40.	1	2	down
41.	-2	2	up
42.	2	2	down

4.13 RESULTS OF CFD AND TANK EXPERIMENTS WHEN LEG ABOVE >20M FROM SEABED

The convergence issue is known in any CFD software. The fluid physics (i.e. mechanic) is always complex area due to its nonlinear behaviour. The CFD results shows promising real-world operations. One of the major validation techniques followed in CFD is convergence. The fine mesh always helps in achieving convergence of the range 1E-05. During our CFD analysis, we struggled to achieve the convergence of range 1E-05 but 1E-03 is achieved. Different CFD software were tried to see if this convergence issues are due to student version or something else. The commercial software was used to check the convergence issue. However, it was concluded from the results the convergence of 1E-05 not achievable even in commercial CFD software. It was then decided to continue the CFD simulation in Ansys AIM CFD software. During the CFD analysis, the author observed vortex around leg. The oscillation forces may be due to fluids passing through the holes. This was also observed during the tank experiment from the load cell reading. In short, both CFD and tank experiment results were complementing each other. One of the possible reasons of non-steadiness in drag and transverse forces (Fx & Fy) could be these vortex as shown in Figure 4-11 and Figure 4-12 vortices causing vibration preventing convergence to 1E-05 but 1E-03 is achieved. In the fluid dynamics a vortex is a region in a fluid in which the flow revolves around an axis line, which may be curved. The stirred fluid will disturb the fluid acting on the leg spudcan. In our case, since the current acting on the leg from X-axis, the vortices formed induces vibration on the leg structure. The vibration then disturbs the fluid flow and main reason for convergence issue.

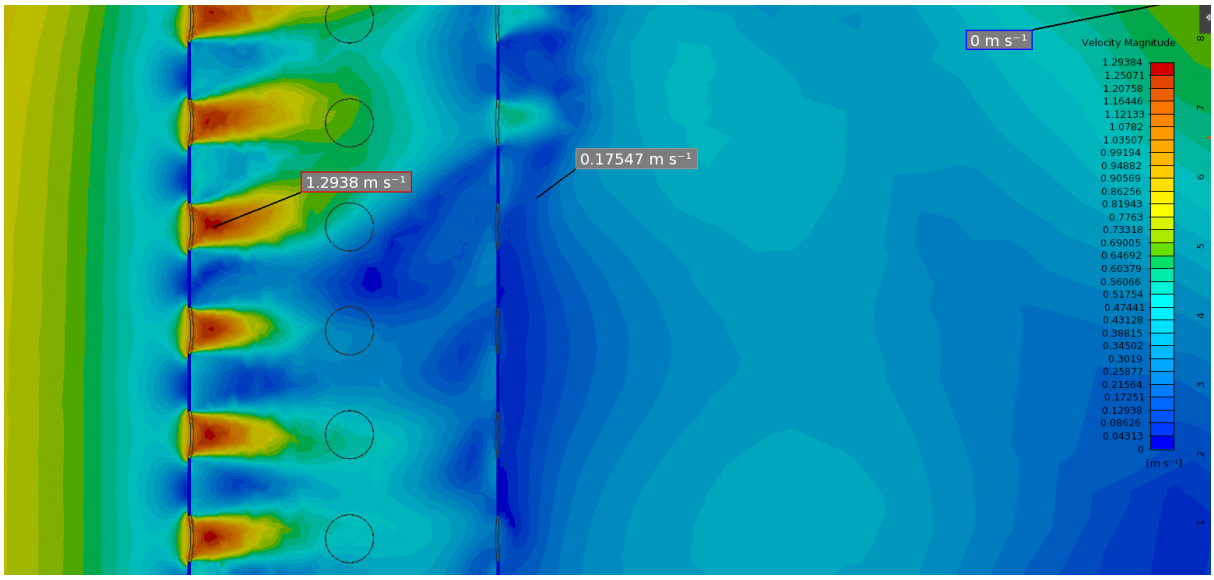

Figure 4-11 Vortices around the leg front view

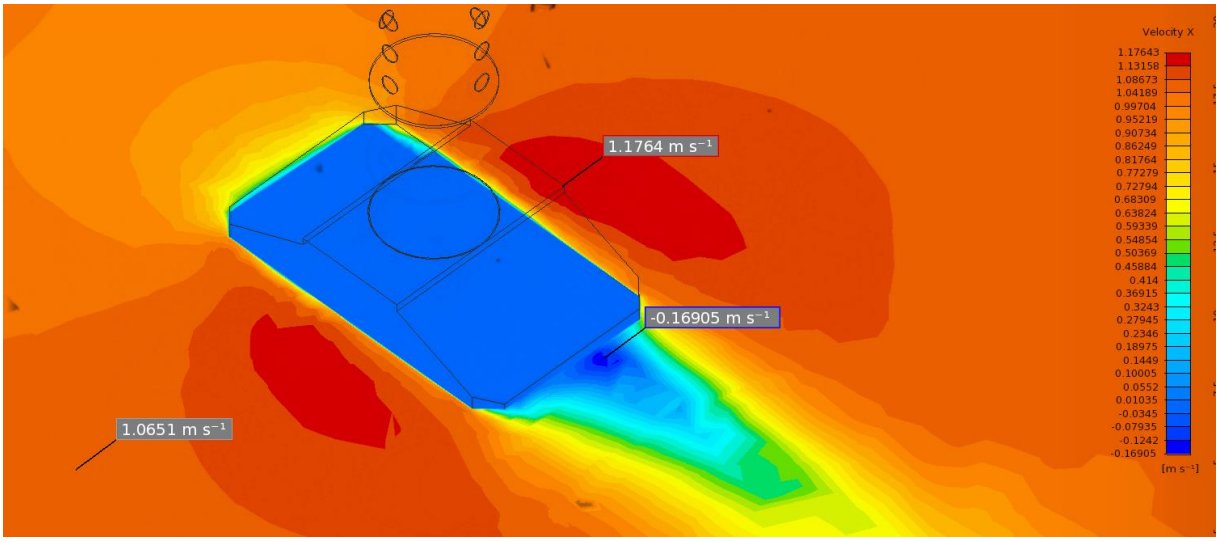

Figure 4-12 Velocity profile showing Vortex for Case 42

The CFD streamline clearly shows in Figure 4-13, the flow of the fluid particles which are responsible of vortex creation. The vortex velocity responsible for the vibration on the leg spud assembly.

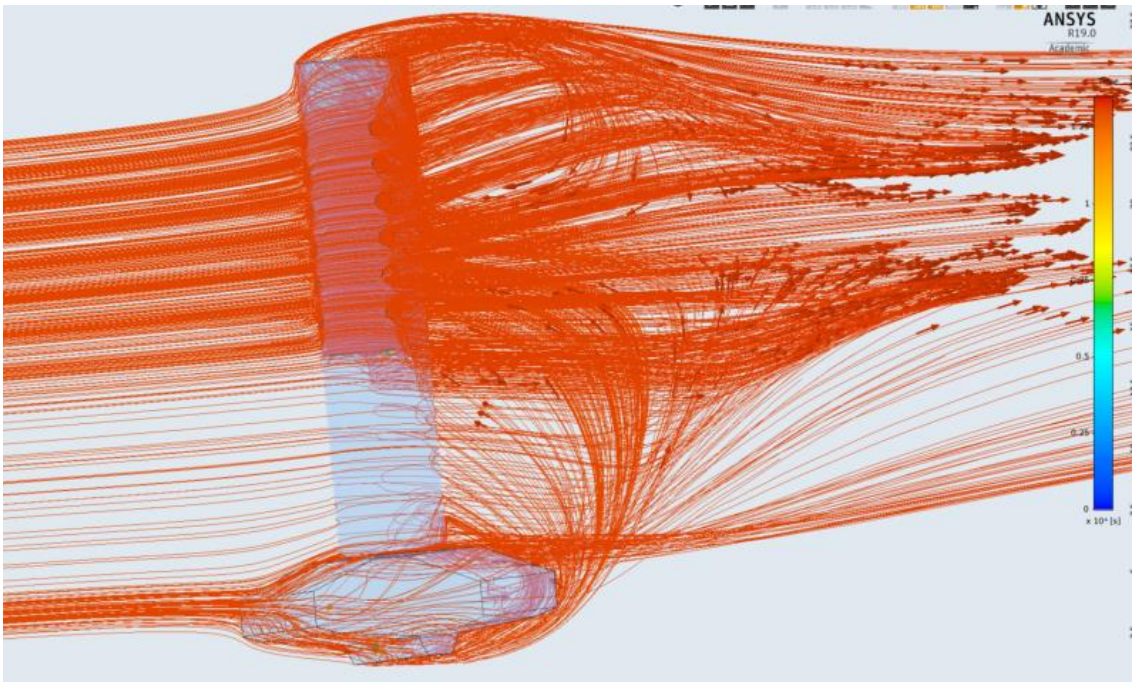

Figure 4-13 Velocity streamline interaction

4.14 DRAG FORCES FX (N) RESPONSE FOR LEG LOWERING & LIFTING CASES

The CFD setup for leg is moving direction indicated by arrow for downward and upward movement in Figure 4-14 and Figure 4-15 respectively.

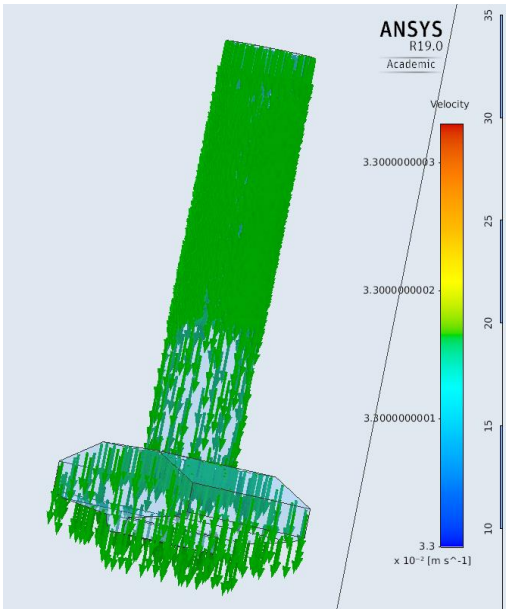

Figure 4-14 Leg lowering down

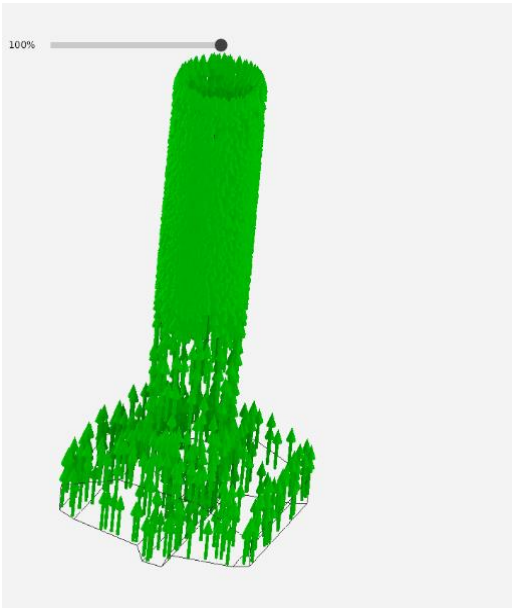

Figure 4-15 Leg lifting up

The hydrodynamic drag forces acting on the composite leg-spudcan are measured for various current and leg speed case. As current increases the drag force acting on leg-spudcan increase, however change in leg speed from 0.5 m/min to 2 m/min does not have any impact on drag Fx force for cases not in closed vicinity of the seabed. It is also noted that up and down leg movement does not have any impact on drag forces. The results obtained in the CFD are shown below in Figure 4-16. clearly shows the leg lowering and lifting speed do not really affect drag force. However, it must be noted these values are simulated at a distance (>)10~15 m above from the seabed.

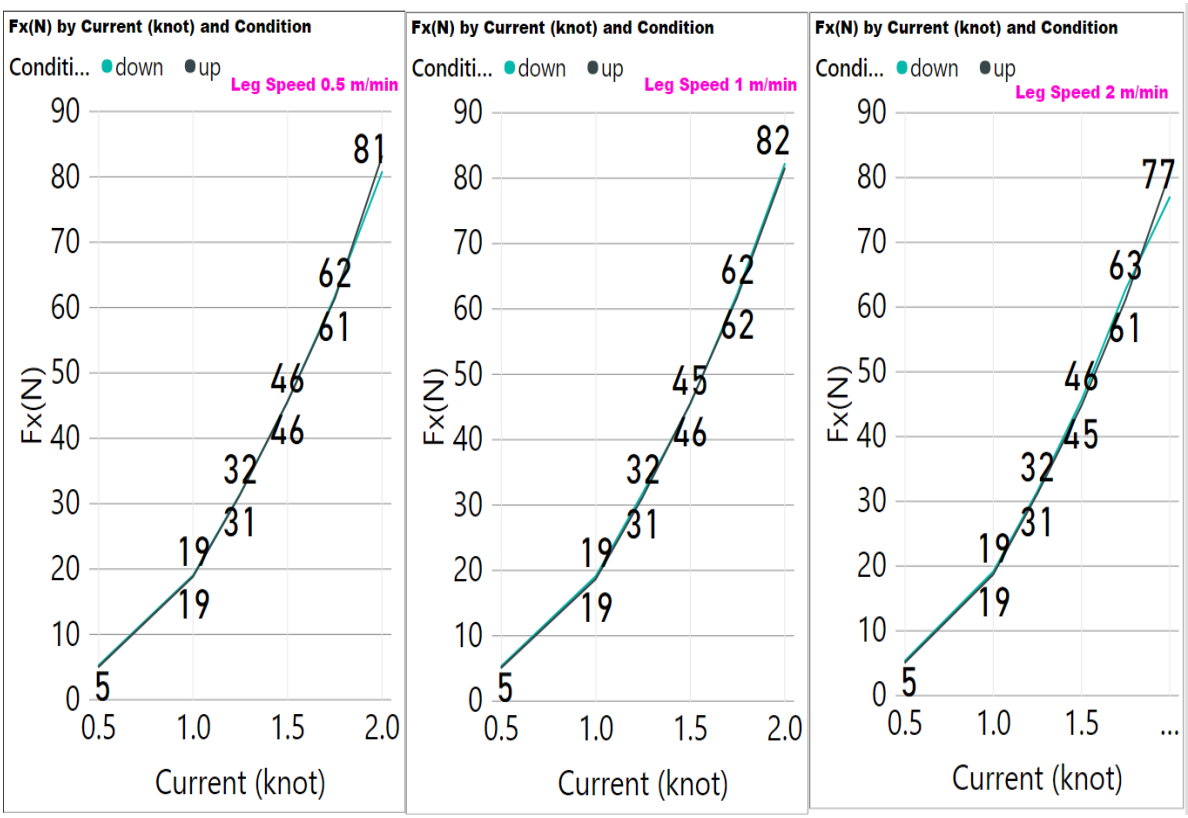

Figure 4-16 Drag forces Fx (N) for UP and DN response

The above results help us to conclude, the jacking speed which is relatively very slow (0.5 – 2 m/min), when compared to the environmental current of 0.5 knot (15 m/min) to 2.0 knots (60 m/min) do not really matters. Although a very slight difference was observed among drag forces values when leg and spudcan evaluate for lowering and lifting operations. However, these results do not show seabed effects. They are verified at later stage and indicated in the section 4.16.

4.15 LIFT FORCES FY (N) RESPONSE FOR LOWERING & LIFTING CASES

The hydrodynamic lift force measurements acting on the composite leg-spudcan are measured for various current and leg speed cases. The result shown below in Figure 4-17 indicates as the current increases the force acting on leg-spudcan also increase. The change in leg speed from 0.5 m/min to 2 m/min clearly shows impact on forces. It is also noted that lift forces Fy(N) are higher when lowering the leg then the lift forces measured in when the leg is moving in up direction. It is also seen that as the leg speed increases the difference of forces from up to down also increases.

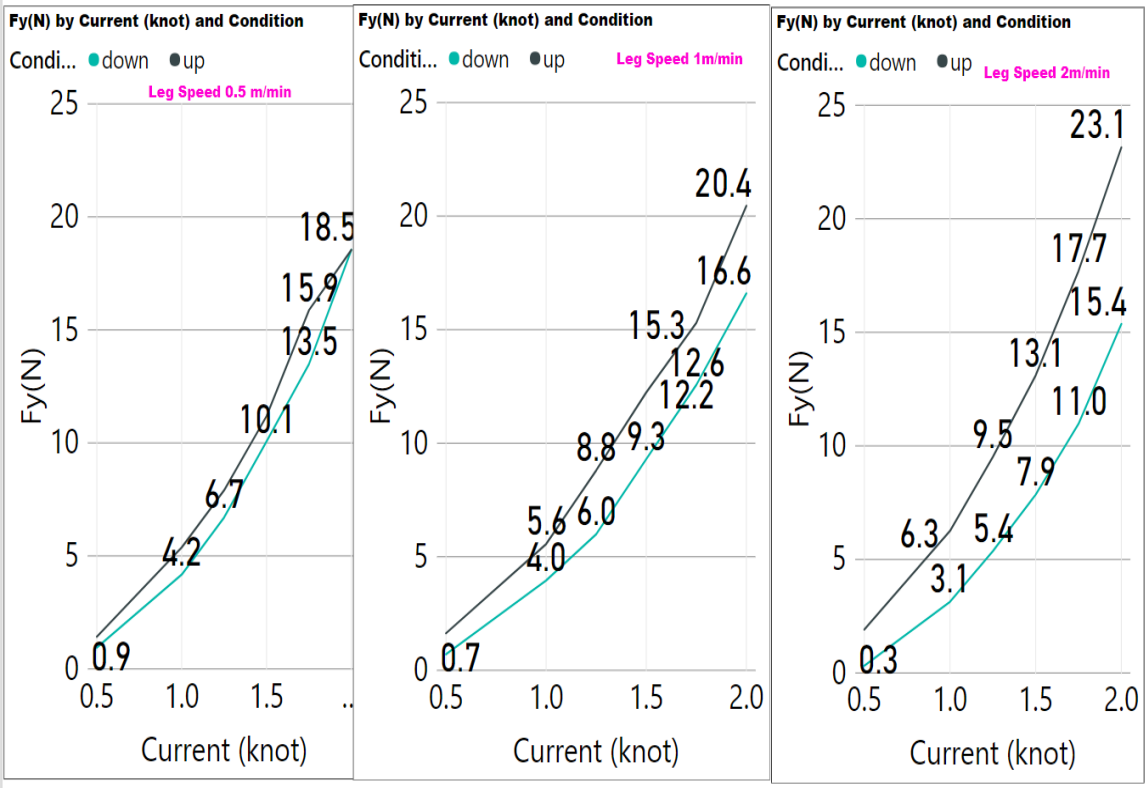

Figure 4-17 Life forces Fy (N) for UP and DN response

The absolute lift forces (Fy) influence in up and down direction of leg-spud can be seen in Figure 4-18. The plot is calculated by summing force for UP and DN cases which have same environmental current and leg speed for instance, in case of a 2knots current and 2m/min leg speed, the force of the upward motion, Fy=23.1363N, (case 42) is added to the force of the downward motion, Fy=15.3640N (case 41). This results to a total force of 38.5003N which will refer to the 100% force for this case of current and leg speed. The individual force Fy for UP or DN motion is compared with the aforementioned total force in order to calculate the relevant percentage weightage.

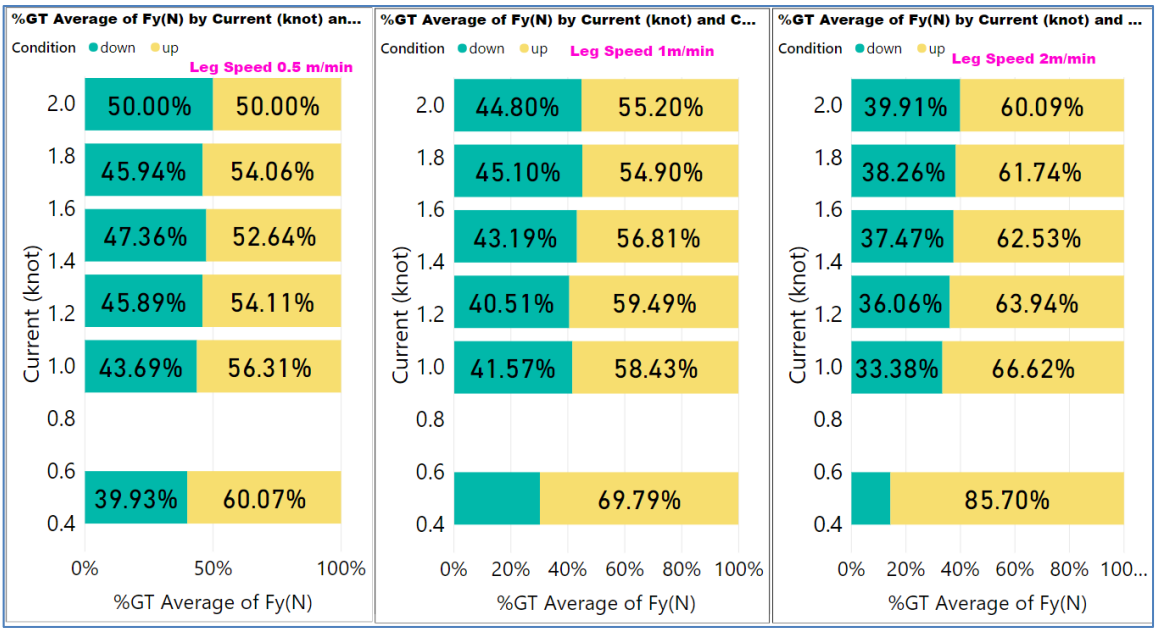

Figure 4-18 Lift Forces Fy weightage for UP and DN cases

The difference of lift forces increases as the leg speed increases and current decreases. The highest difference is observed for a current of 0.5 knot and when the leg is moving at 2 m/min. This force variation could play an important role in tuning the DP mathematical model for DP jack-up vessels, which currently operates without any hydrodynamic force measurement of leg and spudcan. The CFD and experiment results of drag force Fx are compared and tabulated below. The highest differential error between CFD and experimental results found in case 41 (i.e., 2kt, 2m/min) UP direction and it is approximately 18.42%.

The trend of hydrodynamic forces for CFD and tank experiment is similar as shown in Figure 4-19 and Figure 4-20 respectively. The CFD results difference in transverse forces Fx in up / down direction leg motions, does ensue closely between CFD and tank experiment and shown below in Table 4-3 Comparison of experimental and CFD results

Table 4-3 Comparison of CFD and Tank Experiment Results

Current (Knot)	Leg Speed (m/min)	Leg moving Direction	CFD Fx Force (N)	Experiment Results Fx (N)	Error Fx
0.5	0.5	UP	4.4367	5.069	12.47%
0.5	0.5	DN	4.4441	5.279	15.82%

Current (Knot)	Leg Speed (m/min)	Leg moving Direction	CFD Fx Force (N)	Experiment Results Fx (N)	Error Fx
1	1	UP	16.987	18.681	9.07%
1	1	DN	17.118	19.129	10.51%
1	2	UP	16.94	18.7399	9.60%
1	2	DN	17.1470	19.1567	10.49%
1.75	0.5	UP	51.438	61.358	16.17%
1.75	0.5	DN	51.103	61.741	17.23%
2	2	UP	65.823	80.681	18.42%
2	2	DN	65.882	76.945	14.38%

It is evident from the characteristics both CFD and tank experiment results follow each other. The conclusion can be drawn from both tank and CFD analysis the validation process works.

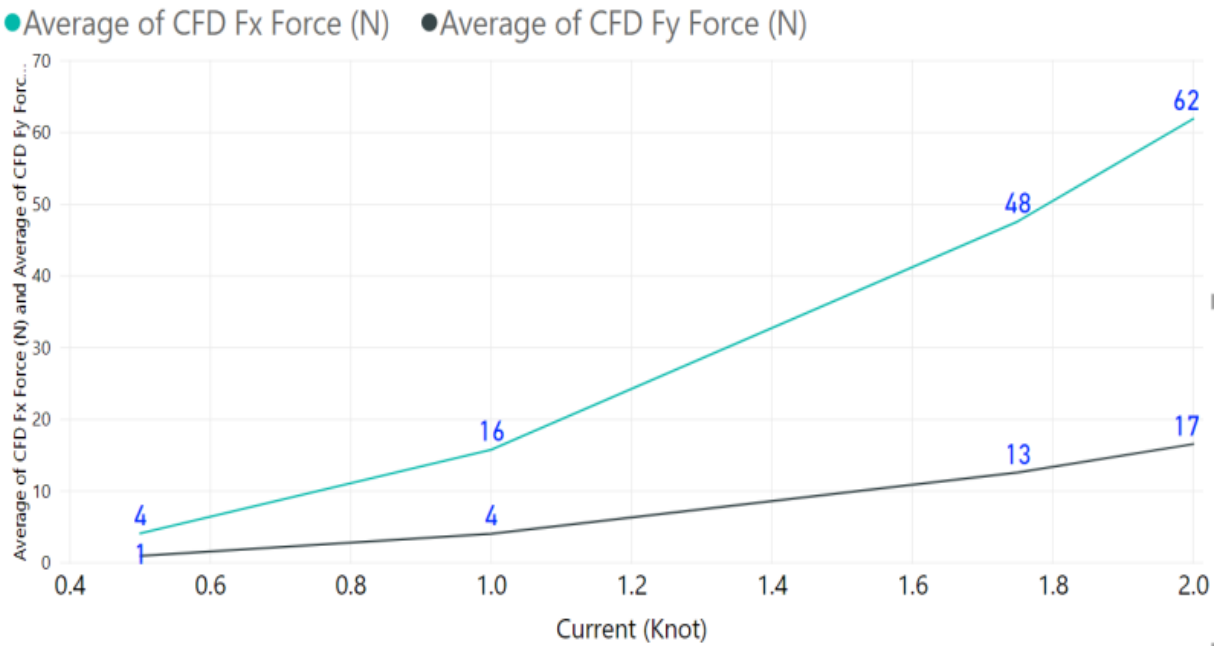

Figure 4-19 CFD force for hydrodynamics Fx(N) &Fy(N) forces

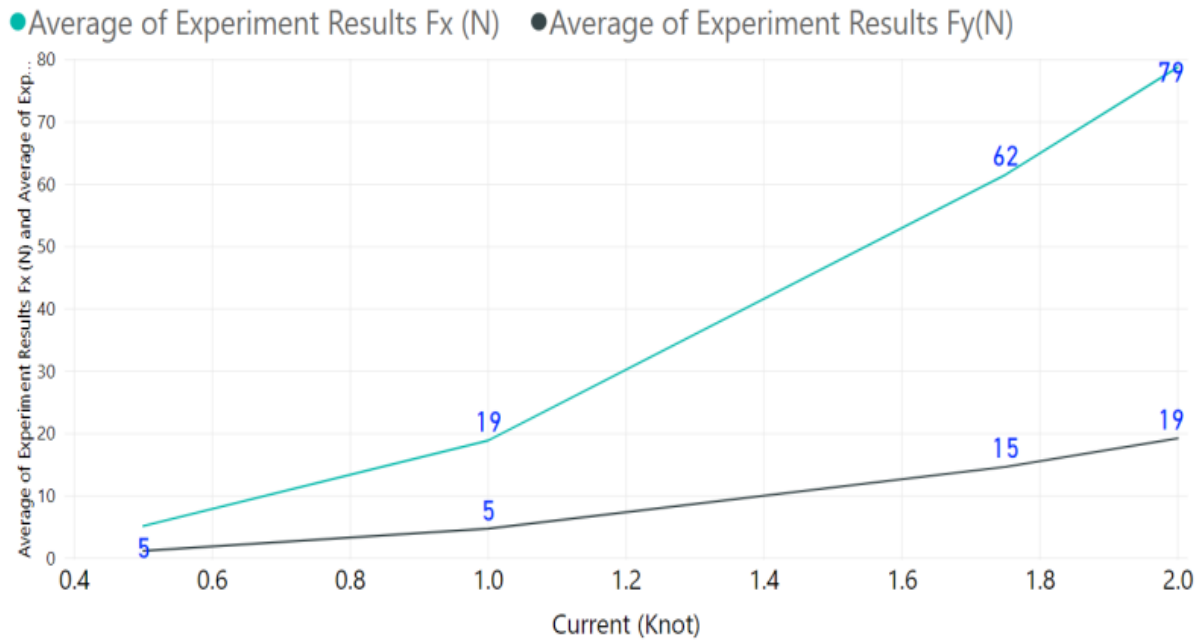

Figure 4-20 Experimental force for hydrodynamics Fx(N) &Fy(N) forces

The CFD analysis also carried out on full scale model having leg diameter of approximately 4.4m. The results shown in Figure 4-21 confirm similar trends between the tank model experiment and the small scale CFD.

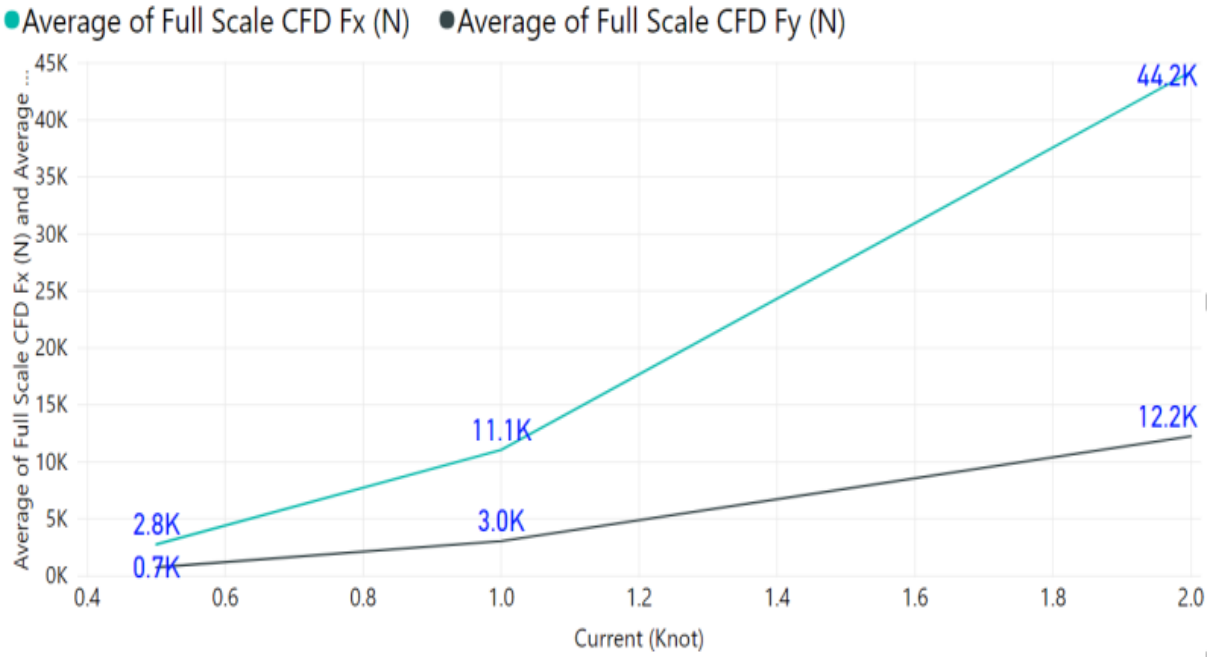

Figure 4-21 Full scale CFD for hydrodynamics Fx(N) &Fy(N) forces

4.16 BOTTOM EFFECT ON HYDRODYNAMIC FORCES OF CYLINDRICAL LEG

In order to see the effect of seabed vicinity on the drag and lift force during touchdown and lift off operational condition for DP jack-up vessels, it was decided to carry out both CFD and tank experiment. The focus area in the range of ½ diameter of spudcan from seabed.

To simulate the effect of seabed bottom on the leg-spudcan, the full scale CFD model domain was modified. The leg-spudcan lowermost position adjusted for following cases above the seabed.

The simulation cases near seabed are selected to find the impact on the drag forces and vessel moments due to seabed vicinity of spudcan (e.g., 50, 1000, 1500,1800,2000, 2200 mm etc). In fact, half of the spudcan diameter from the seabed has been reported to be causing large positional and heading deviations, which can jeopardize the critical offshore operations. Both jacking and DP system remains operational during jack-up installation for work and when leaving the location after the work. The water displacement below the spudcan near to seabed can impact the hydrodynamic forces of DP jack-ups vessels and author is aiming through our study to narrow down the research area on what is causing the positional and heading deviation. One of our aims, is to provide experimental and CFD results to maker of DP system to aware them about forces responses when closed to seabed to improve the station, keeping performance of the DP jack-ups.

The load cases for closed seabed vicinity CFD calculations performed are shown in Table 4-4. These are also validated using tank experiment.

Table 4-4 Closed to seabed simulation case setup

Case	Leg Moving Direction	Current (knot)	Leg Speed (m/min)	Distance from seabed (mm)
Steady State Cases				
1.	Static	2	0	50
2.	Static	2	0	1000
3.	Static	2	0	1500
4.	Static	2	0	1800
5.	Static	2	0	2000

Case	Leg Moving Direction	Current (knot)	Leg Speed (m/min)	Distance from seabed (mm)
6.	Static	2	0	2200
7.	Static	2	0	3000
8.	Static	2	0	5000
9.	Static	1	0	50
10.	Static	1	0	1000
11.	Static	1	0	1500
12.	Static	1	0	1800
13.	Static	1	0	2000
14.	Static	1	0	2200
15.	Static	1	0	3000
16.	Static	1	0	5000
17.	Static	0.5	0	50
18.	Static	0.5	0	1000
19.	Static	0.5	0	1500
20.	Static	0.5	0	1800
21.	Static	0.5	0	2000
22.	Static	0.5	0	2200
23.	Static	0.5	0	3000
24.	Static	0.5	0	5000
Lowering Case				
25.	DN	2	2	50
26.	DN	2	2	1000
27.	DN	2	2	1500
28.	DN	2	2	1800

Case	Leg Moving Direction	Current (knot)	Leg Speed (m/min)	Distance from seabed (mm)
29.	DN	2	2	2000
30.	DN	2	2	2200
31.	DN	2	2	3000
Lifting Case				
32.	UP	2	2	50
33.	UP	2	2	1000
34.	UP	2	2	1500
35.	UP	2	2	1800
36.	UP	2	2	2000
37.	UP	2	2	2200
38.	UP	2	2	3000
Transient Cases				
39.	DN	2	2	5000 to 50
40.	UP	2	2	50 to 5000

The results are evaluated against variable current and distance from the seabed for twenty-four (24) cases with a stationary leg, seven (7) cases showing during leg lowering and seven (7) cases showing during the leg lifting. Two (2) transient cases are performed as well. During the transient case the leg and spudcan moved at a speed of 2 m/min in a current of 2 knots applied for both lowering and lifting cases. In all total 40 cases simulated to see the response of hydrodynamic forces acting on the leg spudcan.

It is decided first to calculate only the drag and lift forces in-order to monitor the effect of the hydrodynamic forces. However, the drag as well as lift force results show a surprising behaviour due to the seabed effect. To understand the cause of this, it is decided to monitor the pressure force on the top and bottom spudcan plates to identify the effect of changes in shape and area change on the drag and lift forces, based on the Bernoulli principle. The water density and current are kept constant. The shape and area change the pressure on the top

and bottom plates. When multiplied by the respective areas, these give the net force acting on the spudcan plates. The force is obtained from the following (Eq. 4-6)

$$Force\ (F) = \ Pressure\ (P)\ x\ Area\ (A) \qquad \text{(Eq. 4-6)}$$

The following five elements are measured using CFD analysis.

- Drag force (Fx)
- Lift force (Fy)
- Drag coefficient of (Cd)
- Top spudcan plate pressure force y direction (PF_{TOP}.Fy)
- Bottom spudcan plate pressure force y direction (PF_{BTM}. Fy)

4.17 RESULTS OF CFD WHEN LEG SPUDCAN CLOSED TO SEABED VICINITY

4.17.1 Effect of sea bottom on drag force (Fx)

Drag force results for the static cases (i.e.,1 to 8) defined in Table 4-4 are presented in Figure 4-22 for currents of 2 knots. The results show the drag force when the leg and spudcan are held at the specified distances from the seabed.

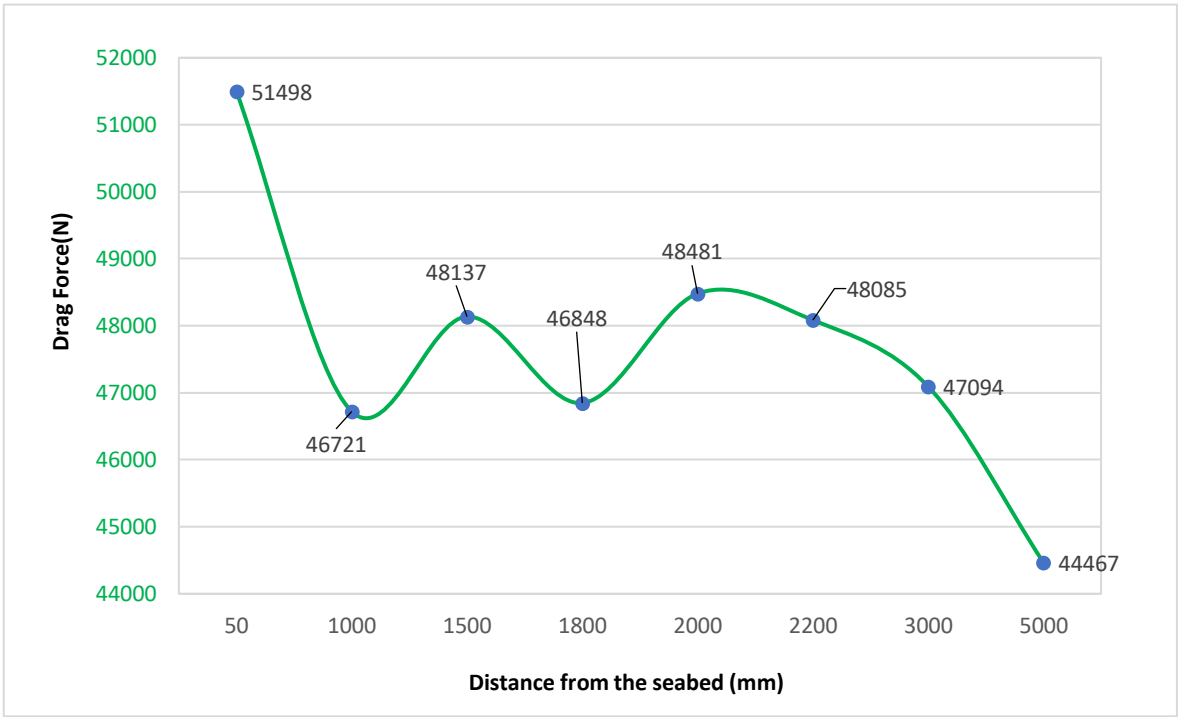

Figure 4-22 Drag force at distance from seabed in 2 knots current

Drag force results for the static cases (i.e.,9 to 16) defined in Table 4-4 are presented in Figure 4-23 for currents of 1 knot. The results show the drag force when the leg and spudcan are held at the specified distances from the seabed.

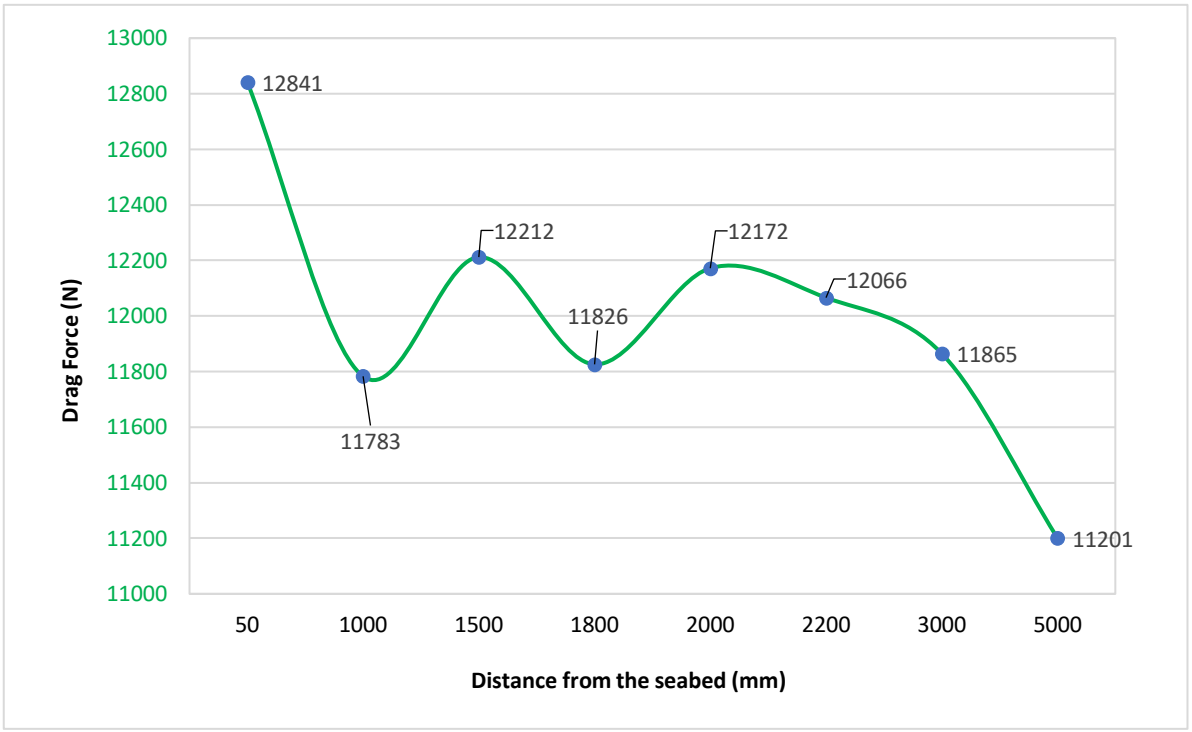

Figure 4-23 Drag force at distance from seabed in 1 knot current

Drag force results for the static cases (i.e.,17 to 24) defined in Table 4-4 are presented in Figure 4-24. for currents of 0.5 knot. The results show the drag force when the leg and spudcan are held at the specified distances from the seabed.

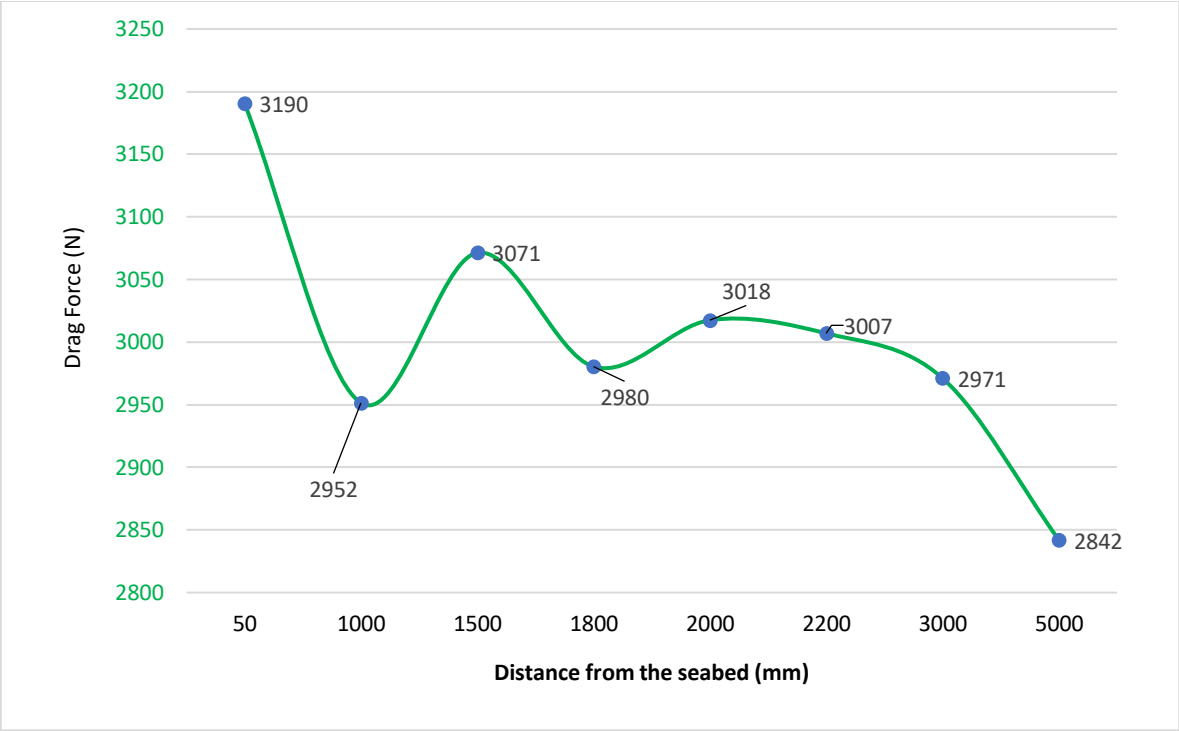

Figure 4-24 Drag force at distance from seabed in 0.5 knot current

The results for each current speed show similar drag force behaviour. The increase in drag force with increasing current is clearly seen. The results are evident for all the 24 cases assessed. The drag force increases by approximately 12~16% when the spudcan move from 5m above the seabed to the seabed for 0.5 knot, 1 knot and 2 knots currents. A sinusoidal cyclic behaviour in drag force in the range of 2.9~3.9%, is also evident when the spudcan move from 1.5m to 2m. The peculiar cyclic behaviour in the drag forces need further investigation by evaluating effect on pressure variance on spudcan top and bottom plate as well as variation in lift forces. An increase of approximately 7~9 % in forces is observed when the spudcan moves from 5m above seabed down to 2m above seabed level. The effect on drag force amplifies as current increases from 0.5 knot to 2 knots.

4.17.2 Effect of sea bottom on lift force (Fy)

Lift force results for the static cases (i.e.,1 to 8) defined in Table 4-4 are presented in Figure 4-25 for currents of 2 knots. The results show the lift force when the leg and spudcan are held at the specified distances from the seabed.

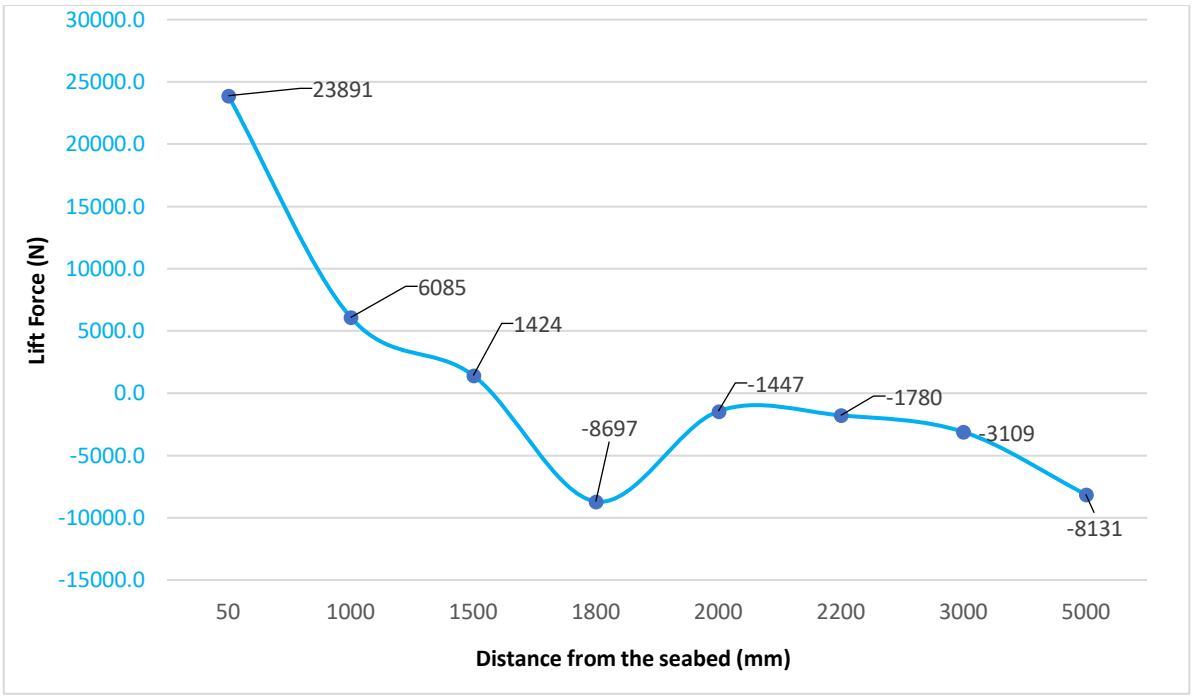

Figure 4-25 Lift force at distance from seabed in 2 knots current

4.17.3 Lift force results for the static cases (i.e.,9 to 16) defined in Table 4-4 are presented in Figure 4-26. for currents of 1 knot. The results show the lift force when the leg and spudcan are held at the specified distances from the seabed.

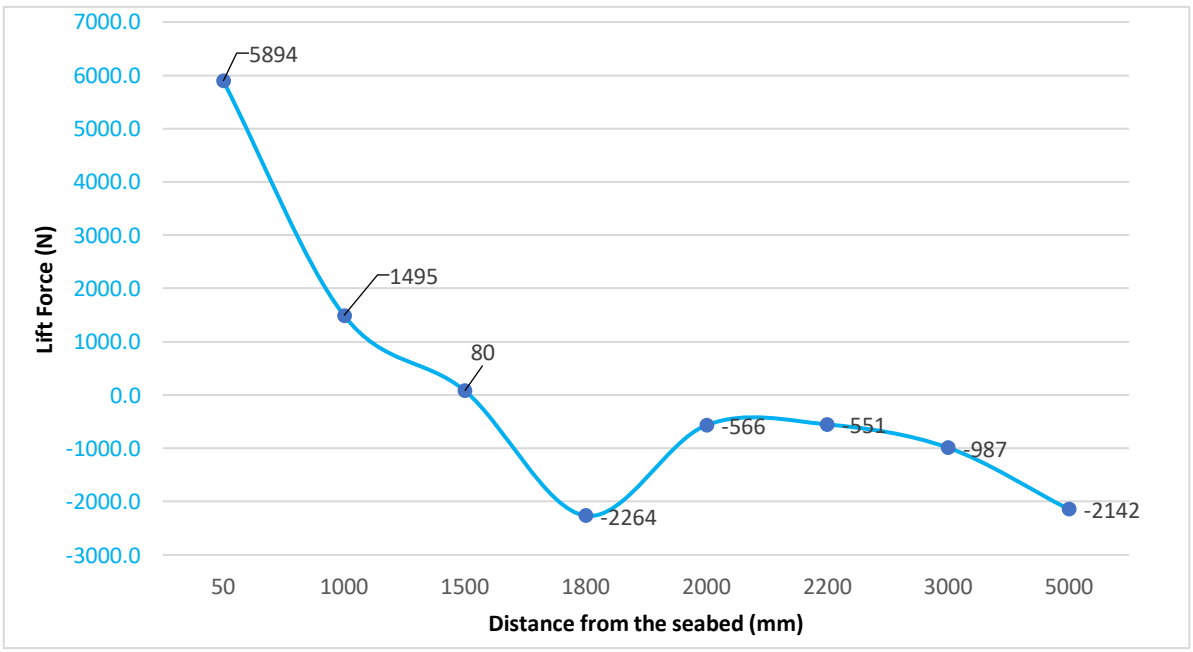

Figure 4-26 Lift force at distance from seabed in 1 knot current

4.17.4 Lift force results for the static cases (i.e.,17 to 24) defined in Table 4-4 are presented in Figure 4-27 for currents of 0.5 knot. The results show the lift force when the leg and spudcan are held at the specified distances from the seabed.

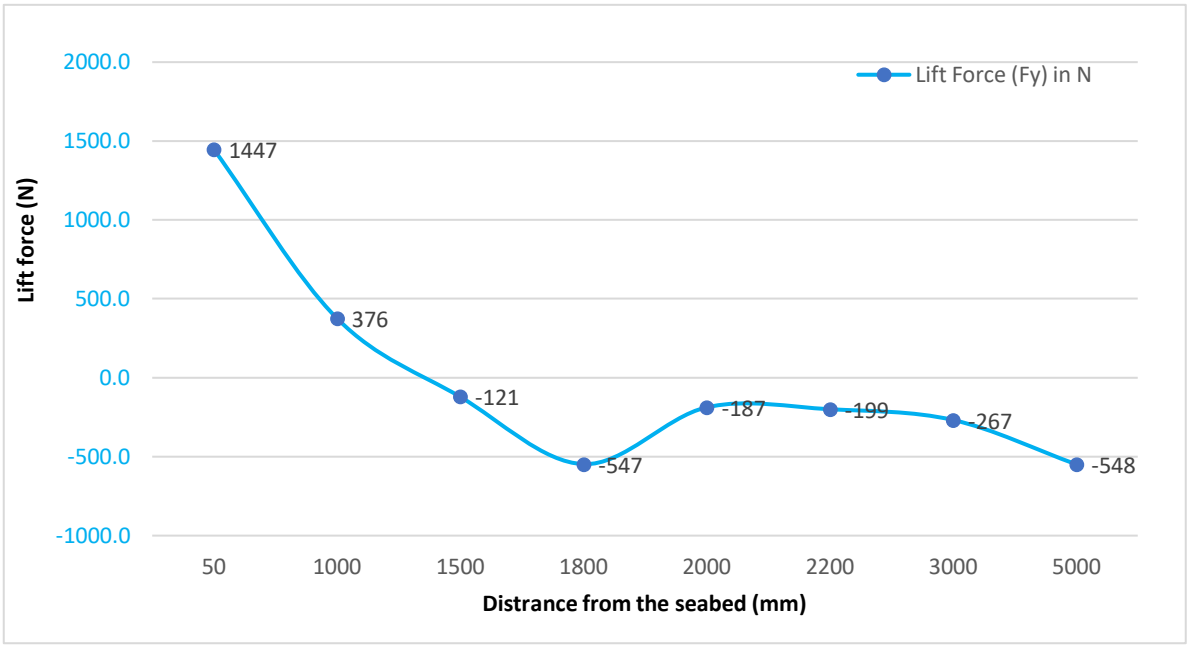

Figure 4-27 Lift force at distance from seabed in 0.5 knot current

The CFD results show that both the current speed and the distance above the seabed have a significant impact on the lift force. The lift force changes at approximately 1800mm above the seabed and it changes with acting current from case 1 to 24 results. The change in lift force sign confirms that the water fluid between the spudcan and the seabed is supporting lift. This is visible from the results. As the spudcan approaches to the seabed the lift force turns positive meaning the lift is supported by the current flow and seabed water compression. However, when the distance between spudcan and seabed increase the lift forces do not support by seabed, and this is evident from the results and indicated by the negative sign. As noted above, in Figure 4-25, Figure 4-26 and Figure 4-27 the lift force is recorded high at 50mm from the sea bottom. The lift force changes by approximately 400% as the leg and spudcan move away from the seabed from 50 mm to 5 m. A sharp increase in the lift force of approximately 300% is also evident when the spudcan moves closer to the seabed from 1 m to 50 mm above it at 2 knot currents. The lift forces also show drops of lift forces from 1500 mm to 1800 mm and then increase from 1800 mm to 2000 mm. The cyclic variations of drag force behaviours around 1800 mm proves vicinity effect of seabed and clear from the lift forces results.

4.18 LIFT AND DRAG FORCE BEHAVIOURS

To evaluate further the cause of this lift and drag force behaviour, the author decided to monitor the pressure force in the y-direction on the top and bottom plates of the spudcan. For a constant fluid density and current, the pressures can be used to evaluate the peculiar behaviour of the lift and drag forces. Additional CFD analysis are performed by considering the leg handing speed of 2 m/min in leg lowering towards seabed and leg lifting away from the seabed.

4.19 EFFECT OF SEABED ON TOP SPUDCAN PRESSURE FORCE (PFTOP.FY)

The top pressure force in the y-direction is calculated for the spudcan shown in Figure 4-28

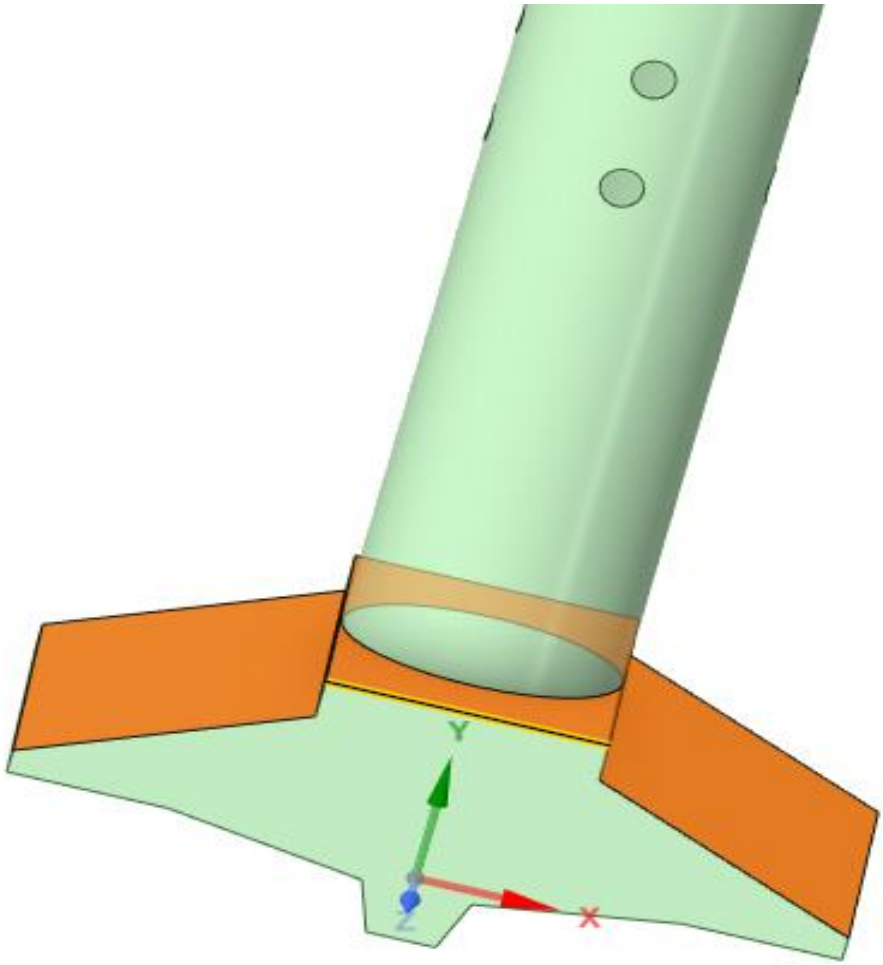

Figure 4-28 Spudcan top plate cross section overview

4.20 EFFECT OF SEABED ON BOTTOM SPUDCAN PRESSURE FORCE (PF BTM.FY)

4.20.1 The bottom pressure force in the y-direction is calculated for the spudcan shown Figure 4-29

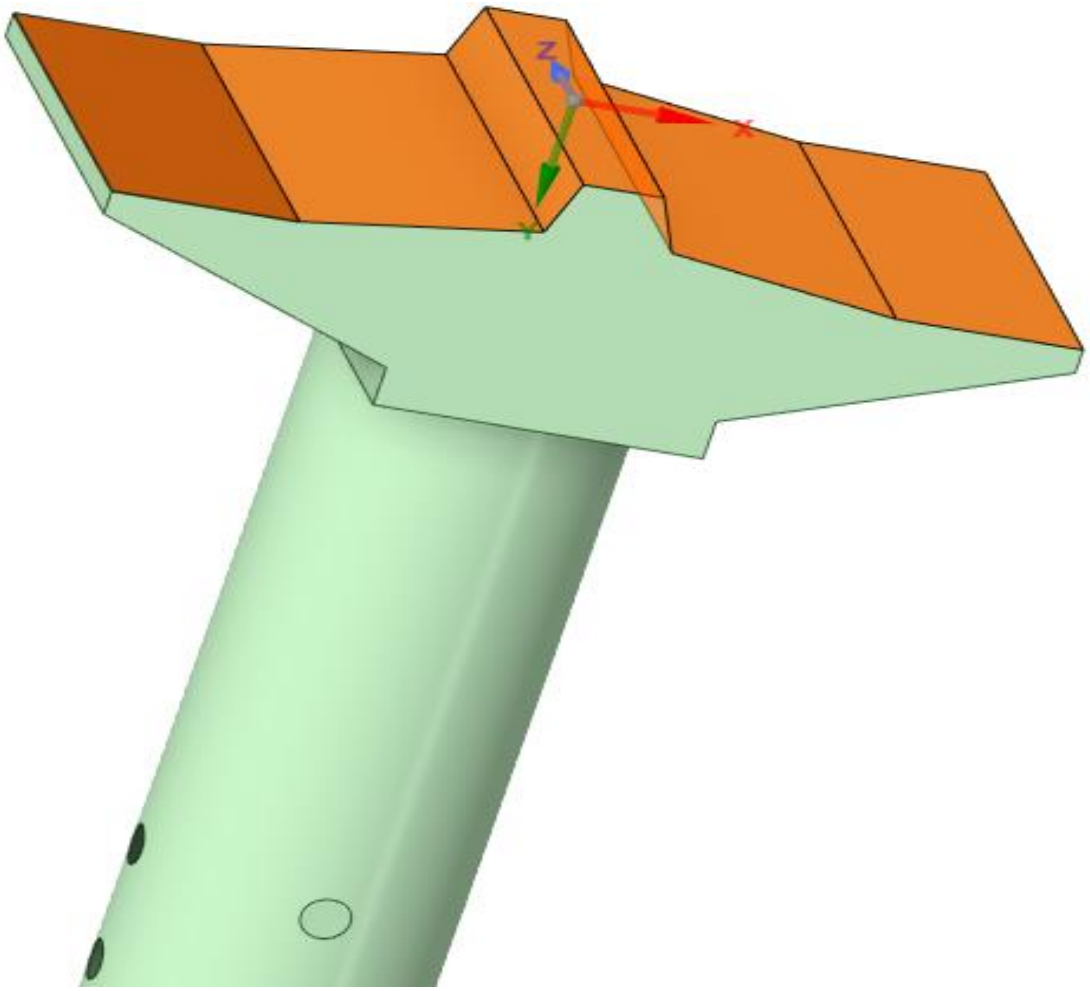

Figure 4-29 Spudcan bottom plate pressure

CFD analysis is performed for the cases indicated in Table 4-4 for leg lowering (cases 25 to 31) and leg lifting (cases 32 to 38). For these calculations, the current acting on the leg is set to 2 knots, and the leg speed set to 2 m/min. The continuous hydraulic jacking system does need time to retract and engage pin at every cylinder stroke length. Typically jack leg weight various from 300 ton to 1000 ton compared to hull weight from 5000 ton to 30000 ton. Since leg weight is lower than the hull the leg handling speed is faster when compared to hull handling speed in UP/DN direction.

The results of the twenty-four static cases showed a large variation in the observed drag and lift force when the spudcan set at 50 mm from 1 m above the seabed. Also, the lift force

transition between positive and negative is observed at approximately 1800 mm above the seabed for 2 knot current case 4. As a result, we decided to monitor the vertical pressure force in the y-direction on the top and the bottom spudcan plates from 50 mm to 3 m above the seabed. The parameters are measured in both leg lifting and lowering conditions at a speed of 2 m/min and 2 knots of current acting on the leg in the x-direction. Since a DP jack-up vessel always undergoes these operating scenarios, the CFD analysis will provide valuable leads of leg speed effect when operating near to the seabed.

4.21 BEHAVIOUR OF PRESSURE FORCE IN Y-DIRECTION DURING LEG LOWERING

The leg lowering CFD simulation results are based on the conditions described in Table 4-4, cases 25 to 31. In these cases, the current is set to 2 knots and the leg lowered towards the seabed at a speed of 2 m/min. The cases are studied with the spudcan set at 50 mm, 1000 mm, 1500 mm, 1800 mm, 2000 mm, 2200 mm and 3000 mm above the seabed, shown as the horizontal axis in Figure 4-30. The simulation results for the spudcan top and bottom plate pressures clearly show that the behaviour of both drag and lift forces is linked with the y-direction pressure force behaviour. The positive spudcan pressure force on the top spudcan plate and the negative pressure force on the bottom spudcan plate are observed high at 50 mm.

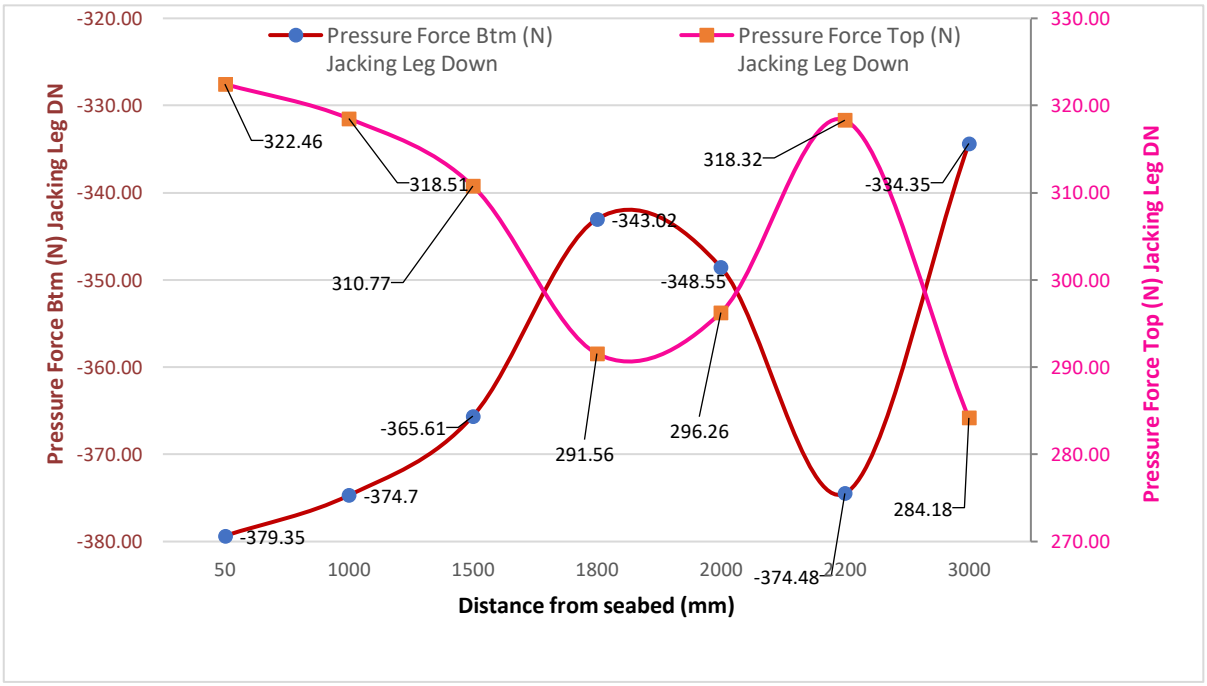

Figure 4-30 Top and bottom spudcan surface pressure force at 2 knots during leg lowering

The pressure force changes are also measured on the spudcan top and bottom plates during jacking up. The results are shown in Figure 4-31. The simulation setup of current and leg speed is shown in Table 4-4, cases 32 to 38.

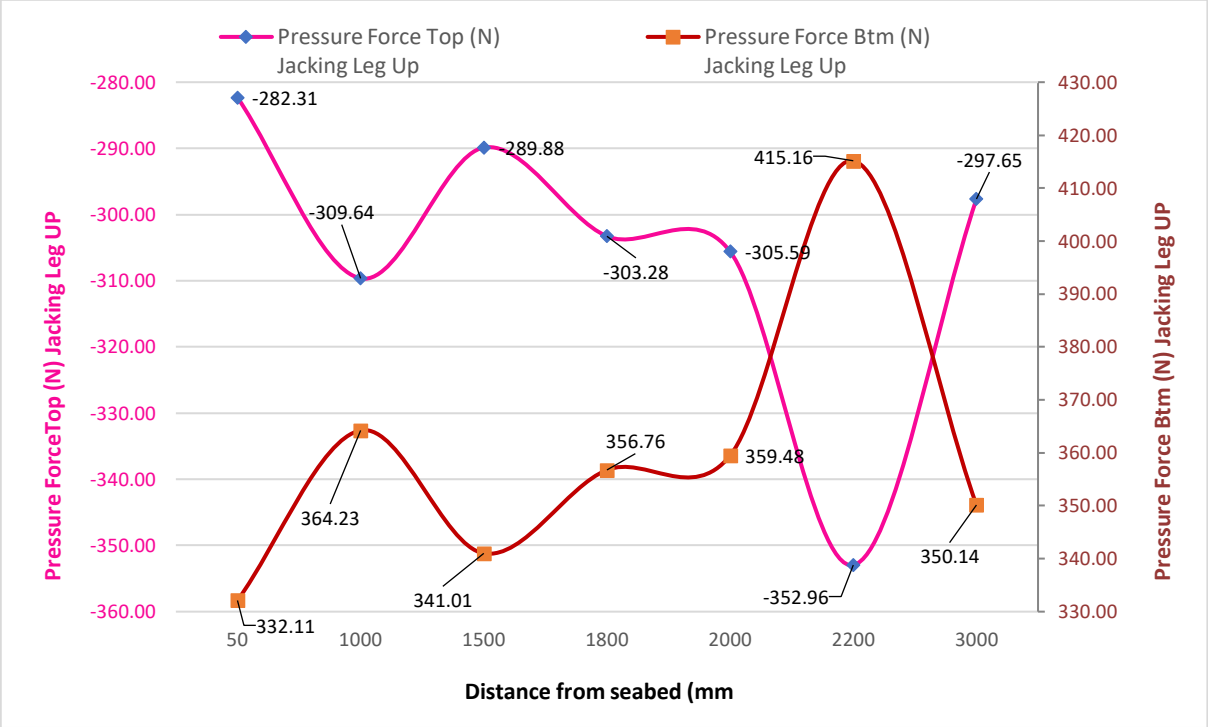

Figure 4-31 Top and bottom spudcan surface pressure force at 2 knots current during leg lifting up

The Figure 4-31 shows peculiar behaviours during the jacking leg up process of the decrease and then the increase in the drag forces seen in similar to Figure 4-22 between 1m and 2.2 m.

The analysis results shown in Figure 4-30 and Figure 4-31 confirms the pressure force pattern on the spudcan plate reverses when jacking down operations change to jacking up. The spudcan top plate pressure force shows positive during jacking the leg down (i.e., approaching the seabed), while the same pressure force shows the negative sign when jacking the leg up. Similar behaviour is observed on the spudcan bottom plate, which shows the negative sign during jacking the leg down and positive during jacking the leg up. The negative sign of pressure force indicates resistance to the direction of acting force.

To understand spudcan pressure behaviour on top plate during leg lowering and lifting the results are compared and shown in Figure 4-32. The results clearly show different behaviour of pressure force pattern on top plate during jacking up and down

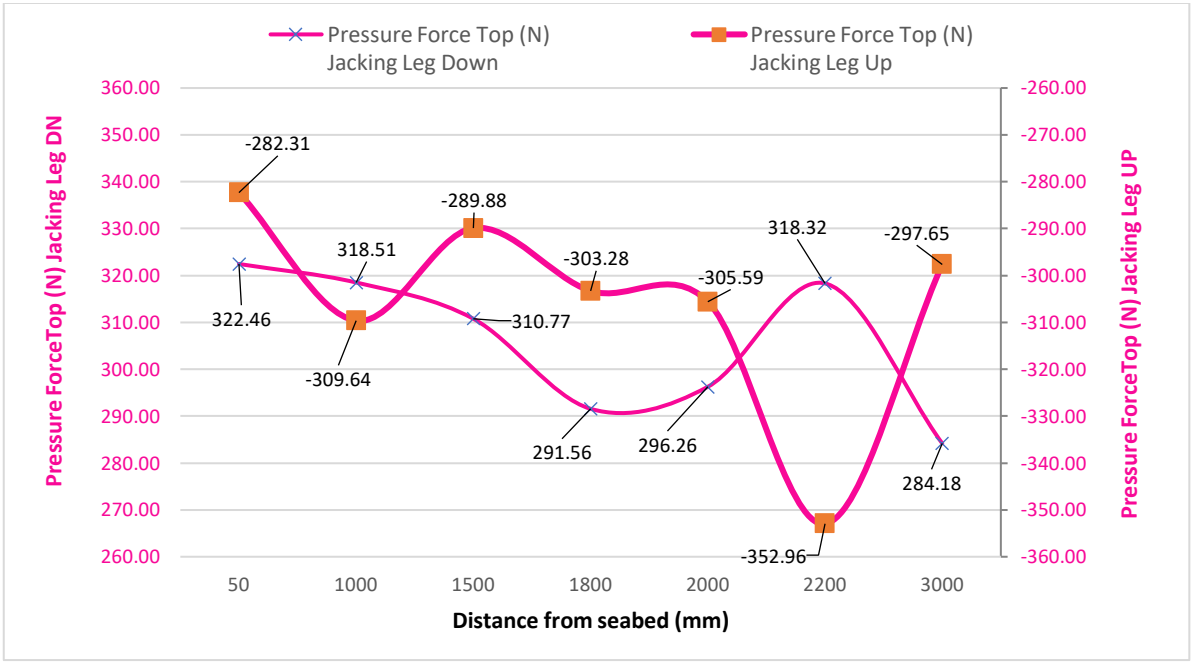

Figure 4-32 Spudcan top pressure force in jacking leg lowering and lifting

To understand spudcan pressure behaviour on bottom plate during leg lowering and lifting the results are compared and shown in Figure 4-33. The results clearly show different behaviour of pressure force pattern on top plate during jacking leg lifting up and lowering down.

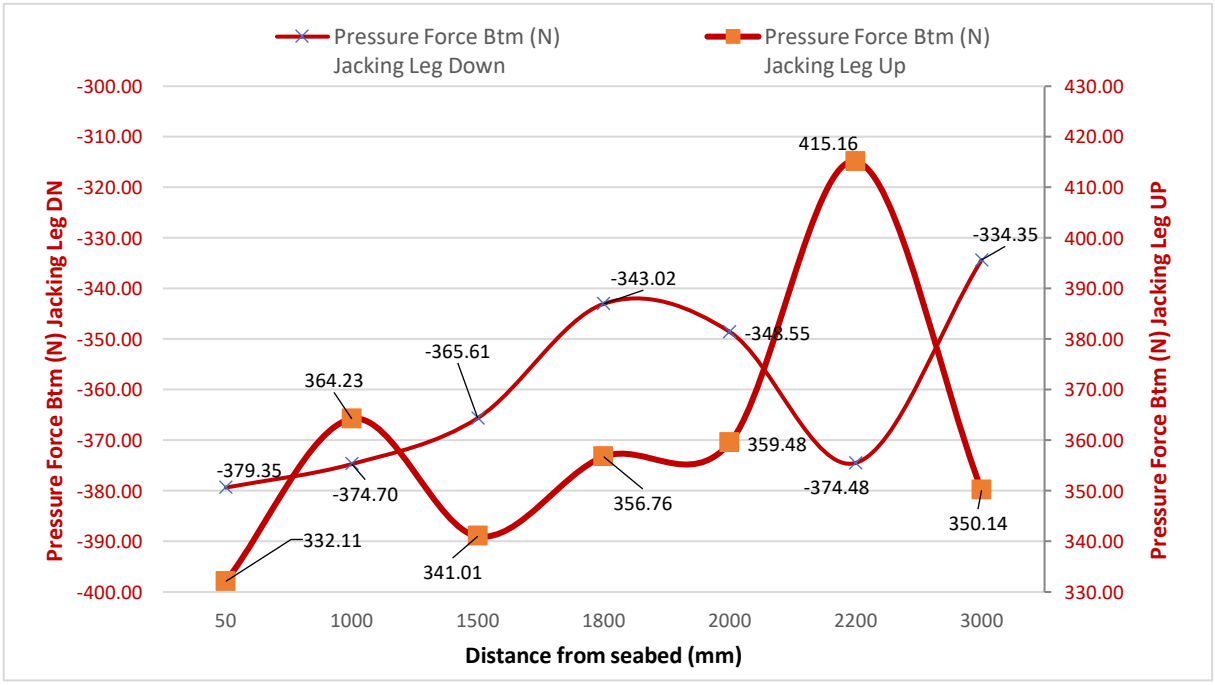

Figure 4-33 Spudcan bottom pressure force in jacking leg lowering and lifting

The behaviour of the drag forces is also measured with the leg and spudcan moving at a speed of 2 m/min towards seabed in a current of 2 knots. Figure 4-34 indicate the comparative drag force behaviour of the static cases (i.e., cases 1, 2, 5 &7), leg lowering (i.e., cases 25 to 28) and leg lifting (i.e., cases 29 to 32). The comparative graphs show that the drag forces follow each other closely with only slight differences. This means that the impact of leg movement on the drag forces is minor in comparison to the seabed impact on these forces.

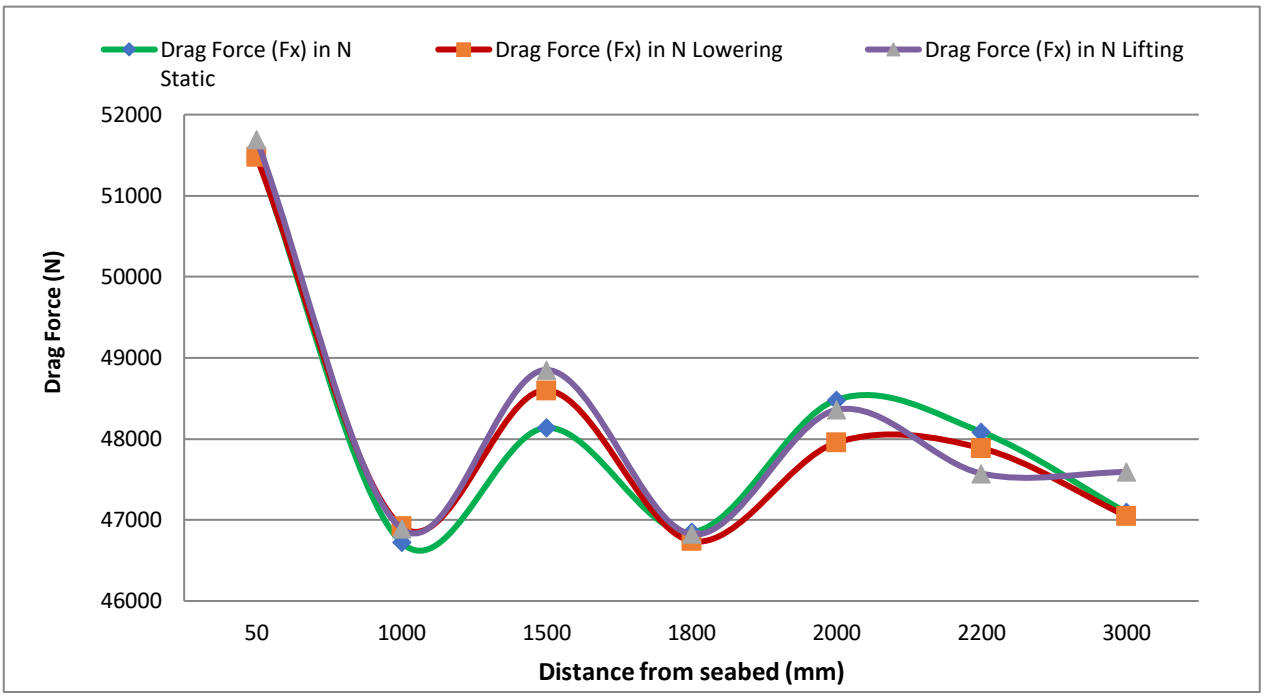

Figure 4-34 Drag force behaviour comparing static, jacking leg lowering and lifting

The behaviour of the lift forces is also measured with the leg and spudcan moving at a speed of 2 m/min towards seabed in a current of 2 knots. Figure 4-35 indicate the comparative lift force behaviour of the static cases (i.e., cases 1, 2, 5 &7), leg lowering (i.e., cases 25 to 28) and leg lifting (i.e., cases 29 to 32). The comparative graphs show that the lift forces follow each other closely with only slight differences. This means that the impact of leg movement on the lift forces is minor in comparison to the seabed impact on these forces.

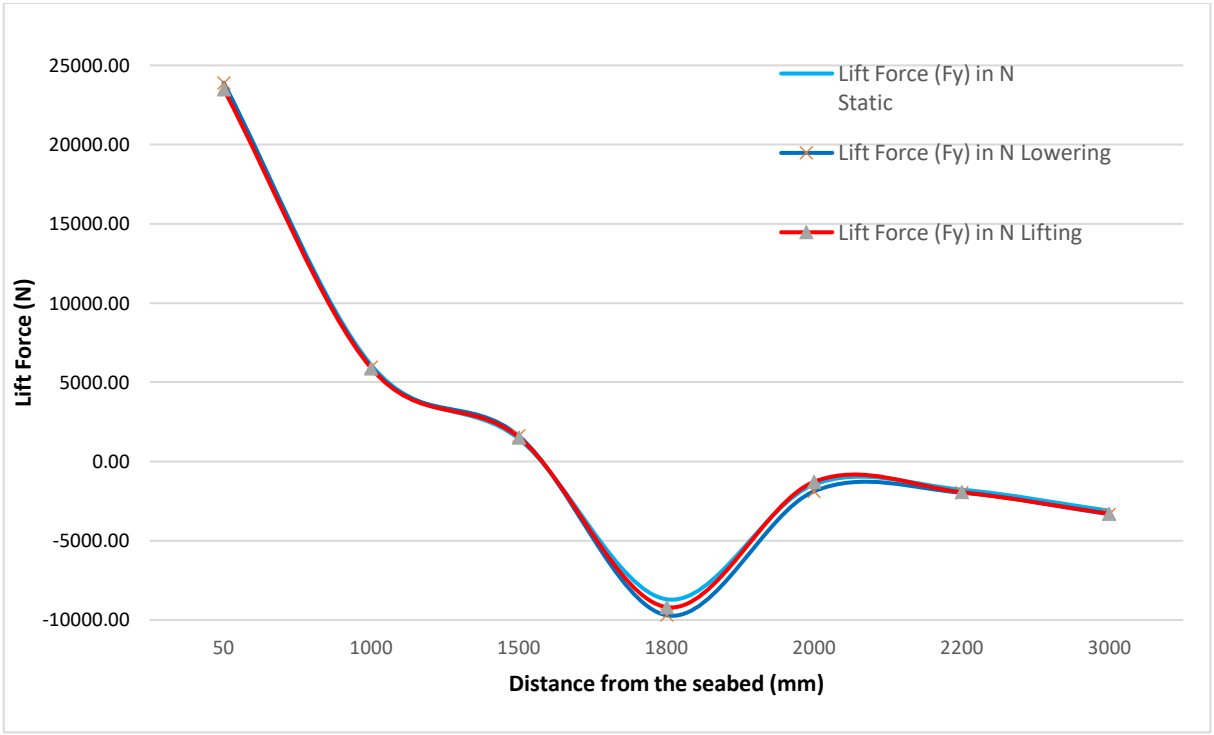

Figure 4-35 Lift force behaviour comparing static, leg lowering and lifting

DP jack-up vessels of similar leg design should focus on this impact, which can cause positional deviation during the critical DP station keeping and the jacking SIMOPS operations.

Liebert (2019) [34] has also reported difference in force coefficients legs down / legs up. The paper echo, the critical moment just before the initial contact of legs and seabed which corresponds to maximum current loads during the SIMOPS.

The DP vendor must consider this effect in their mathematical model. Since the spudcan shape influence the behaviour of the pressure or forces, it is important DP system designer consider tailer made solutions for better station keeping performance during SIMOPS operations for each DP Jack ups vessel.

The highest difference in drag force between static case 5 and lowering case 29 is measured to 528 N, with the spudcan set at 2 m from the seabed. The lift force difference of 1000.9 N observed at approximately 1.8m between case 4 and case 28.

The spudcan top plate has a surface area of 100.6 m^2, the bottom plate has a surface area of 114.2 m^2. The difference is due to the geometry of the spudcan. The pressure change between the spudcan bottom and top occurs at approximately 1800 mm from seabed. This changed

effect of hydrodynamic forces at a distance from the seabed of approximately half the spudcan diameter is also claimed in the paper of Hoes (2012).

4.22 EFFECT OF SEA BOTTOM ON DRAG COEFFICIENT (CD)

The static cases defined in Table 4-4 (i.e.,1 to 8) are set for CFD simulation. The results are presented below in Figure 4-36 for currents of 2 knots. They show how the drag coefficient is affected as the leg and the spudcan move away from the seabed.

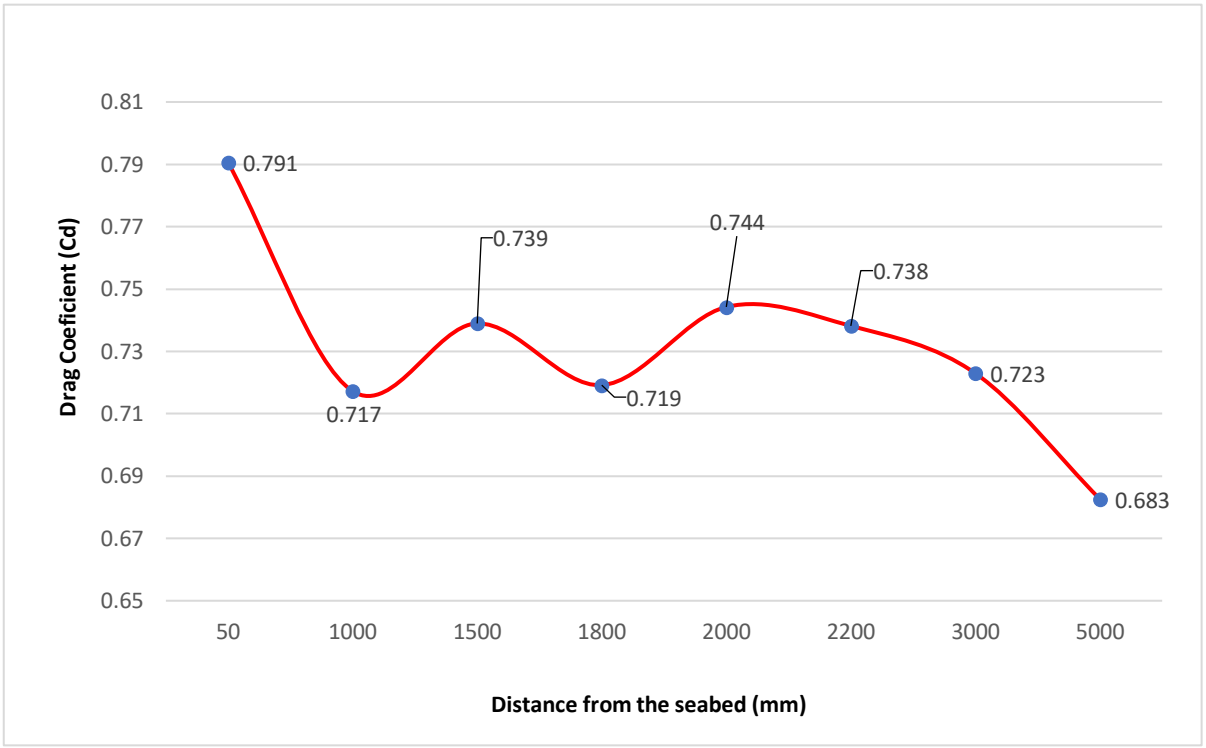

Figure 4-36 Cd behaviour at distance from seabed in 2 knots current

The static cases defined in Table 4-4 (i.e.,9 to 16) are set for CFD simulation. The results are presented below in Figure 4-37 for currents of 1 knot. They show how the drag coefficient is affected as the leg and the spudcan move away from the seabed.

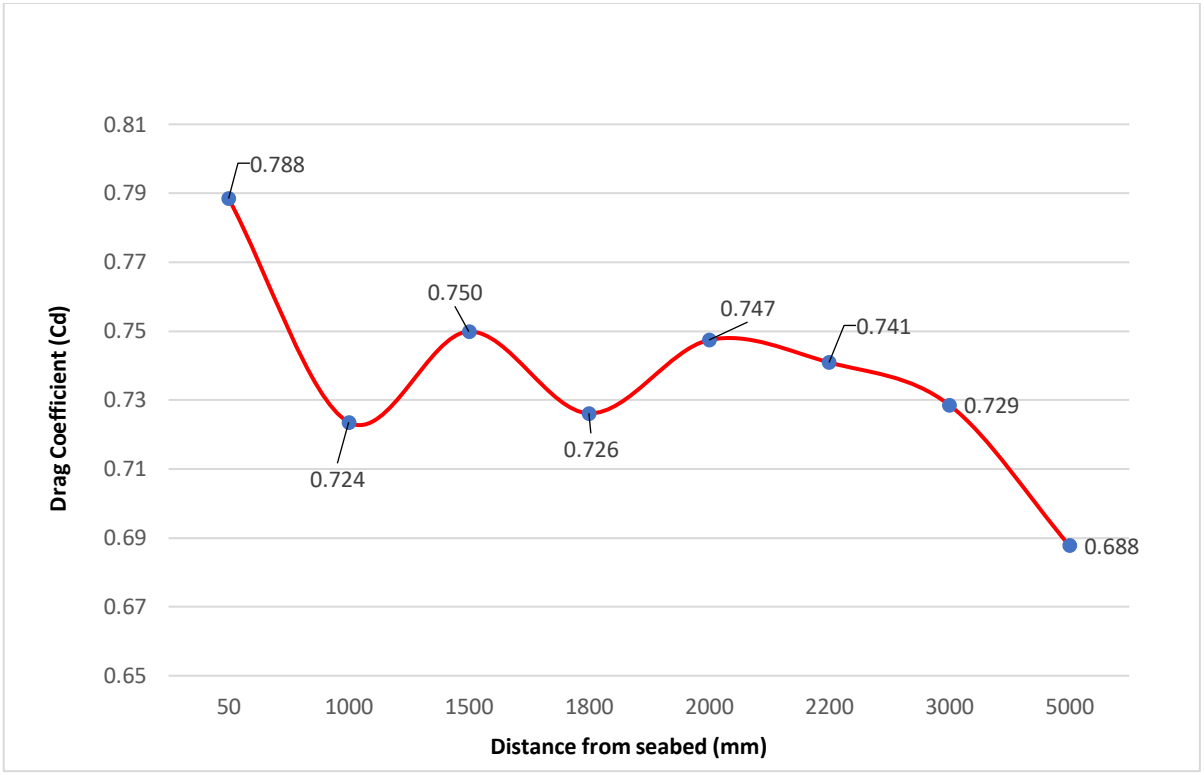

Figure 4-37 Cd behaviour at distance from seabed in1 knot current

The static cases defined in Table 4-4 (i.e.,17 to 24) are set for CFD simulation. The results are presented below in Figure 4-38 for currents of 0.5 knot. They show how the drag coefficient is affected as the leg and the spudcan move away from the seabed.

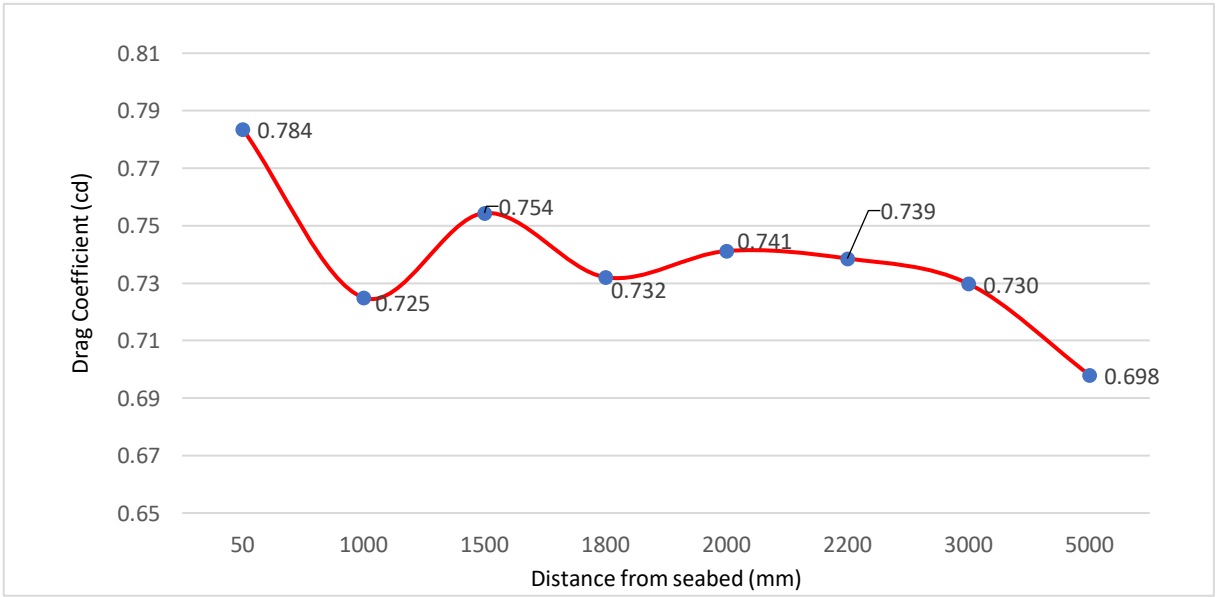

Figure 4-38 Cd behaviour at distance from seabed in 0.5 knot current

The CFD results show how the drag coefficient reduces as the leg and spudcan move away from the seabed. The results show similar trends for each current and show an increase of approximately 16%.

The DP vessel mathematical model uses a drag coefficient to estimate the drag forces on the jack-up leg and spudcan. Since it is important to know how the seabed vicinity affects this drag coefficient (Cd), CFD calculations are also carried out.

A DP vessel usually requires minimum 23-30 minutes to adapt the DP mathematical model to the environmental conditions. The DP system kept on during the leg spudcan removal from the seabed, however the hydrodynamic model building is a challenge as vessel position and heading remains stationary when spudcan in the seabed.

Once all the legs are detached, the DP system should ideally take over and hold the position and heading of the vessel as set. Since the DP mathematical model do not really update due to spudcan in the seabed. The thruster in relax mode during spudcan in seabed need to act aggressively soon after spudcan out of seabed to control the vessel drifting.

It is often observed the vessel drifted soon after the spudcan detach from the seabed. This poses the biggest risk to the offshore industrial mission.

The DP system receives the vessel's actual location and heading information as input from position reference sensors and from the gyro compass. The mathematical model based on environmental data calculates the impact on the vessel's station keeping of position and heading. The DP system then generates counter thrust by issuing the required thrust and steering angle commands to the available thrusters. The aim of the DP control system is to keep the position and heading errors close to zero.

To understand how the hydrodynamic forces on the leg and spudcan change when the leg and spudcan are operating in close vicinity to the seabed could be beneficial to dynamic position assessors. In my opinion, this information is critical for DP vendors to achieve tight control on position and heading of the vessel. The Richard Ian Stephens, US Patent 8992126 in 2015 also advised to install strain sensor on at least one support leg of the jack-up vessel for a dynamic positioning (DP) system of the jack-up vessel to determine a suitable thrust to apply to the vessel as the support legs of the vessel are raised. This is good solutions; however, considering single failure, it is highly recommended to consider redundancy in strain sensors preferably on cross diagonal legs.

4.22.1 The snapshot of the CFD velocity flow around the leg and spudcan. Vortices behind the leg are clearly seen in Figure 4-39

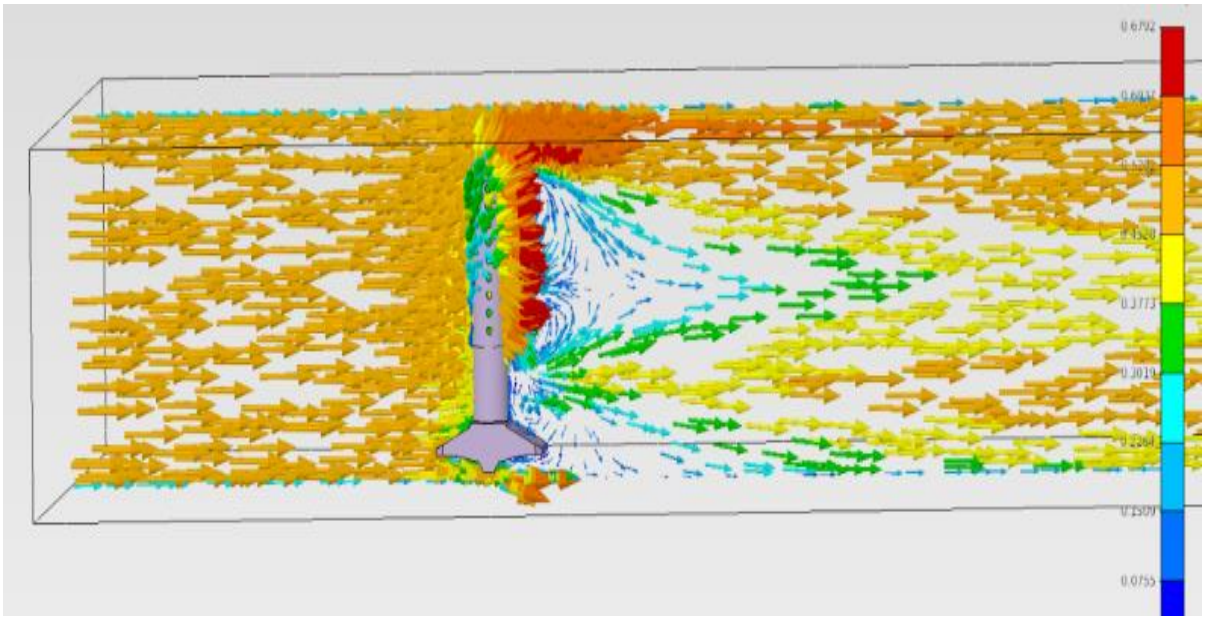

Figure 4-39 Side view showing the current acting on the leg and spudcan (Vortex points)

The streamlines flow clearly show the vortex generation due to diverted cross fluid flow in Figure 4-40. The hydraulic jacking system have holes for hydraulic pin insertion, this provides the fluid path and caused cross flows, the leg movement and spudcan disturb the cross flow and as result some of these flows redirected towards leg creating vortex vibration.

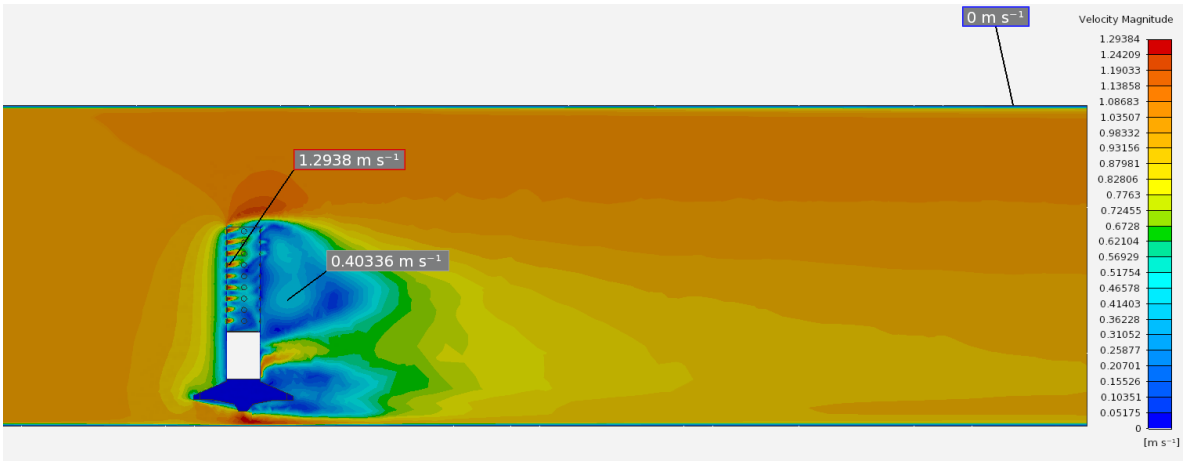

Figure 4-40 Side view showing the velocity flow around the leg and spudcan.

4.23 TRANSIENT EFFECT DURING LEG MOVEMENT TO & FROM SEABED

The transient effects are analysed to determine the variation of drag coefficient (Cd), drag force (Fx), lift force (Fy) and spudcan pressures. The purpose of the analysis is to find how the dynamics of leg movement with respect to time affect each parameter. The simulation conditions setup shown below in Table 4-5.

Table 4-5 Transient effect simulation case

Case	Description of Case	CFD Setup
Lowering case	Leg and spudcan moved from 5 m towards seabed at speed of 2 m/min.	Current – 2 knot @ X directions. Time Duration 148.5 sec Leg speed 2 m/min @ Y direction (-lowering)
Lifting case:	Leg and spudcan moved away from seabed at a speed of 2 m/min.	Current – 2 knot @ X directions. Time Duration 148.5 sec Leg speed 2 m/min @ Y direction (-lowering)

The variation of drag coefficient during lowering and lifting the spudcan toward and away from the seabed is shown in Figure 4-41 and Figure 4-42. Since the speed of the leg is set at 2 m/min and the distance of the spudcan from the bottom is set at 5 m, the leg should touch down 50 mm above seabed in a time of 148.5 seconds. The transient time is set to 148.5 sec to ensure the touch down effect is accommodated. The results show that, during the transient case, the drag coefficient remains high at the start and slowly reaches the typical steady state values published in DNVGL-RP-C205 [11]. The reason of such response could be vortex induce due to cross flow. Vortices around the leg are formed by the disturbed flow due to leg movement and by fluid flow from the leg jacking pin holes. Based on DNVGL-RP-C205,2010 Sec 9.2.2, the impact on drag coefficient due to vortex induced vibration can be calculated using (Eq. 4-7) below

$$C_{dviv} = C_d \left[1 + 2.1 \times \left(\frac{A}{D}\right)\right] \quad \text{(Eq. 4-7)}$$

Whereas,

Cd – Drag Coefficient for the stationary leg spudcan.

D – Diameter of leg (4500 mm)

A – Amplitude of the crossflow vibration

The Figure 4-41 shows the behaviour of the drag coefficient during the transient analysis. The drag coefficient reduces sharply over approximately the first 40sec visible before it goes to steady state. When near to the seabed the rise in drag coefficient due to the seabed effect is observed as shown in Figure 4-36 The vortices are clearly visible in Figure 4-39. This cross flow creates disturbance to the flow. As a result, the convergence criteria of E-05 cannot be achieved but E-03 is achievable.

The reason for the drag coefficient increase can be calculated using (Eq. 4-7). At approximately 7.66 sec when the leg is at 4750mm approximately above the seabed, the steady state drag coefficient from Figure 4-36 is found to be 0.69. The amplitude of cross flow vibration estimated 1150 mm resulting in the ViV drag coefficient during leg lowering (jacking down case) from equation (5) being calculated to be:

$$Jacking\ leg\ lowering\ case\ C_{dviv} = 0.69\left[1 + 2.1 \times \left(\frac{1150}{4500}\right)\right] = 1.06$$

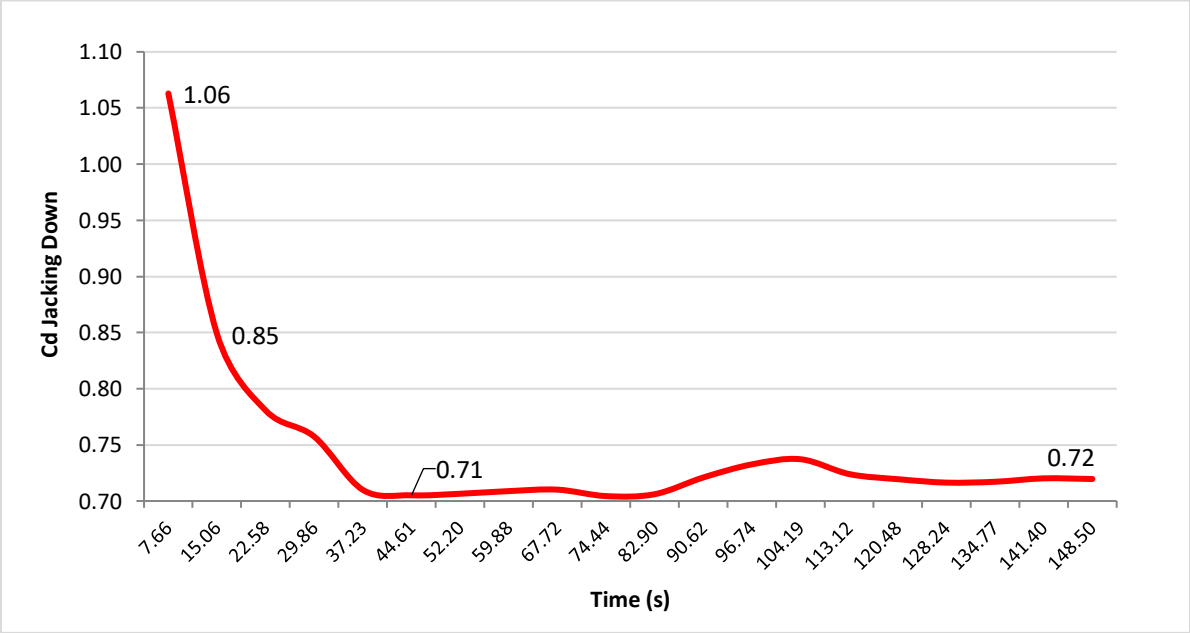

Figure 4-41 Drag coefficient jacking leg lowering from 5000mm to 50mm above seabed

The Figure 4-42 shows the transient behaviour of the drag coefficient when the leg and spudcan are jacked up from the seabed. The results show similar behaviour i.e sharp change at approximately 40sec and then settling to steady state values.

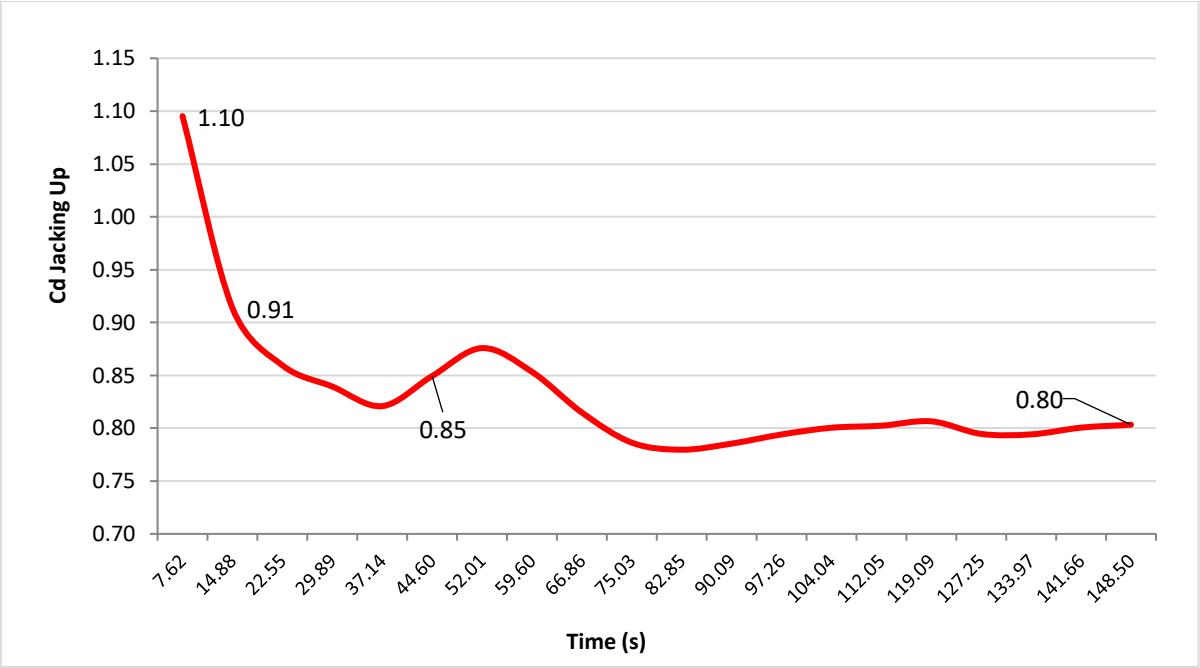

Figure 4-42 Drag coefficient jacking leg lifting from 50 mm to 5000 mm above seabed

The steady state distance at 7.62 s at a leg speed of 2 m/min is 300 mm. The steady state Cd value from Figure 4-36 is 0.76. The amplitude of the crossflow vibration estimated 950 mm such that Cdviv using value (jacking up case) is calculated using (Eq. 4-7) to be:

$$Jacking\ leg\ lifting\ case\ C_{dviv} = 0.76\left[1 + 2.1\ \times \left(\frac{950}{4500}\right)\right] = 1.08$$

This means, the amplitude of cross flow vibration (1150 mm Vs 950 mm) during leg lowering is relatively higher than leg lifting, when worked reversely. These results could be very useful to the DP vendors who should consider such changes to their mathematical models. The simultaneous operation of DP jack-ups has various transit phases such as leg in air, lowering leg to the seabed, close vicinity of the seabed during approach, removal of spudcan from the seabed, etc. It is very important that DP system designer carefully consider these transient phases for better station keeping stability.

The drag force (Fx) variation is as shown below in Figure 4-43 and shows large force variations similar to the drag coefficient. Irrespective of lowering or lifting of the leg and spudcan, the drag force is measured higher in the beginning before reducing. The lifting case shows at approximately 50 sec, 3% increase in drag force then drops to approximately 10%, a peculiar behaviour during lifting. The pressure force changes between top plate and bottom plate near seabed vicinity as shown in Figure 4-31 shows similar trends of drag forces. The fluid below spudcan bottom plates might be exerting forces on the spudcan.

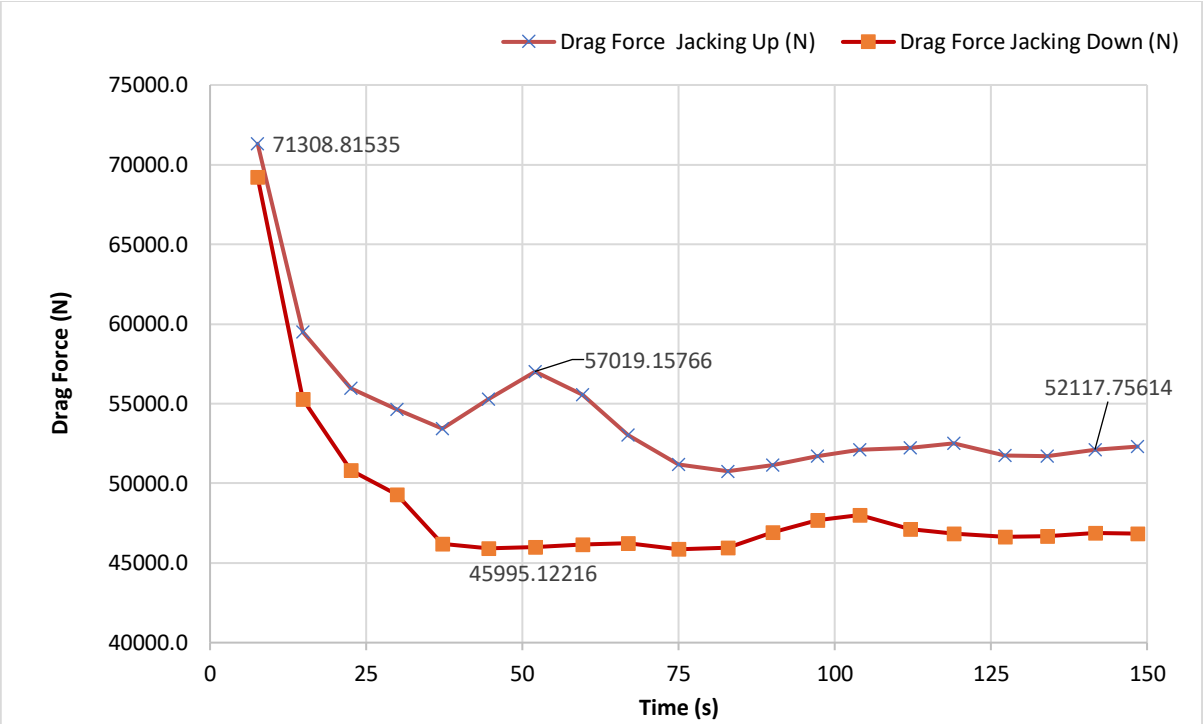

Figure 4-43 Drag force (Fx) variation during jacking lifting and lowering

The time domain analysis shows similar behaviour of drag forces as shown in Figure 4-43. Although the value at starting shows higher and the main reasons behind this could be vortex vibrations due to cross flow, which caused increased in the drag coefficient.

The overview of all five parameters (i.e., Cd, Fx, Fy, P_{BTM} and $P_{TOP,)}$ clearly shows the large variation of hydrodynamic forces in lifting and lowering operations. The DP control system for the jack-up must be designed to take into consideration the full effect of all the force variations to achieve better station keeping during these very critical modes of operation. The jack-up works very close to the field assets and errors in the mathematical model can lead to collision. Currently, the DP officer and the jack-up master are handling this risk manually.

4.24 MODEL TESTING - VALIDATION EXPERIMENTAL RESULTS

The CFD results are validated by tank experiments at a model scale of 1:27. The Kyushu university tank is 2 m in depth and experiment setup shown in Figure 4-44 and Figure 4-45.

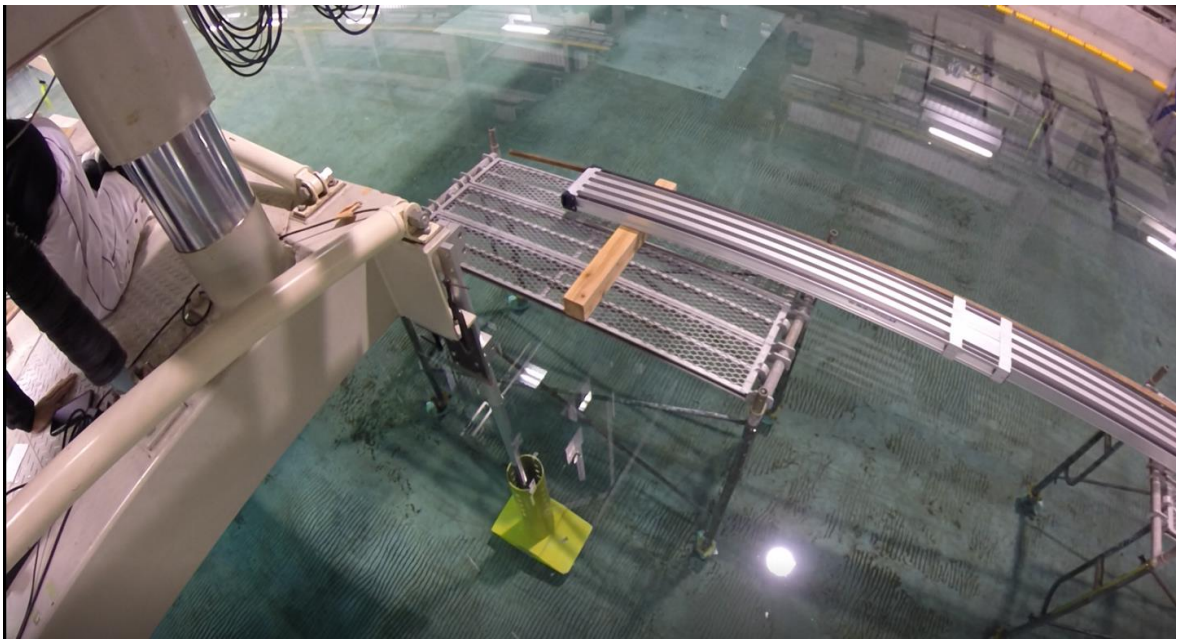

Figure 4-44 Tank experiment arrangement

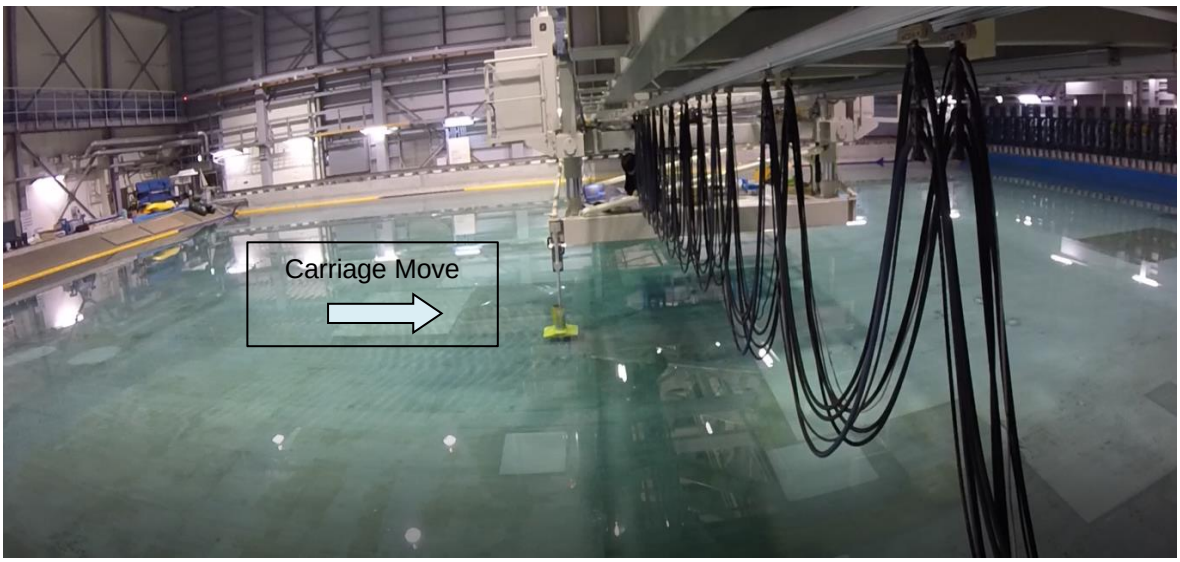

Figure 4-45 Tank experimental carriage motion

The carriage holding the leg model set to move at a speed, simulating the current acting on the leg. The load cells are mounted to measure the drag forces acting on the leg. The load cell is used during the experiment for interpreting voltage signal to the force. The raw voltage signal

is measured by the computer. This is then interpreted to calculate the actual value of drag force.

The carriage needs some momentum to reach desired current speed. Once carriage reach this speed after some time gap the readings are used for validation purpose. The carriage stops once the sufficient data collected. During the experiment, the author noticed variations of the reading. The vortex vibration was also noticed during the experiment from the video footage camera. The figure below shows the experimental recording and zoom view of variation.

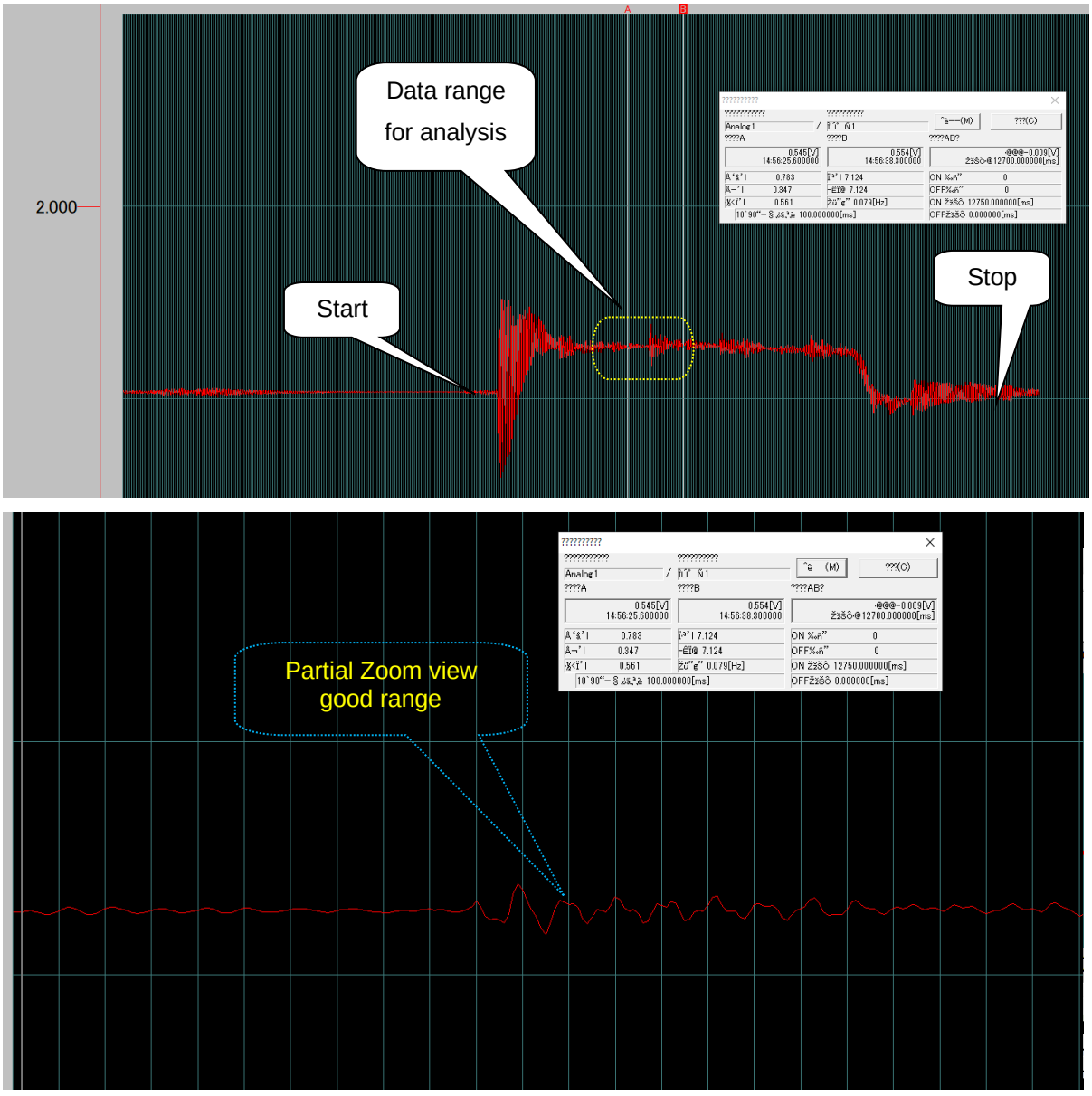

Figure 4-46 Experiment data logger

Cases to validate the bottom effect are run with the spudcan base set at 182.8 mm, 109.7 mm, 73.1 mm and 36.6 mm above the seabed. To simulate the current flow, the tank carriage is used to tow the spudcan model. The leg lowering/ lifting cases are not performed but the spudcan is set at the fixed distances to validate the results. Once the carriage achieved the required steady state condition the load cell results are averaged out to obtain the readings for comparison with the CFD results.

The specific tank experiment cases are also analysed by CFD. The laboratory result of case 2 having distance from the seabed 182.8 mm for 1 knot current is shown below in Figure 4-47

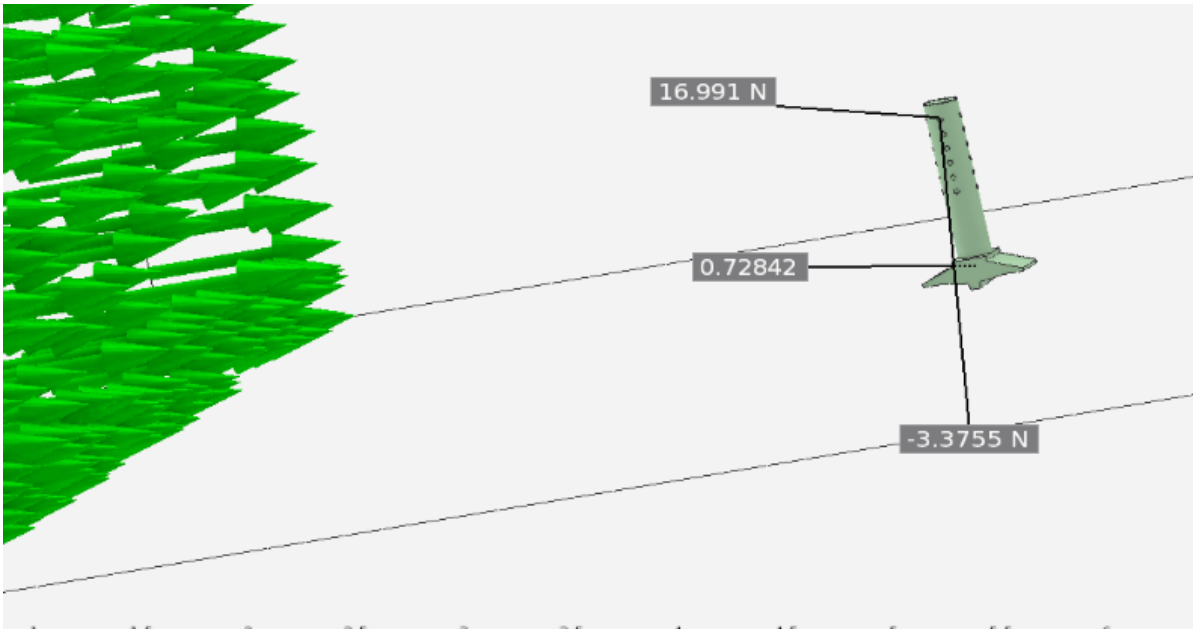

Figure 4-47 CFD results of lab experiment Test 2

The tank experiment results are compared with the CFD calculations. The results are shown in Table 4-6

Table 4-6 Tank experiment vs CFD results

Test	Cur (Knot)	Dist. Btm (mm)	CFD Fx(N)	Lab Fx (N)	% Error Fx	CFD Cd	Lab Cd	% Error Cd
1	0.5	182.8	4.389	4.759	7.8	0.753	0.801	6.0
2	1	182.8	16.991	17.982	5.5	0.728	0.757	3.7
3	0.5	109.7	4.457	4.882	8.7	0.764	0.821	6.9

Test	Cur (Knot)	Dist. Btm (mm)	CFD Fx(N)	Lab Fx (N)	% Error Fx	CFD Cd	Lab Cd	% Error Cd
4	1	109.7	16.977	18.370	7.6	0.728	0.773	5.9
5	0.5	73.1	4.860	4.953	1.9	0.833	0.834	0.0
6	1	73.1	18.743	18.452	-1.6	0.804	0.776	-3.5
7	0.5	36.6	4.886	4.943	1.2	0.838	0.832	-0.8
8	1	36.6	18.334	19.476	5.9	0.786	0.819	4.1

The CFD and tank experiment results show that both drag force and drag coefficient follow the same trends. The discrepancy between the CFD and experimental results is less than 10%. This proves that CFD analysis results can be applied to the full-scale leg model to determine the impact of the seabed bottom effect, which could be significant to the DP system.

4.25 CFD ANALYSIS ON TRUSSED LEGS FOR DP JACK UP

The CFD simulation was carried out to measure the response of drag and lift forces of triangular trussed type lattice leg chord design. The CFD analysis is performed exclusively to see the trends of drag and lift forces of cylindrical leg type with another popular trussed type lattices leg consist of braces, rack and chord. The leg has three chords of legs and most of the DP jack vessels has four vertical leg structure. The advantage of four leg structure over 3 legs is mainly fast preload operation compared to 3 legs jack ups. Currently, industry has over 450 operational jack ups operational worldwide, out of which approximately 300 jack ups have trussed type legs. The trussed type of legs is dominating due to optimal utilization of steel and predominantly less drag loads due to reduce cross section area. Moreover, trussed type legs are very stiffed. The cross-bracing connection between the two chords helps to increase the load handling capacity.

The lattices leg design used for analysis is shown below in Figure 4-48. The chord diameter of 356mm and rack width 550 mm. The distance between each chord is approximately.5236 mm, while height of the leg consider for simulation is 6207 mm. The aim of this analysis is to see the trends of the forces acting on the leg spudcan of trussed type leg and compare this trend with cylindrical leg, which was studied above, and results summarize for bottom effect in Table 4-6.

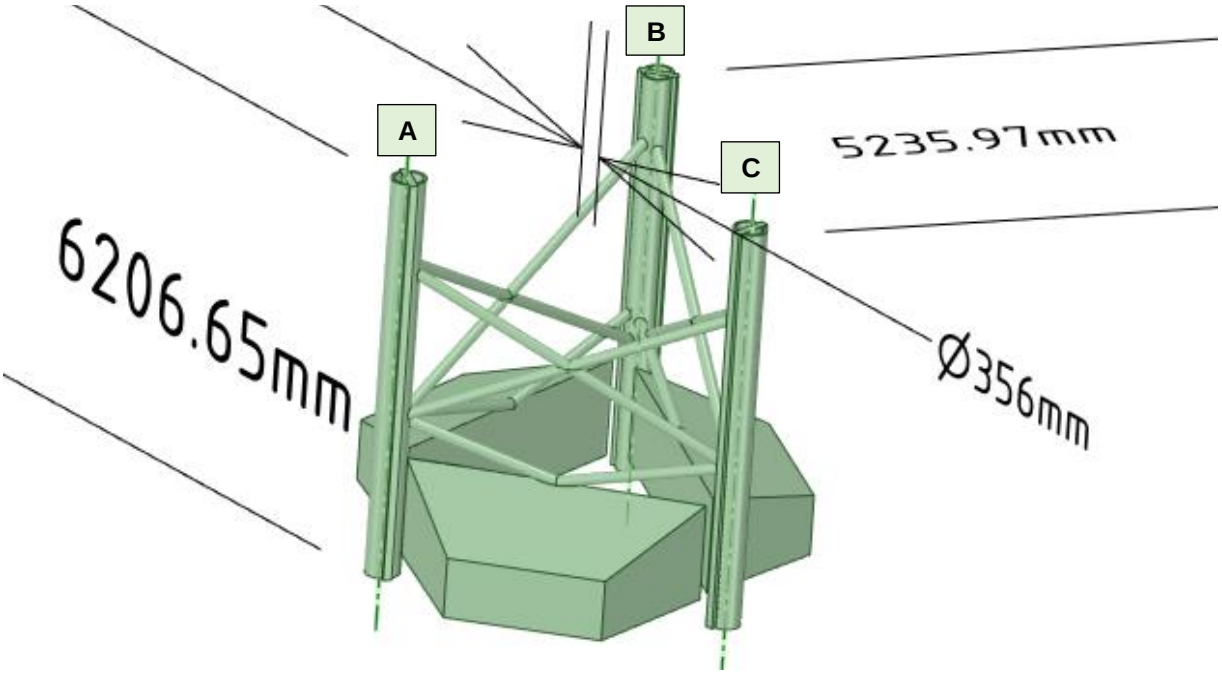

Figure 4-48 Lattice Triangular Leg

The simulated results for lattices leg are tabulated below in Table 4-7 Compared to cylindrical legs the hydrodynamic drag forces are relatively low due to less cross-sectional area of the chord.

Table 4-7 CFD results for lattices leg

Current (knot)	Leg Speed (m/min)	Dir.	CFD Fx Force (N)	CFD Fy Force (N)
0.5	0.5	UP	514.61	65.68
0.5	0.5	DN	513.00	61.44
1	1	UP	1996.80	285.98
1	1	DN	2035	218.51
2	2	UP	8025.5	961.52
2	2	DN	8054.8	1052.7

The CFD Simulation results are shown below in Figure 4-49 and Figure 4-50 showing vortex and drag flows around leg chords and braces A, B and C.

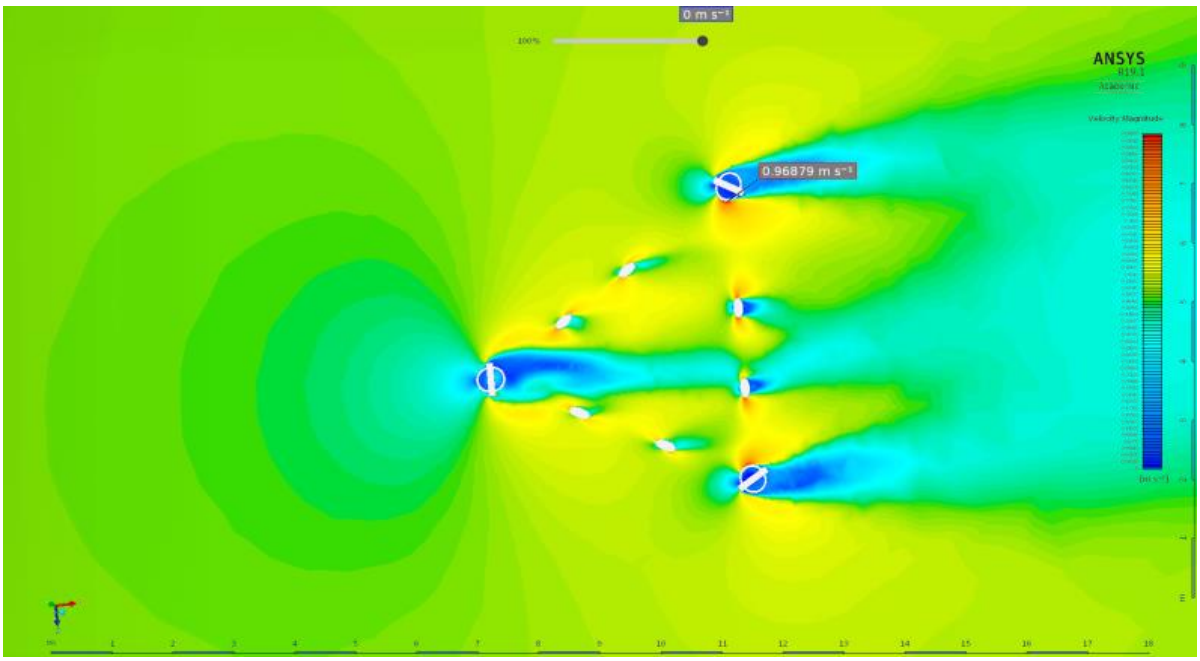

Figure 4-49 Top view of velocity magnitude lattices leg

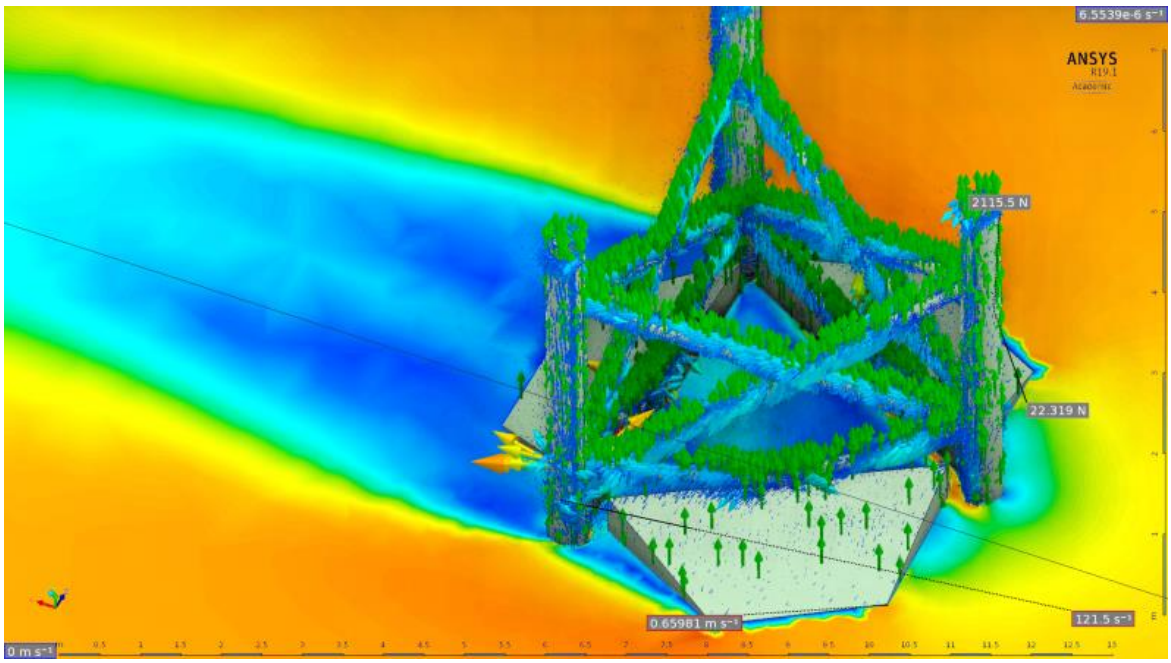

Figure 4-50 Flow velocity magnitude showing force &Vortices

4.26 SEA BOTTOM EFFECT ON TRUSSED TYPE LEG

4.26.1 Steady state conditions

To evaluate the effect of sea bottom on the rack and chord type lattices leg spudcan, the author decided to use CFD analysis tool. The cases analyse are as indicated below in Table 4-8.

Table 4-8 Trussed Leg spudcan sea bottom effect

Case	Current (knot)	Leg Speed (m/min)	Distance from seabed (mm)
1	2	0	0.001
2	2	0	50
3	2	0	1000
4	2	0	2000
5	2	0	3000
6	2	0	5000
7	1	0	0.001
8	1	0	50
9	1	0	1000
10	1	0	2000
11	1	0	3000
12	1	0	5000
13	0.5	0	0.001
14	0.5	0	50
15	0.5	0	1000
16	0.5	0	2000
17	0.5	0	3000
18	0.5	0	5000

The case results at 2 knots are shown below in Figure 4-51 and in Figure 4-52, the drag force observed with increased in forces as approaching to the seabed by about 6%, from 3 m.

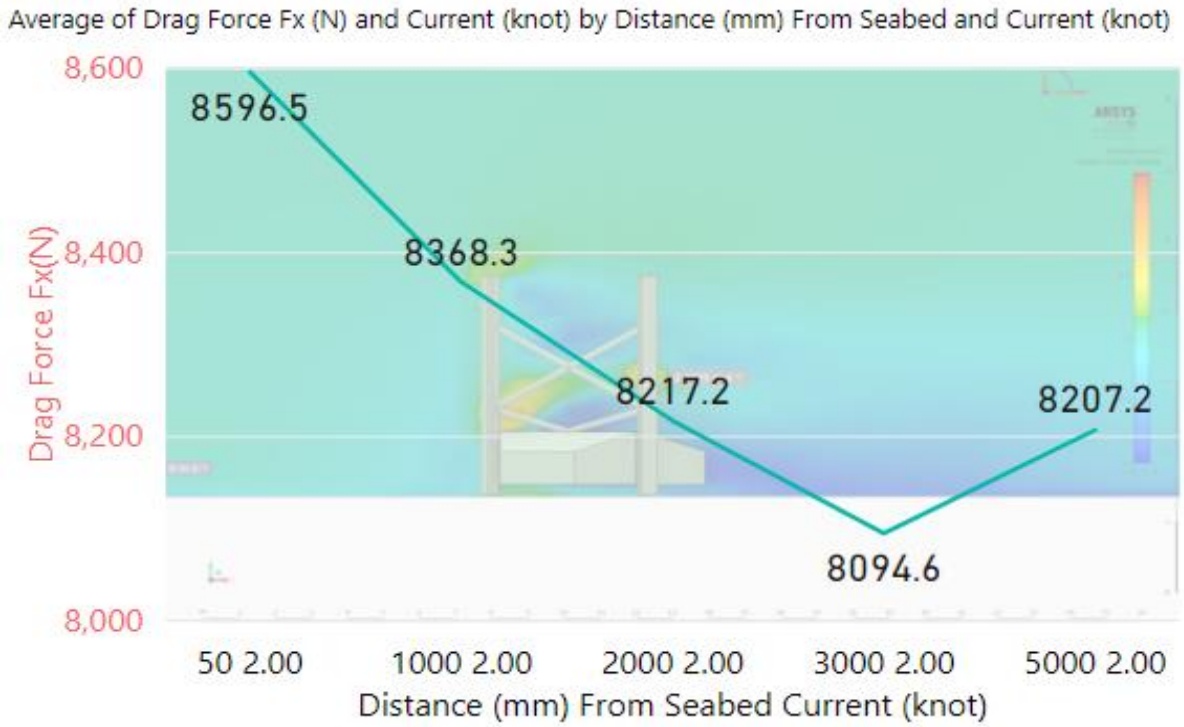

Figure 4-51 Drag force effect near seabed for trussed design legs

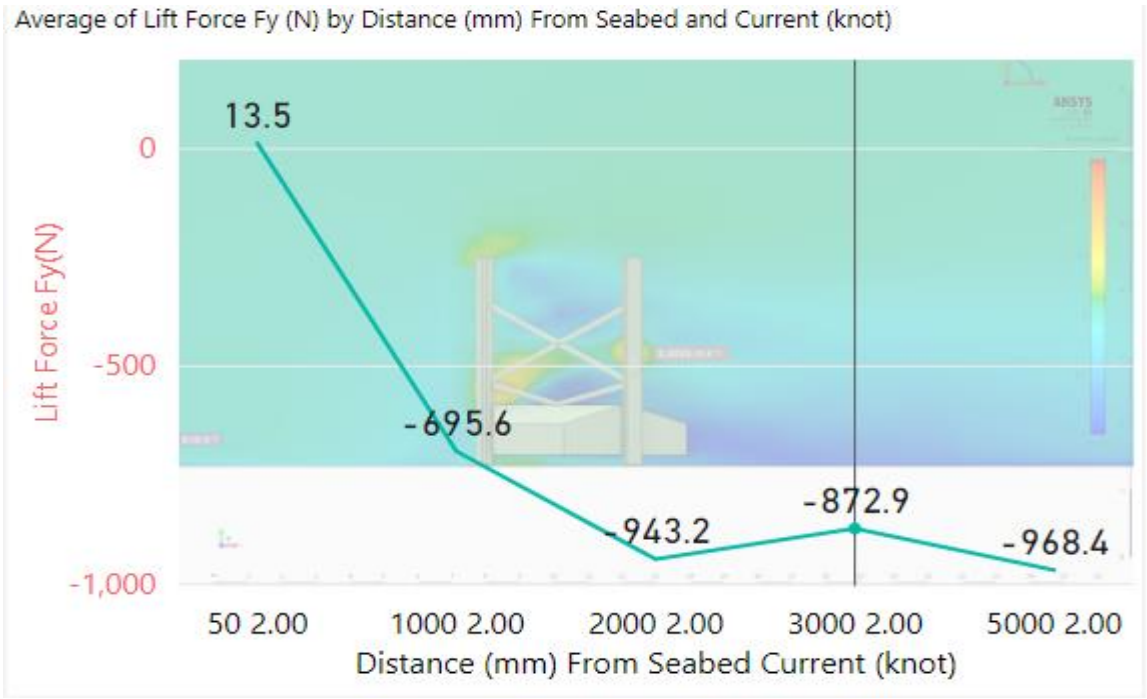

Figure 4-52 Lift force at 2 knot Vs distance from /sea bottom

The lift force on the other hand seen responding in other way, the change in direction indicates it's helping the bottom pressure pushing the spudcan upwards compared to it was opposing when spudcan far from seabed i.e., half of the diameter of the spudcan. The peculiar trends observed for cylindrical legs also observed in the trussed type legs. The CFD results confirms the seabed vicinity on the spudcan remains similar despite the differences in the leg design.

5 OFFSHORE EXPERIMENT DP AND JACK-UPS SIMOPS

5.1 BACKGROUND OF OFFSHORE EXPERIMENT

The offshore industry has a plan to use DP jack up vessel for various installation work in offshore and renewable market. Typical work involved well interventions, lifting of modules, installation of wind turbine and pile etc. One of such installation is 250 piles installation for oil and gas LNG hub development, using DP jack-ups vessels. The piles are densely populated. The piles installed using specially design unit called outrigger, which is installed on DP jack ups vessel. The outrigger has capability to install more piles from same locations in the elevated mode of operations thus helping in reducing number of moves. The solution provides cost effective engineering solution to project and as well as to the industry. The design solution provider claims this will help in reducing the risk of damage to installation as they have DP system capable to maintain the station keeping. The project overview shown below in Figure 5-1

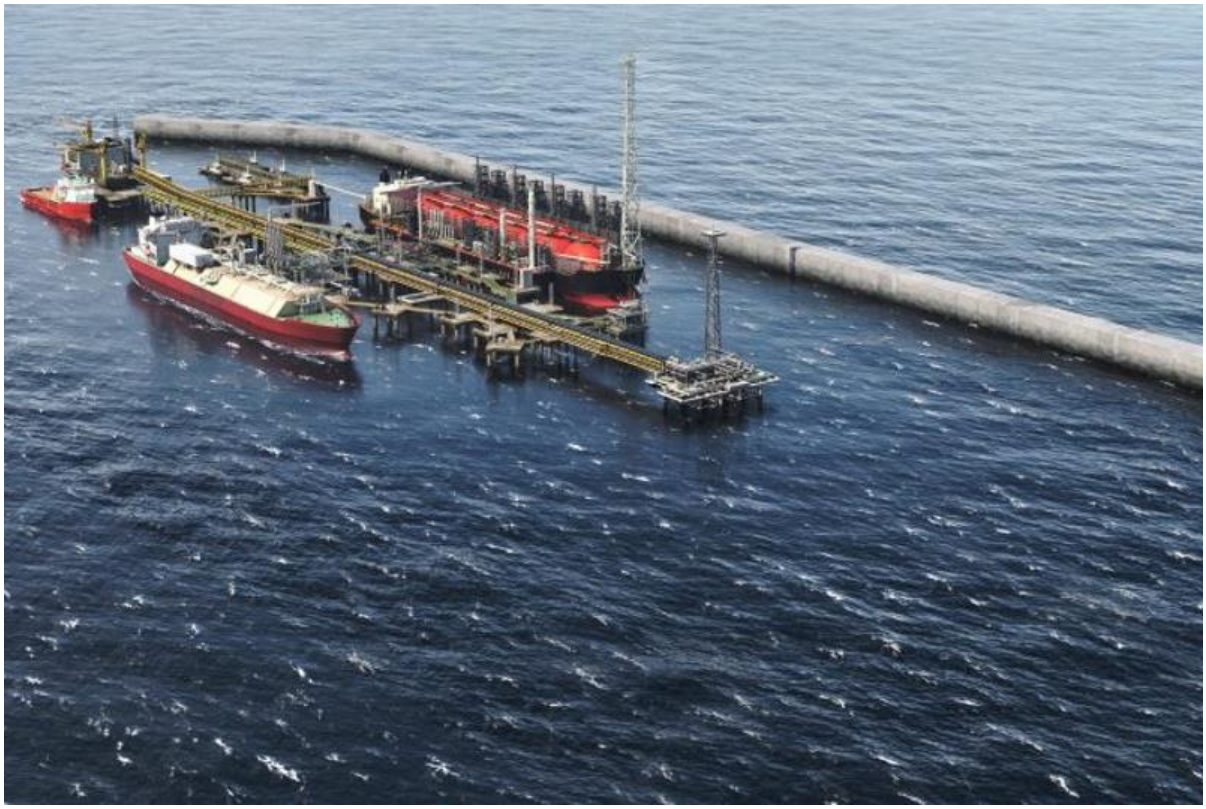

Figure 5-1 Project required 250 piles installations (Courtesy BP)

Being a DP professional one of the authors roles is to assist our client to identify the operational risk by assessing vessel documentation and witness DP trials to access vessel performance

and compare this with project needs. The project outline shows it needs over 100 moves to install 250 piles. Some of the jack ups moves does need very tight position keeping of the marine DP jack-ups vessel. The vessel must control position deviation while approaching and moving away from installation to avoid damage to the assets due to collision. The Figure 5-2 below indicates one of the jack ups positioned and clearance, when vessel motion applied to the DP vessels.

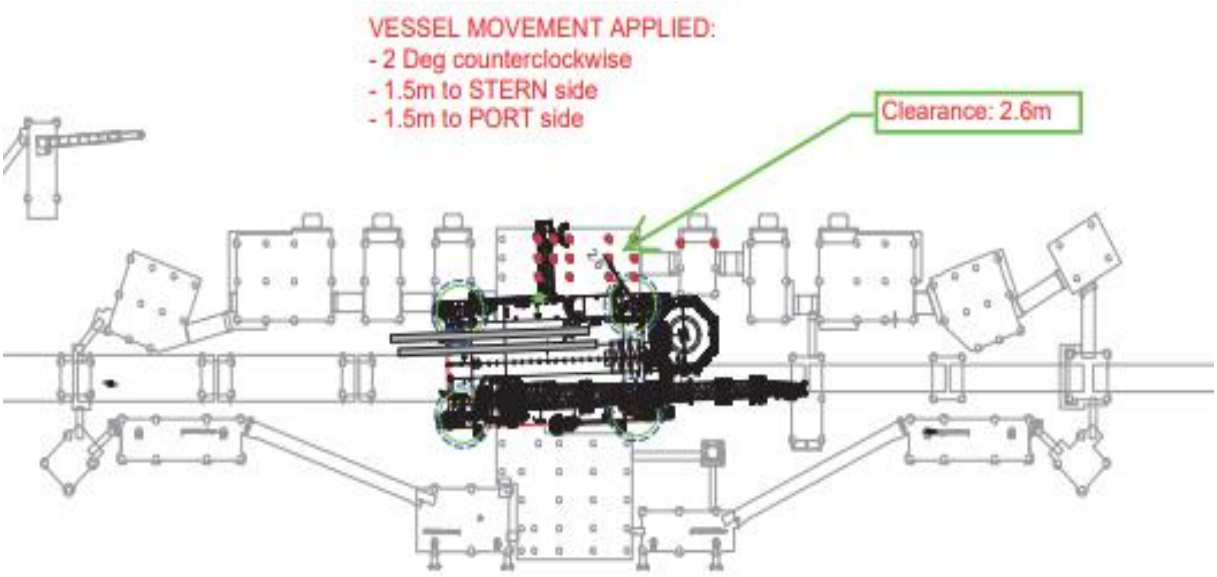

Figure 5-2 Minimum clearance during DP Jack up move

The DP and vessel design documentations reviewed, and various tests were proposed to check fit for purpose. The offshore experiment is conducted on the DP jack-ups vessel, which has a similar cylindrical type of leg and spudcan shape. The experiment is conducted to see the station keeping response of the installed DP system during the SIMOPS operation. Particularly focusing on the leg spudcan lowering to the seabed and lifting of the leg spudcan from the seabed.

The procedure of the vessel followed, during SIMOPS (i.e., DP and Jacking) operations for approaching and leaving the test positions. The DP system designer has modelled the leg without spudcan in his mathematical model for DP system for estimating the vessel position and heading. Since the leg length and load interface between DP and Jack ups were not made ready at the time of test, it was agreed to take the information of leg length from Jacking system and enter manually.

The leg length below the keel line is entered manually in the DP system. The DP vendors are using Morrison equation to calculate the forces in surge, sway direction and moment in yaw direction. The Morrison equation has limitation and recommended ratio for diameter of leg /wavelength < 0.2, however the diameter of the leg is 4.0 m, means for the wavelength of 8 m > above the results of inline drag forces obtained using Morrison equation will provide acceptable results.

These forces are measured in the surge and in sway directions, while moment is measured in yaw direction. The DP system has a mathematical model and non-measured forces are accounted for the DP system as a residual current force. The experiment is conducted for both Leg spudcan lowered (Down) and Leg spudcan removal (Up).

During the spudcan removal the DP system engineer has applied various gain factors in surge, sway, and yaw directions to the mathematical model, to improve the thruster response for maintaining the position and heading of the vessel, which was not successful. The water depth at the location measured using echosounder Figure 5-3

Figure 5-3 Echosounder measurement of water depth from keel

The details of the Spudcan, depth below keel and expected penetration at the experiment site is shown below in Table 5-1

Table 5-1 Details of water depth and expected penetration at offshore experiment site

Water Depth below keel	20.4 m
Spudcan Height	1.8 m
Expected Penetration	1.5 m

Based on above details, leg length on the jacking system will be sum of above = 23.7m. The jacking system overview shows the details of the leg below hull in Figure 5-4

Figure 5-4 Jacking system leg load and distance below hull

5.2 DP STATIC CAPABILITY PLOTS DESCRIBING LEG LOWERING CONDITIONS

5.2.1 DP capability plots are usually used by vessel owners for selecting the vessel for their operations. Typically, it shows four cases

a. Intact – All thrusters working

b. Single failure minimum effect – loss of single thrusters which has minimum effect.
c. Single failure maximum effect – loss of single thruster, which has maximum effect
d. Worst case - Loss of thrusters based on worst case failure design intend effect.

Worst case failure design intend of the vessel can be found in the failure more effect study documents of the vessel.

The limitation of static capability plots, they do not show the time domain response of the vessels, meaning vessel response in real time. The dynamic allowance used in the DP capability plots are nothing but spare thrust to compensate the losses occurred due to wind and wave drift load, typically, these dynamic factors are 1.25 times. The DP Capability plots were prepared by DP system designer to show, DP vessels when operating in different water depth e.g., 29m and 32m.

The vessel particular of the offshore experimental vessel is shown in Table 5-2 below.

Table 5-2 Offshore vessel particulars

1.	Length over all	100.2 m
2.	Length between perpendiculars	75.7 m
3.	Breadth	40.0 m
4.	Draught	3.4 m
5.	Displacement	9723.0 t
6.	Leg diameter	4.3 m
7.	Thrusters (4 nos.) Retractable Azimuth (T1 to T4)	4 x 903 kW
8.	Jacking Speed UP and DN	0.4 m/min and 0.5 m/min

The overview of Jack ups shown below in Figure 5-5.

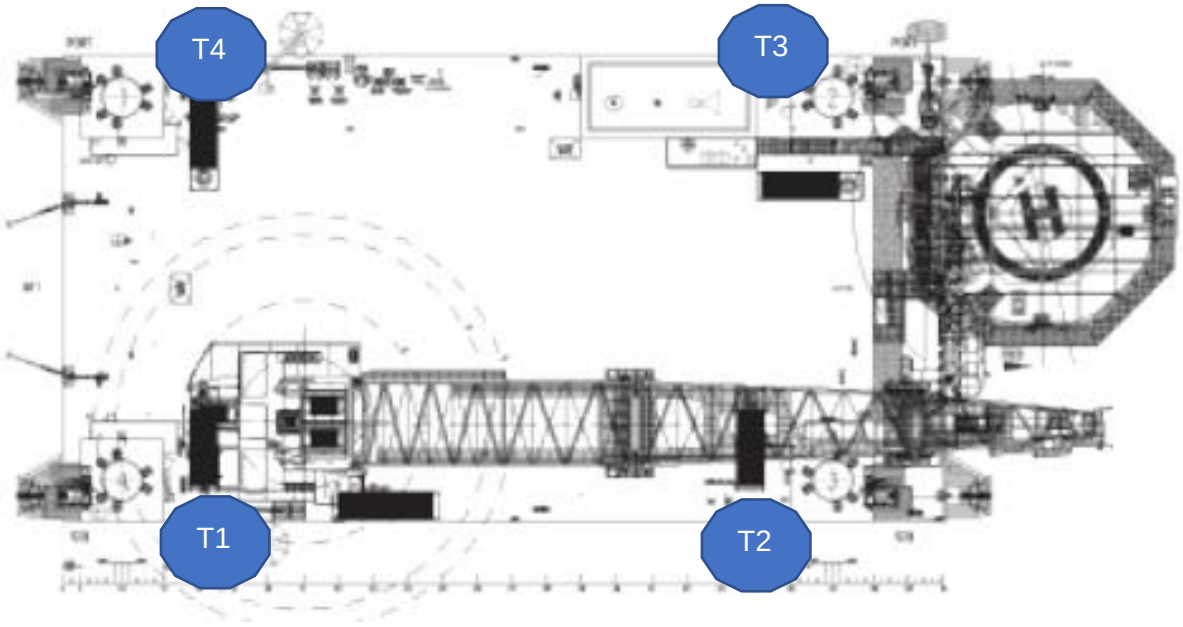

Figure 5-5 General arrangements of Offshore vessel

The static DP capability are produced for wind dominating or power dominating cases. The wind dominating case DP capability plots shows wind envelope, vessel is capable of maintaining position. The power dominating plots typical done for offshore operational conditions. They are producing for fixed worst environment estimated case. The objective of this DP plots is to check if the vessel has sufficient thrust power to support the operations after posts worst case failure so that operation can be safely terminated.

In order to identify the effect of acting wind, current and wave on the station keeping of the vessel the load coefficients are applied. The choice of coefficients depends on area of model test results or CFD analysis and geographical area environmental conditions.

The DP capability plot shown below in Figure 5-6 for Intact case with 10 meters lowered leg. Under these conditions all thrusters are working. The capability plot below is showing thruster loading when constant environment of wind 19.5 knots and significant wave height Hs of 1.5m, wave period Tz 6.2 sec applied acting colinear in rotating envelope to the jack ups vessel. The maximum thruster loading of approximately 55% found when the environment acting at 70 degrees on the beam of the vessel, while minimum thruster loading of approximately 28% found when the environment acting at 0 degrees on the bow of the vessel.

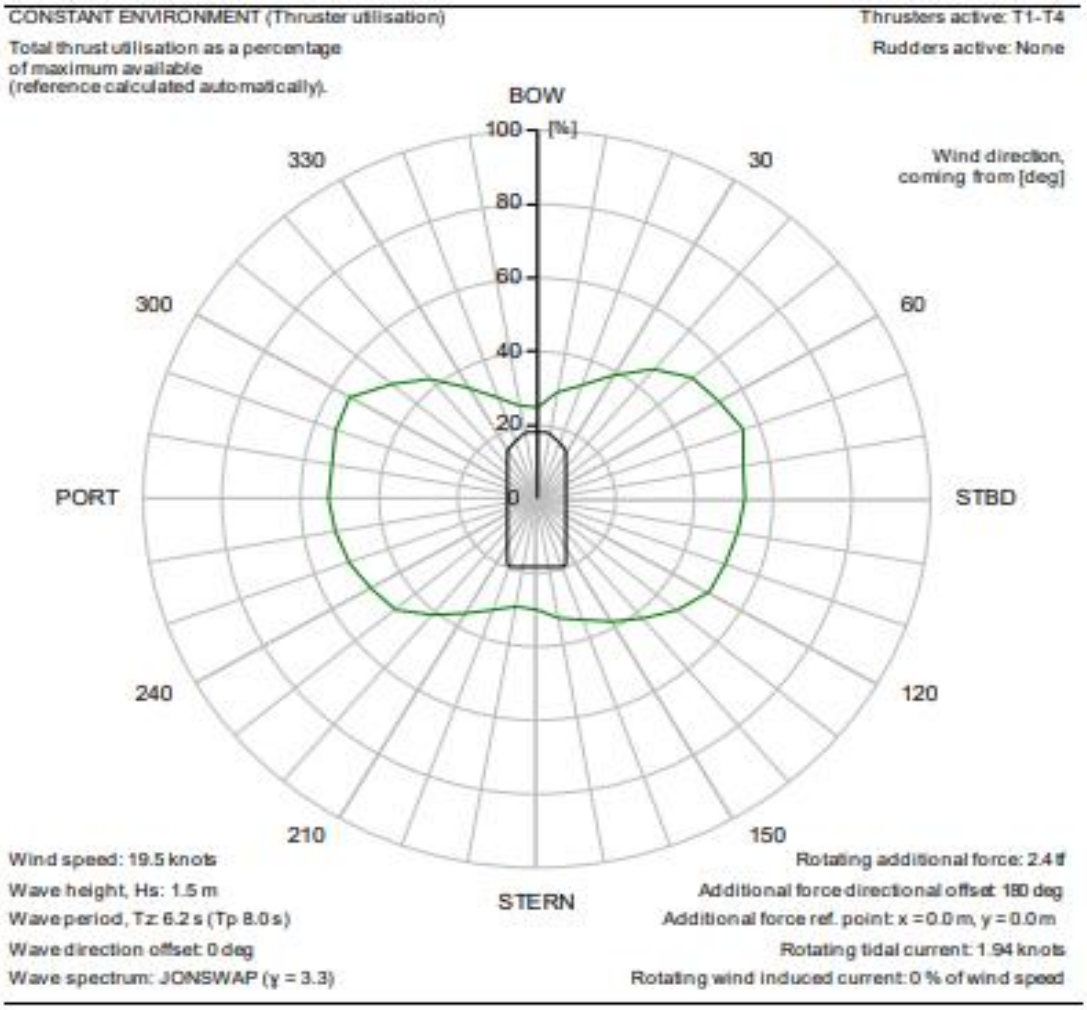

Figure 5-6 DP capability plot for Intact case with leg lowered 10 m below hull.

The DP capability plot shown below in Figure 5-7 for WCF case with 10 meters lowered leg. Under these conditions only T1, T2 and T4 thrusters are working. The capability plot below is showing thruster loading when constant environment of wind 19.5 knots and significant wave height Hs of 1.5m, wave period Tz 6.2 sec applied acting colinear in rotating envelope to the jack ups vessel. The maximum thruster loading of approximately 92% found when the environment acting at 80 degrees on the beam of the vessel, while minimum thruster loading of approximately 32% found when the environment acting at 0 degrees on the bow of the vessel.

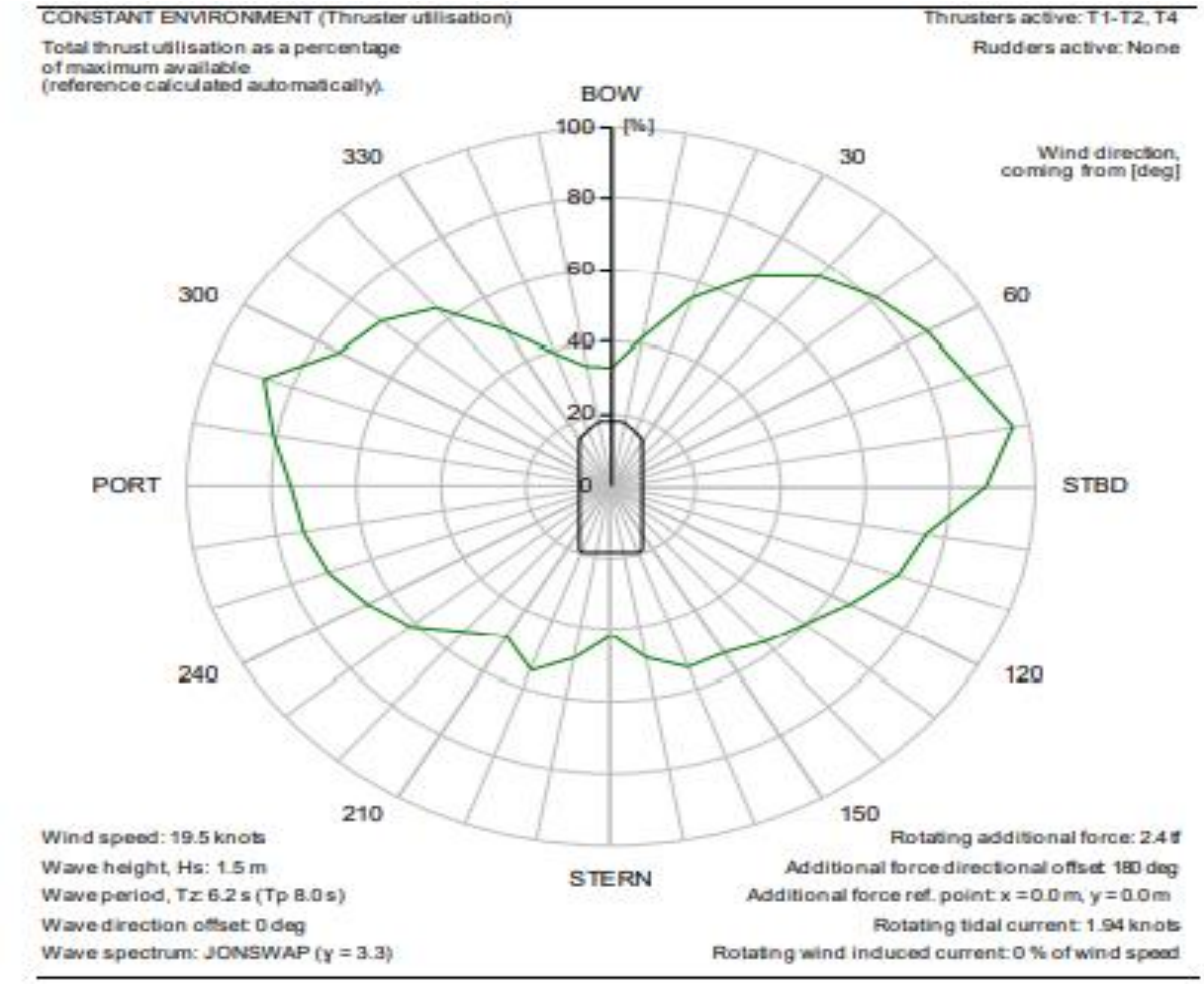

Figure 5-7 DP capability plot for WCF case with leg lowered 10 m below hull.

The DP capability plot shown below in Figure 5-8 for intact case with 30 meters lowered leg. Under these conditions all thrusters are working. The capability plot below is showing thruster loading when constant environment of wind 19.5 knots and significant wave height Hs of 1.5m, wave period Tz 6.2 sec applied acting colinear in rotating envelope to the jack ups vessel. The maximum thruster loading of approximately 60% found when the environment acting at 70 degrees on the beam of the vessel, while minimum thruster loading of approximately 30% found when the environment acting at 0 degrees on the bow of the vessel. The higher thruster utilization confirms the impact of drag forces on station keeping due to the leg spudcan.

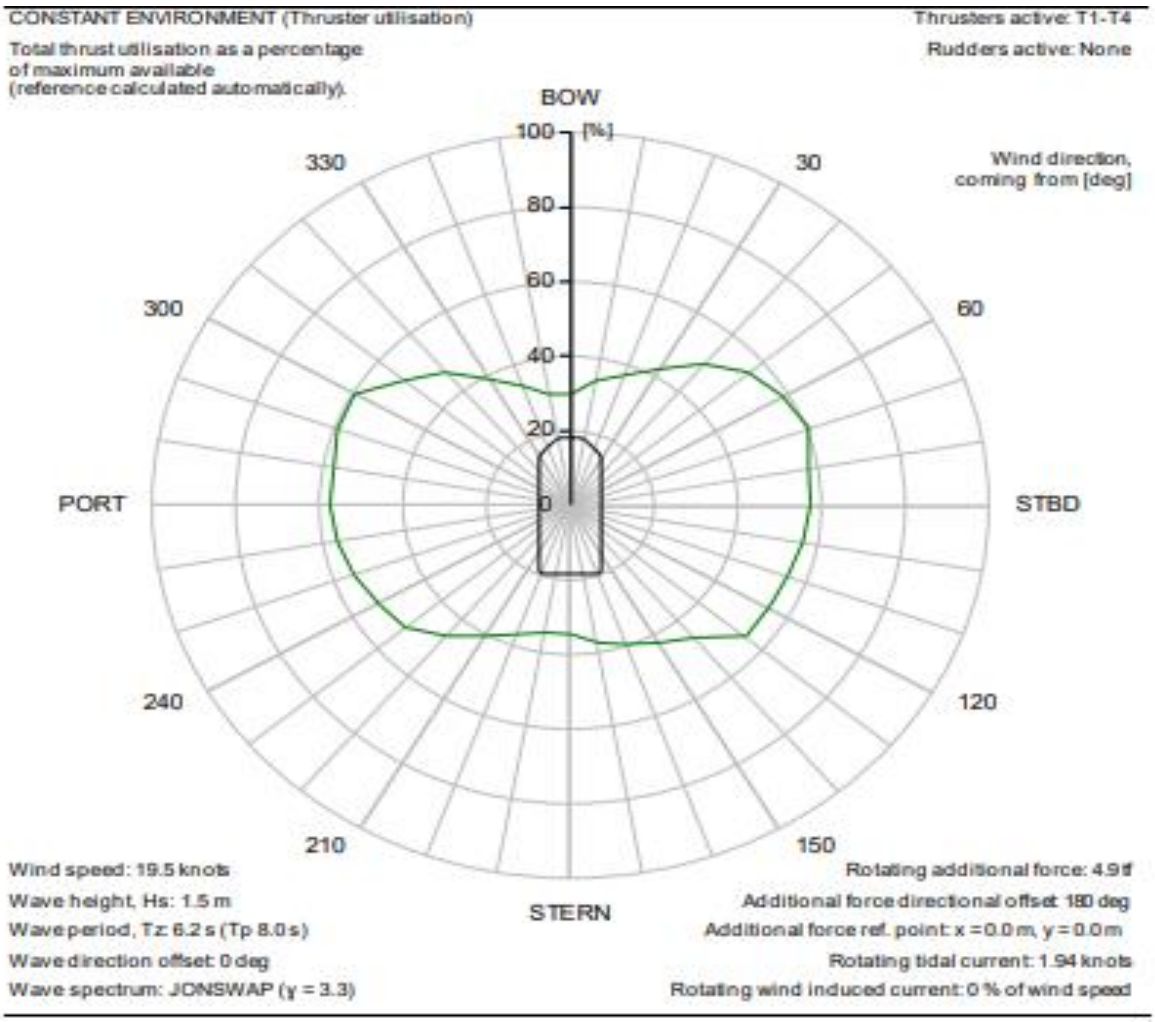

Figure 5-8 DP capability plot for Intact case with leg lowered 30 m below hull.

The DP capability plot shown below in Figure 5-9 for WCF case with 30 meters lowered leg. Under these conditions only T1, T2 and T4 thrusters are working. The capability plot below is showing thruster loading when constant environment of wind 19.5 knots and significant wave height Hs of 1.5m, wave period Tz 6.2 sec applied acting colinear in rotating envelope to the jack ups vessel. The maximum thruster loading of > 100% found when the environment acting at 75-85 degrees on the beam of the vessel, while minimum thruster loading of approximately 40% found when the environment acting at 0 degrees on the bow of the vessel.

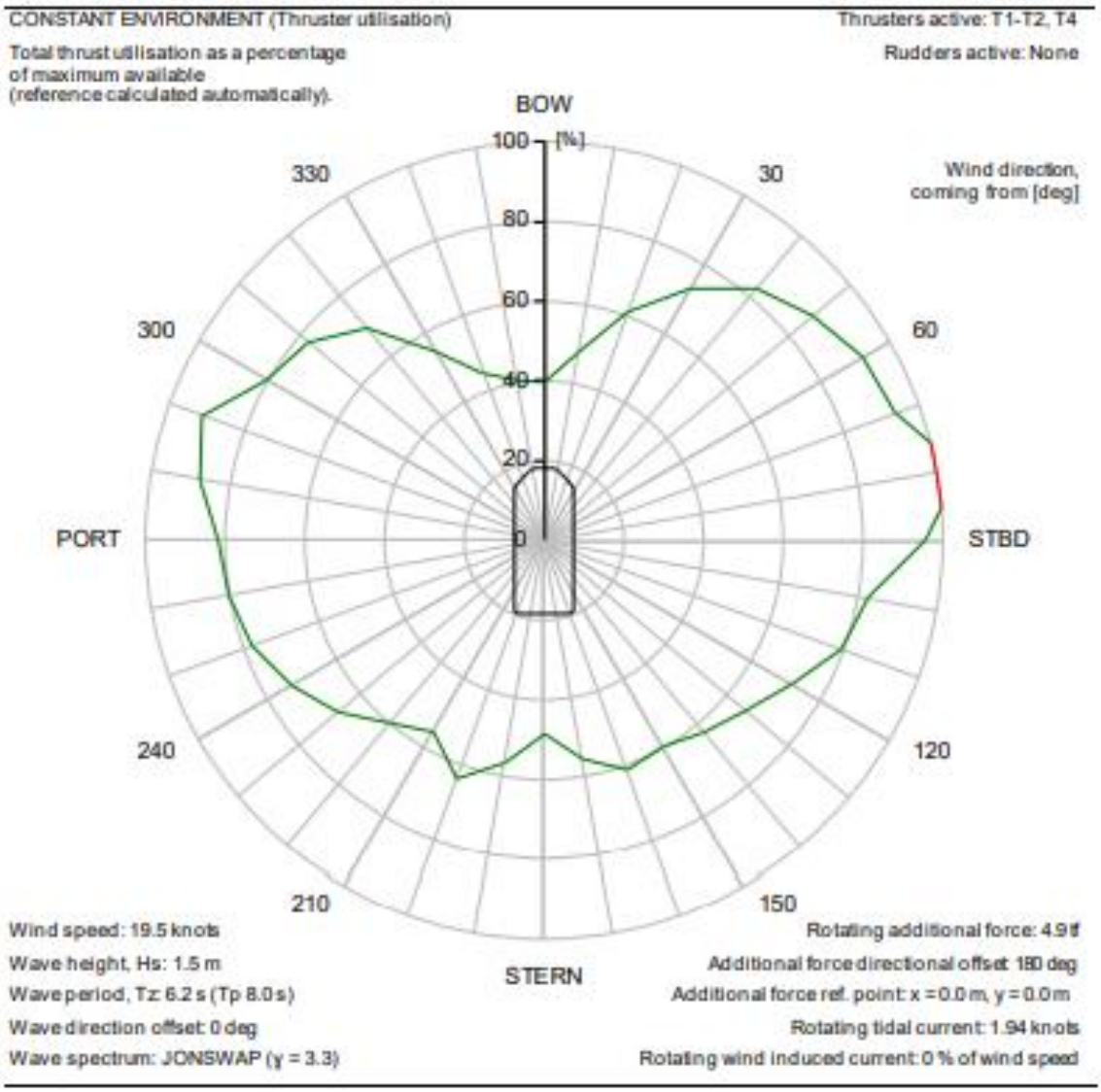

Figure 5-9 DP capability plot for WCFD case with leg lowered 30 m below hull.

5.3 MISINTERPRETATION AND PROJECT RISK

The DP Static capability plots results though shows the vessel has sufficient power to maintain the positions at project desired water depth. The system does not provide the time domain response of station keeping drift / drive off response. The seabed effect completely neglected by many vessel owners and charters. The seabed near effect seen in the chapter 4 above confirms CFD and tank experiments demonstrate increases in sudden drag. This increase in drag not considered by DP mathematical model and as results the vessel drifting become sensitive issue. This is the most critical time for both Jack ups and assets. Our intension of offshore experiment is to demonstrate this gap in risk acceptance to the charter as well as to the vessel owners.

5.4 OFFSHORE EXPERIMENT LEG DOWN CASE

The experiment conducted in North Sea area in a water depth of approximately 20 m. The vessel is equipped with cylindrical legs powered via hydraulic power. The leg lowering 0.4m/min and lifting speed 0.5m/ min. The vessel has four thruster's azimuth retractable type for DP station keeping.

The DP screen seen below in Figure 5-10 shows the jack ups leg length interface (manual input/sensor), leg direction down and up with DP system. During offshore experiment the variable wind was in the range of 8 to 15 knots and estimated sea current 0.4 to 1 kts.

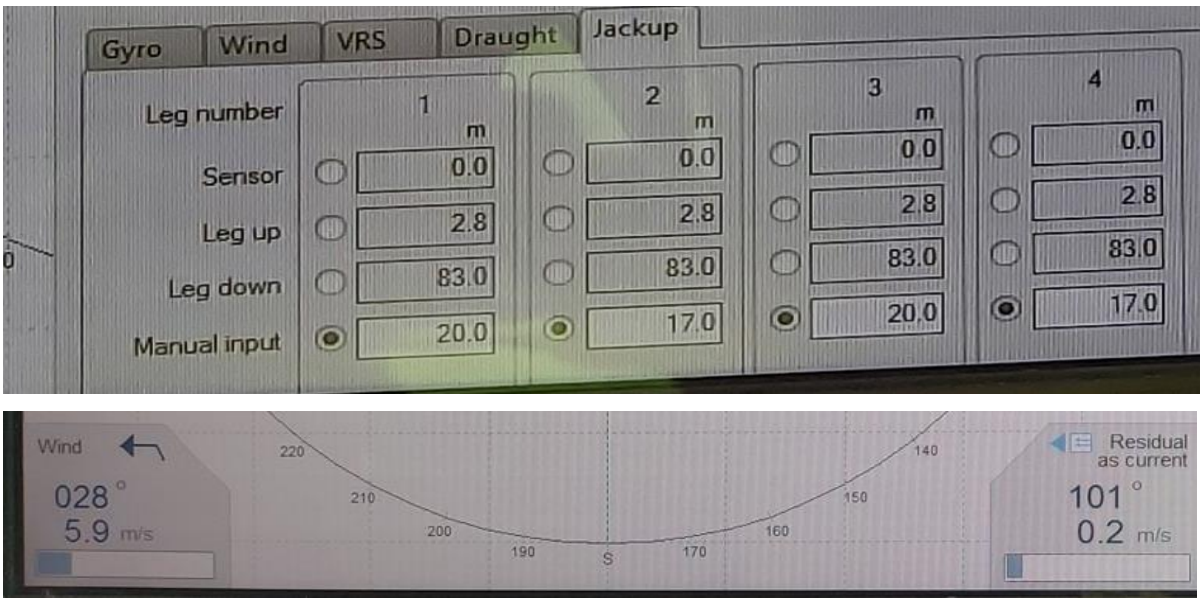

Figure 5-10 Jack up leg interface with DP system and environment

The DP system designer has modelled the leg geometry in the mathematical model to add forces due to legs which could affect station keeping and shown below in Figure 5-11. The equation used by DP vendor is Morrison equation for leg force calculation.

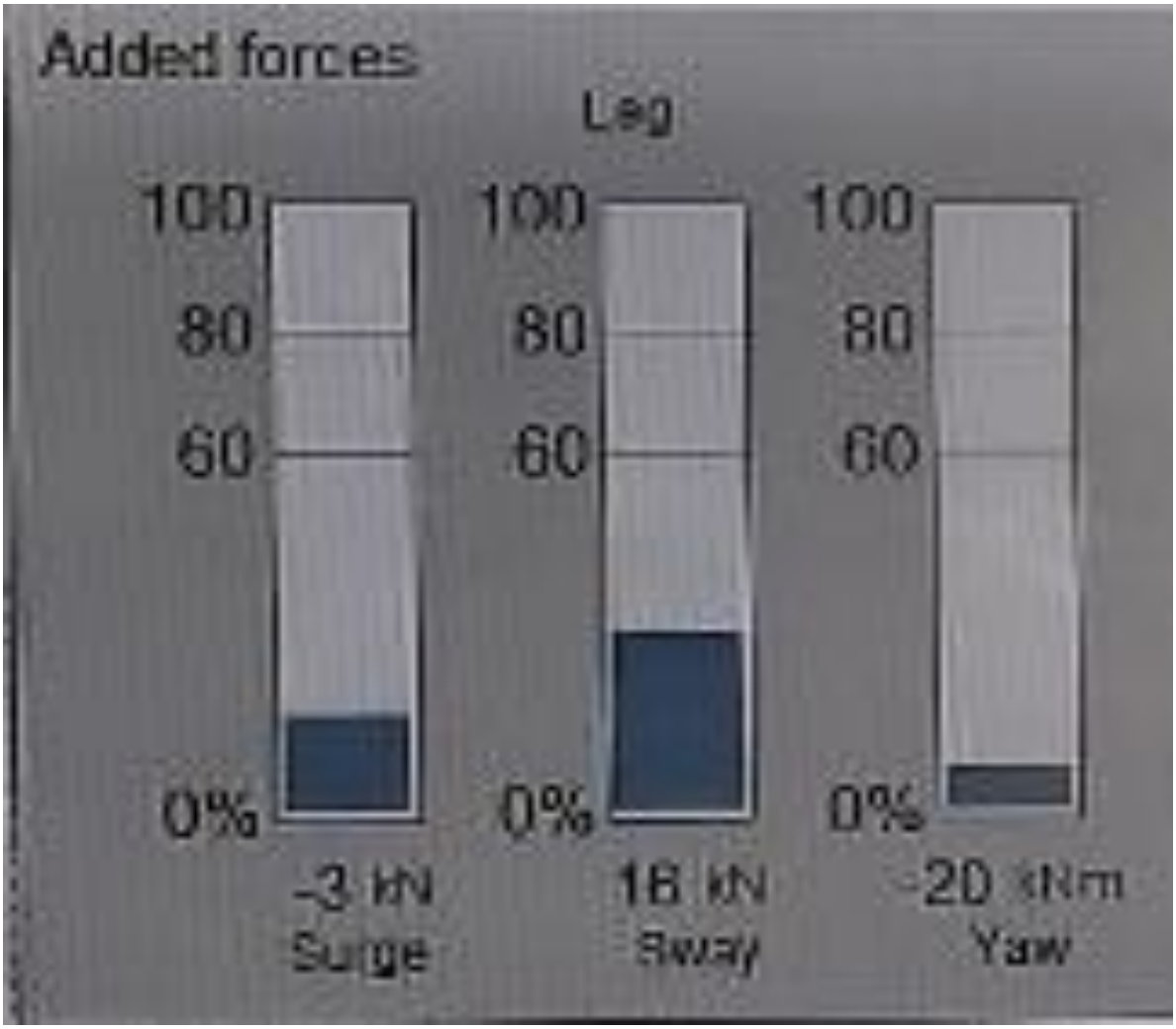

Figure 5-11 Added forces due to leg in DP

During the leg lowering cases, the author first observed the impact on heading changes due to leg lowering measured and this is shown below in Figure 5-12. The deviation clearly shows approximately 1.5 degree heading change.

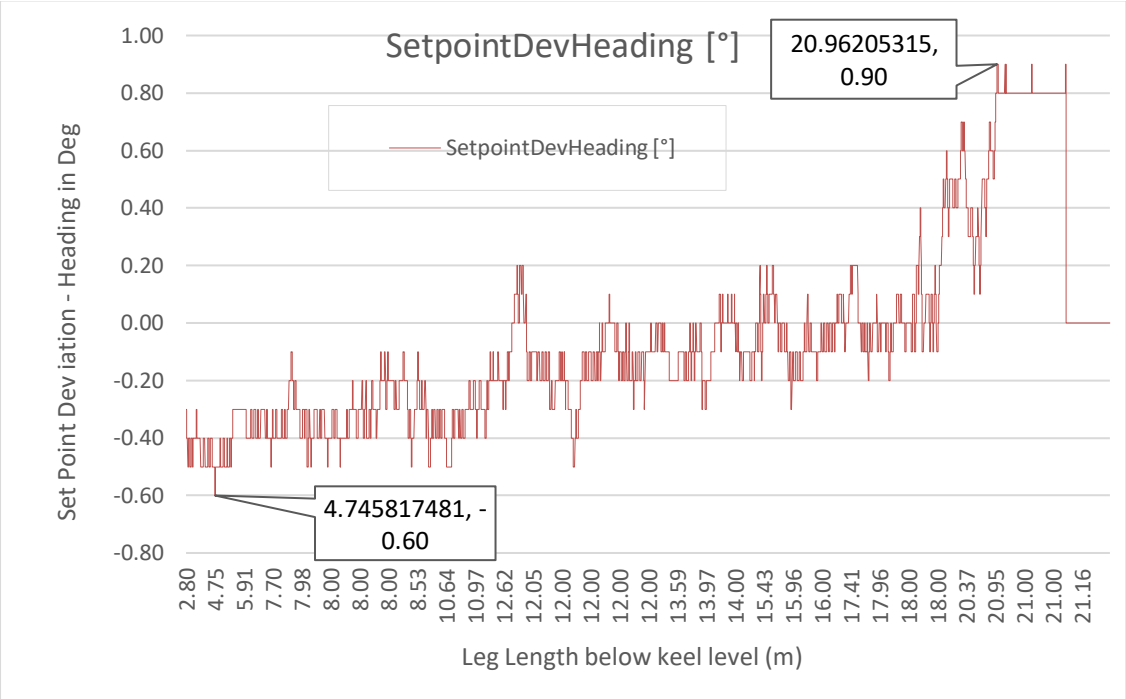

Figure 5-12 Heading change during leg lowering

The impact on the position measured in surge directions during leg lowering is shown below in Figure 5-13. The position deviation noted to be approximately 2.1 from the original position,

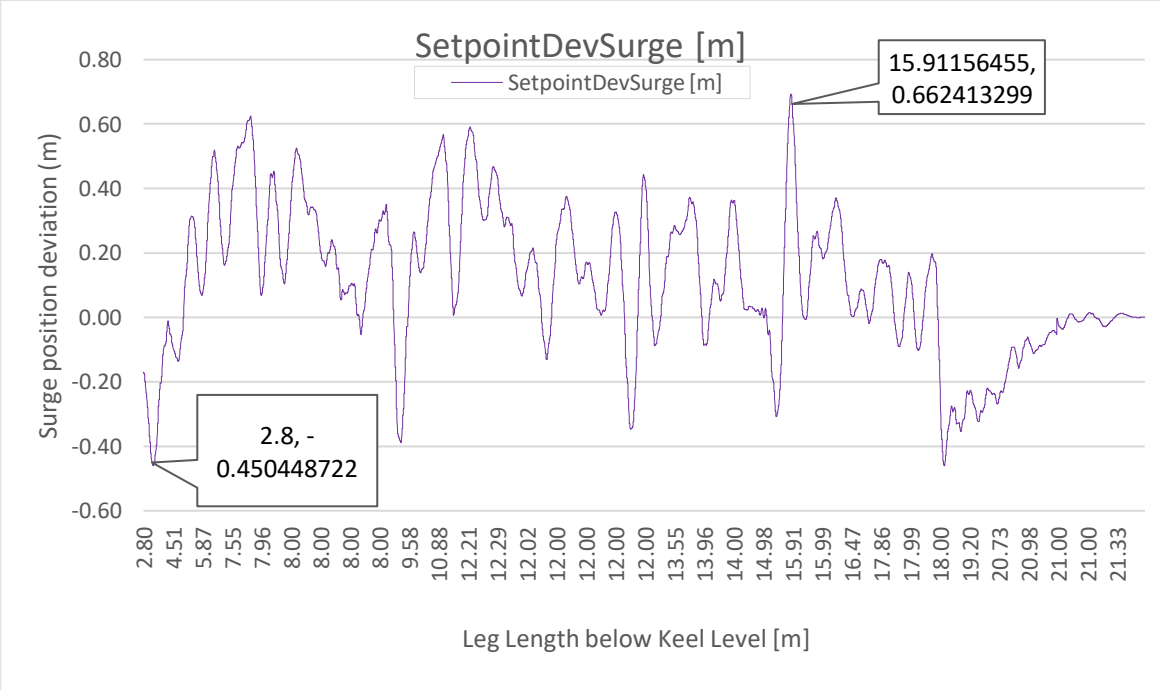

Figure 5-13 Surge position deviation during leg lowering

The impact on the position measured in sway directions during leg lowering is shown below in Figure 5-14. The position deviation noted to be approximately 2.0 from the original position,

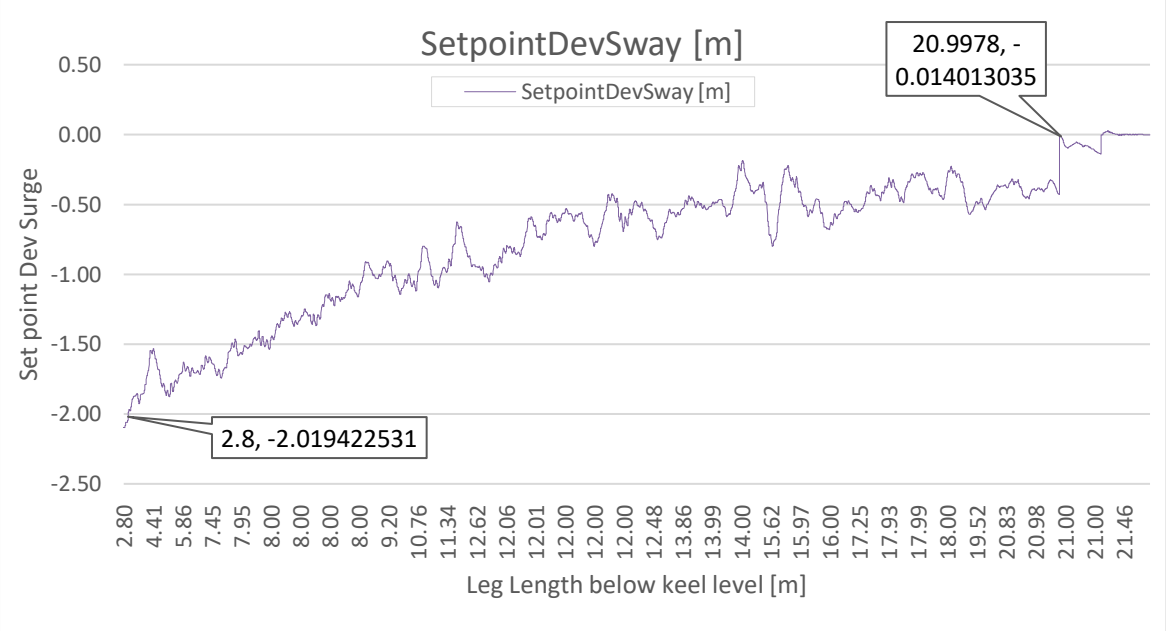

Figure 5-14 Sway position deviation during leg lowering

The DP system mathematical model utilizes wind-current and wind-wave relationships to estimate the forces in surge, sway direction and moment in yaw direction. The unaccounted forces not covered by inputs to mathematical models deal as a residual force. This is achieved by residual/DP current function. The leg lowering sway forces in Figure 5-15 clearly shows peculiar behaviour of increasing and decreasing pattern. When the leg is lowered to 7.8 m, the sway forces calculated by DP system is (-) 26.5kN. However, when the leg is lowered to 8 m, the sway force calculated by DP the system is (-) 20.6 kN. The leg sway force at 20m is calculated by DP system is (-) 21.6 kN, while the sway force at 21.9m calculated as (-) 15.7 kN. The negative sign indicates the force during leg lowering. The increase in forces from 20 to 21.9 m noted as 5.9kN. The increase in forces typically 27%. The increase in sway forces on leg spudcan when in closed vicinity compliment CFD and tank experiments. The Morrison equation in DP system needs careful approach as ratio of diameter of leg to wavelength is greater than 0.2. The reasons of higher sway force at lower leg length also needs investigation.

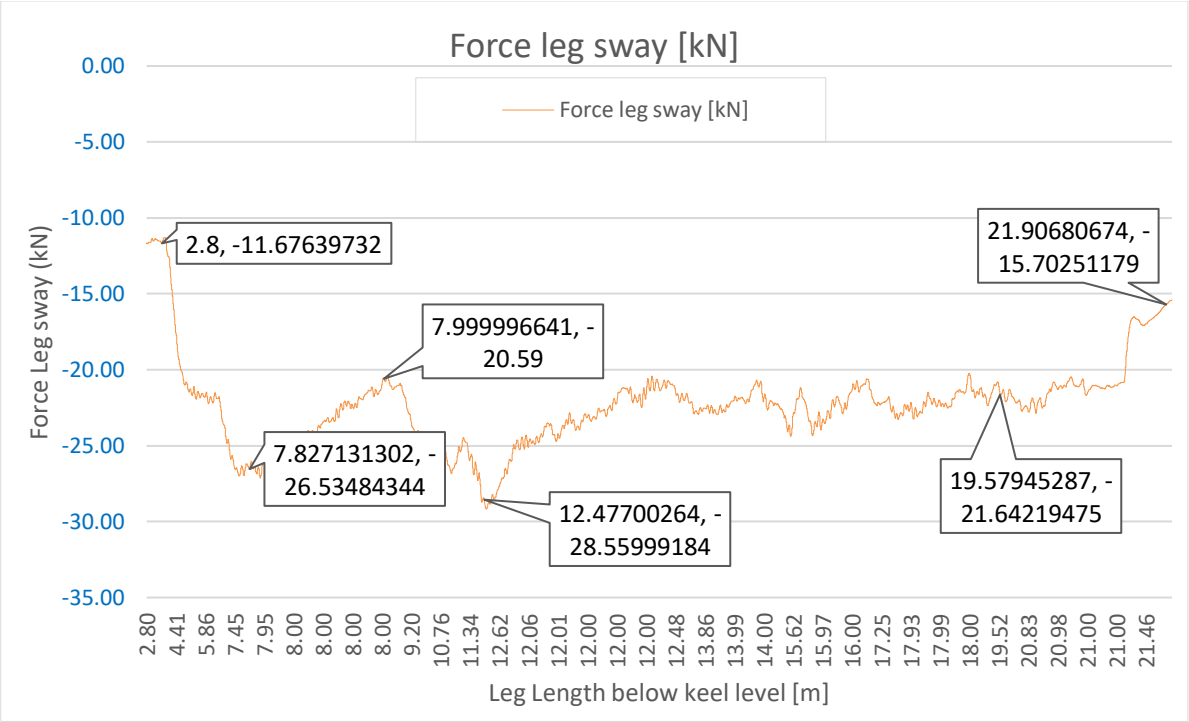

Figure 5-15 Current acting on the vessel during leg lowering – sway leg Force

The leg lowering leg surge force in Figure 5-16 clearly shows peculiar behaviour of increasing and decreasing pattern. From 18 m to 21 m of leg lowered cases, the surge forces increased from 18.3 to 34.7 kN. The drop in surge force indicates soft pining of spudcan in seabed.

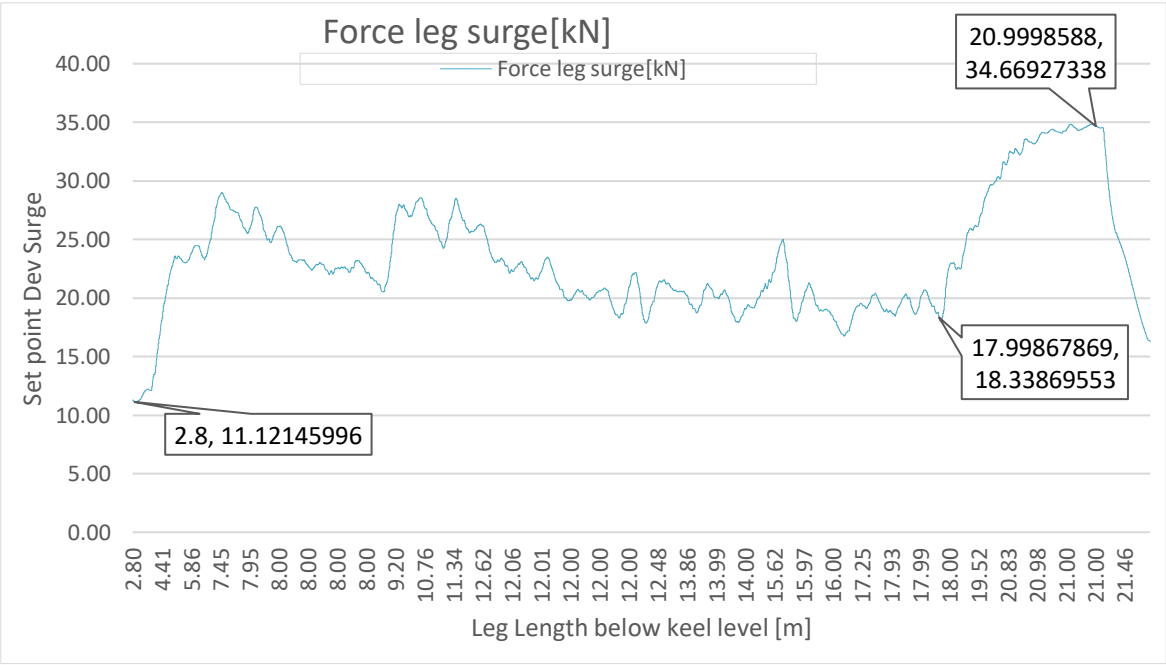

Figure 5-16 Current acting on the vessel during leg lowering – surge leg Force

5.5 OFFSHORE JACK UP EXPERIMENT LEG UP CASE

During spudcan removal case, the DP system was first started and kept in DP joystick mode for approximately 30 min. The jacking master then slowly started retrieving the leg from the seabed.

The heading change is measured over entire leg lifting (i.e. spudcan removal) case and shown below Figure 5-17. The figure clearly demonstrates no change in heading until spudcan in seabed and soon after spudcan detached from the seabed the impact on the vessel heading clearly show. The heading at 22m was noted as 103.2 degrees and soon after spudcan detached from the seabed it was changed to 105.5 deg. The heading change of 2.3 degrees of the vessel can severely impact offshore operations as depending on the size of the vessel the heading change in clockwise or anticlockwise will change bow and stern of the vessel. In case of any assets falling near to bow and aft of the vessel then collision with assets cannot be ruled out.

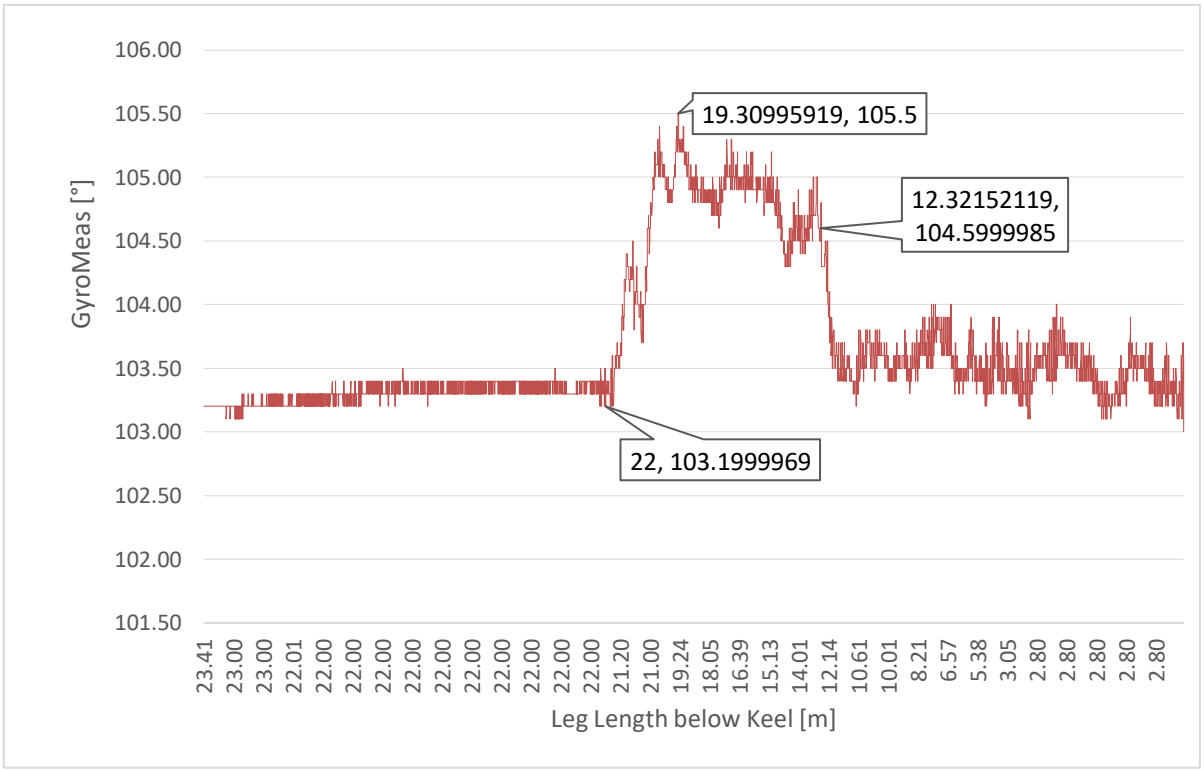

Figure 5-17 Heading change during leg lifting

The position deviation also measured, when carried out operation of jack up spudcan removal and shown below Figure 5-18, capturing the DPO command of DP joystick.

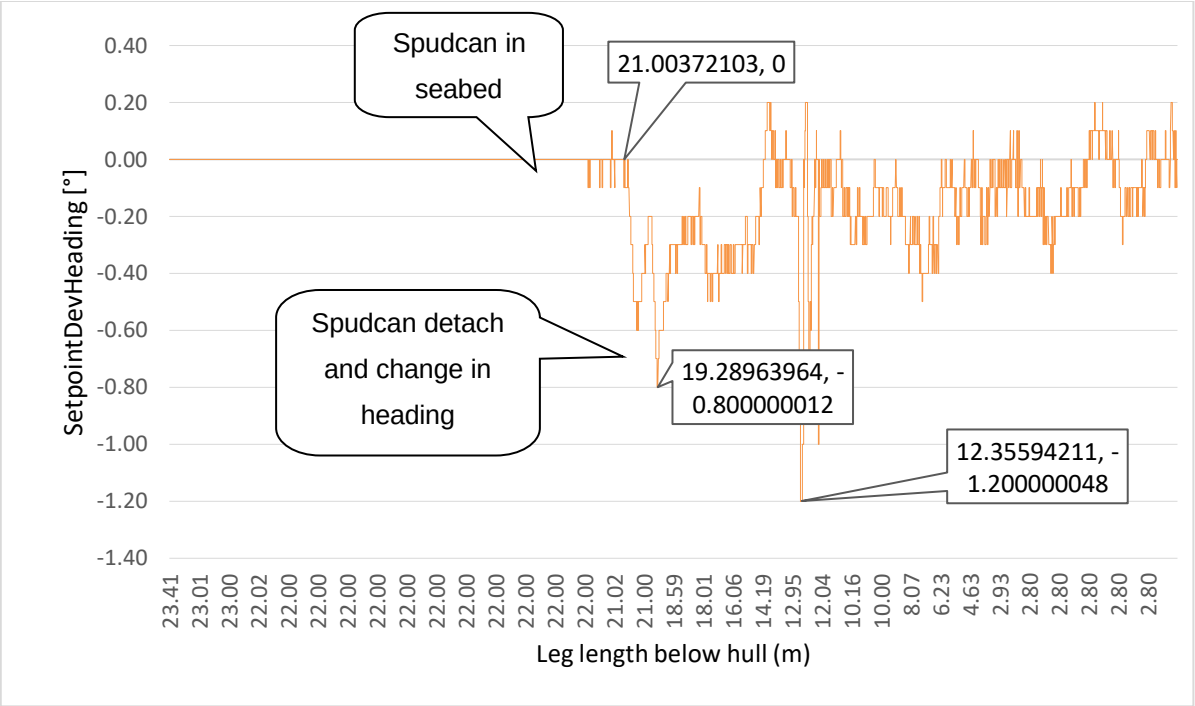

Figure 5-18 Heading set point deviation during leg lifting case

The Figure 5-19 show position deviation in surge direction during leg lifting. When the leg lifted at 21m the position deviation in surge direction noticed to 0.25m from the set point. At 19m the surge deviation noticed 0.26m. The maximum position deviation noted 0.35m, when the leg retracted to 2.8m.

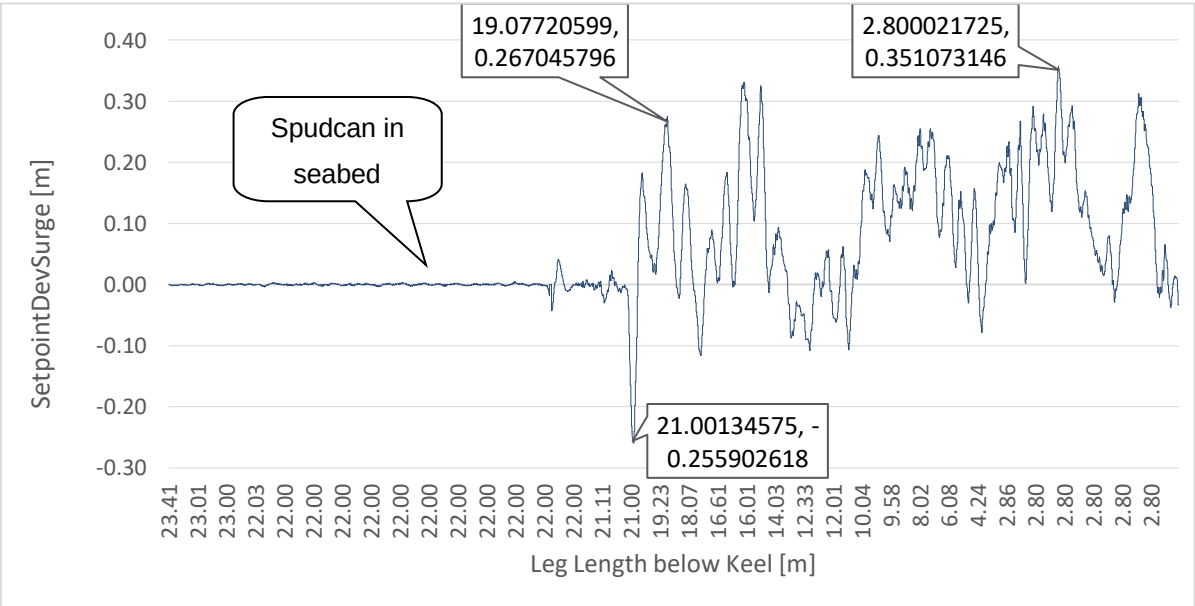

Figure 5-19 Position deviation in surge during leg lifting

The Figure 5-20 shows position deviation in sway direction during leg lifting. It was observed immediately after spudcan detach from the seabed the vessel oscillates among the position set point. When the leg lifted at 21m the position deviation in sway direction noticed to 0.23 m from the set point. At 19m the surge deviation noticed 0.32m. The maximum position deviation noted 0.72m, when the leg retracted to 2.8m.

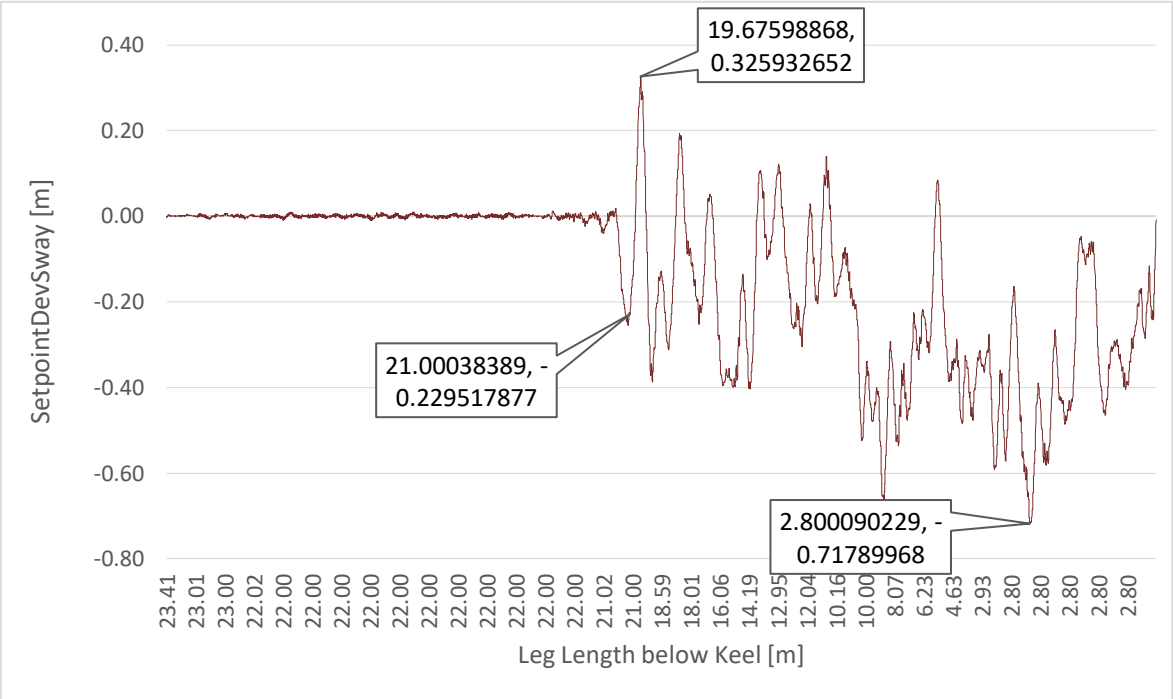

Figure 5-20 Position deviation in sway during leg lifting

It was observed immediately after spudcan detach from the seabed the vessel oscillates among the position set point.

The current acting on the vessel during this experiment was pretty small (approximately 0.05 m/s). The larger current can have bigger deviation among the set points. The evidence proves the position deviation despite vessel in DP to learn the mathematical model for 30 mins. This was predicated before start of experiment as having spudcan in seabed prevents heading and position change means DP mathematical model learning will not help to correct the model.

5.6 DISCUSSION ON THE RESULTS

The forces are measured in the surge and in sway directions, while moment is measured in yaw direction. The DP system has a mathematical model and non-measured forces are accounted for the DP system as a residual current force. The experiment is conducted for both spudcan lowered and spudcan removal. During the spudcan removal the DP engineer has applied various gain factors in surge, sway, and yaw directions to the mathematical model, to improve the thruster response for maintaining the position and heading of the vessel. However, the vessel drifted in a range of 6.8 m to 11 m during various experimental phases and shown below in Figure 5-21 is one of these out of position results, noted soon after spudcan detached from the seabed (i.e.,8.6m)

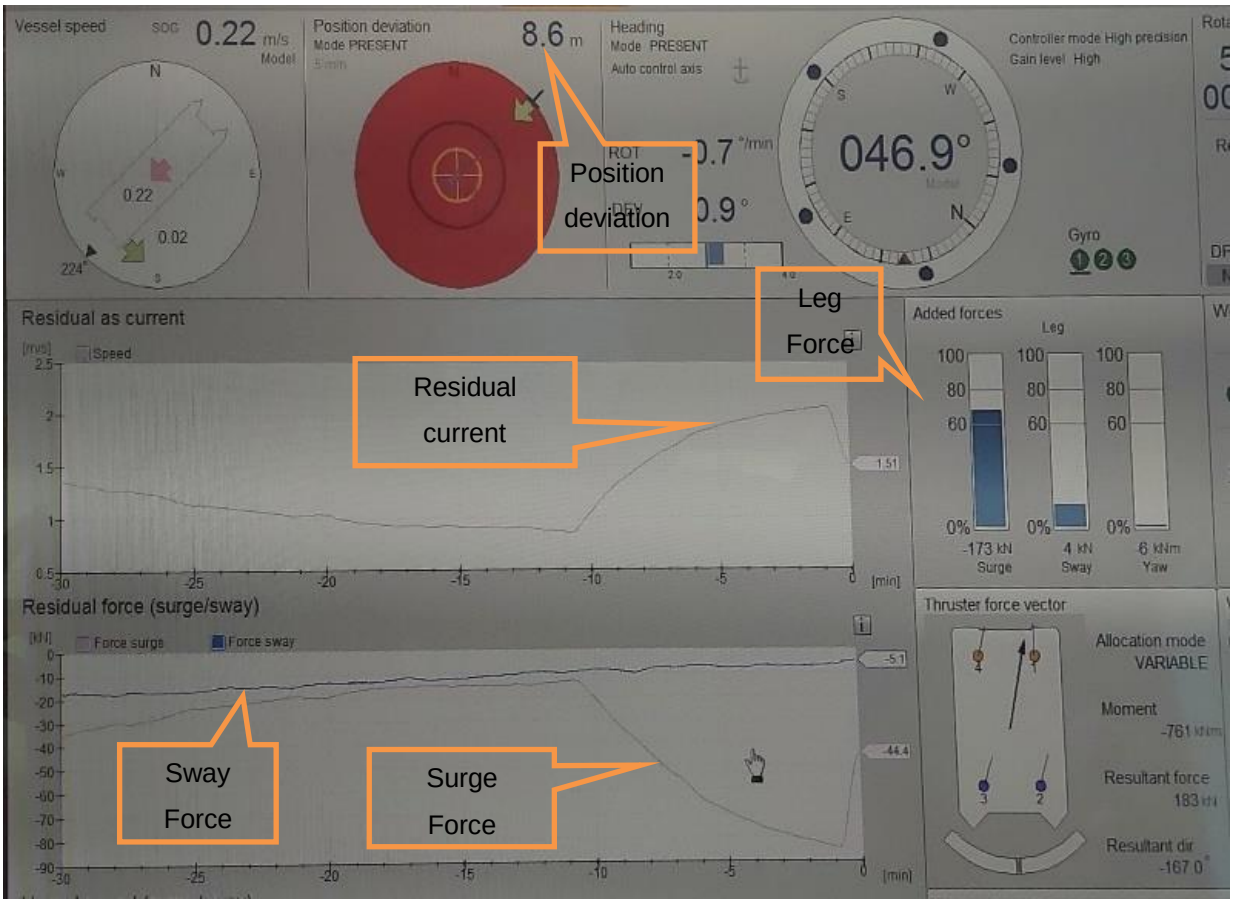

Figure 5-21 Vessel drift when the spudcan was extracted from seabed

The DP residual current functions which are one of the best functions for any DP model is used to account forces not measured by sensors. It also helps in auto correcting DP mathematical model which has error in models in bringing stability in both position and heading.

The notch filter as shown in Figure 5-22, typically used for DP heavy lift crane vessel.

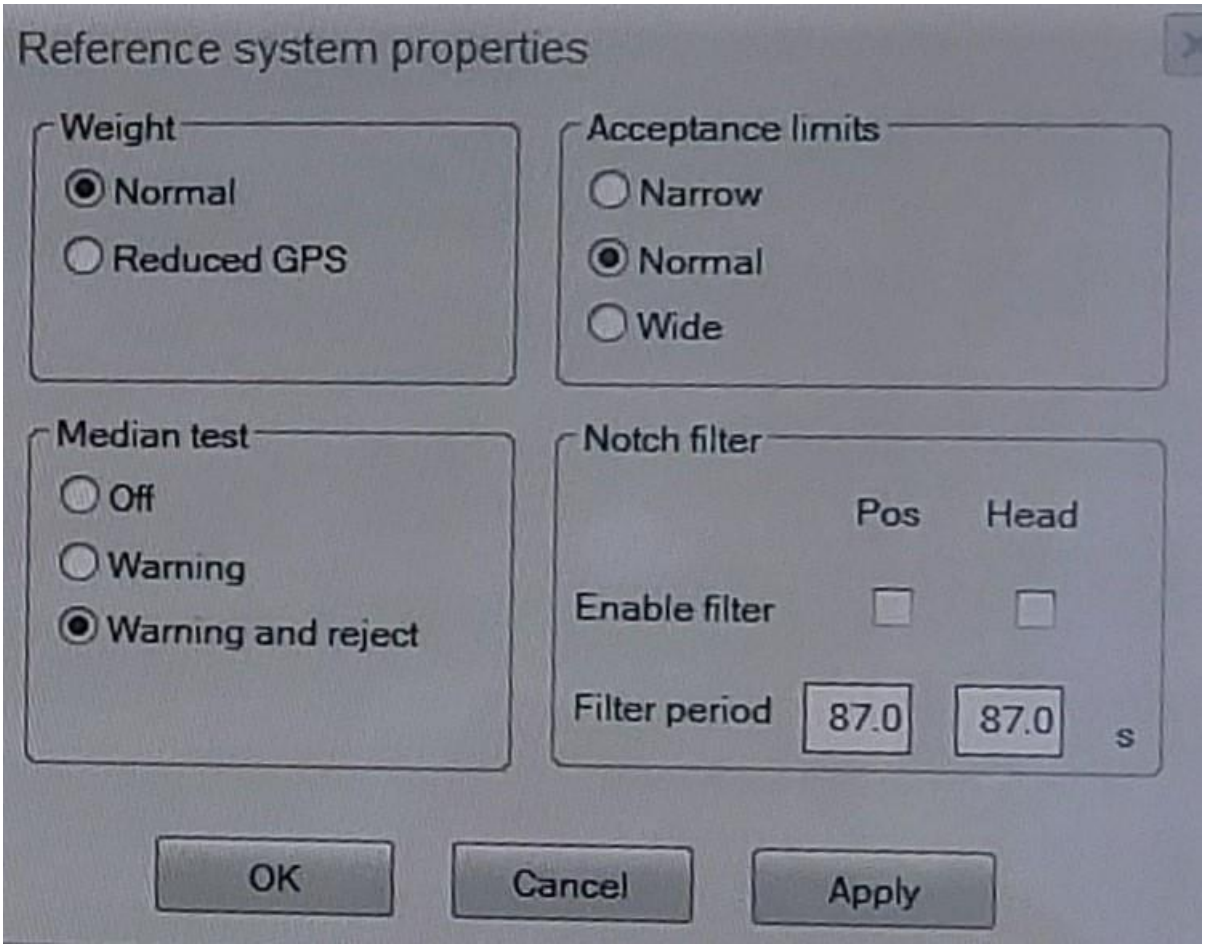

Figure 5-22 Notch filter application to improve DP station keeping during SIMOPS

The DP engineer then activated this function to check the performance of DP system during leg move. In addition, he applied gain factors in surges, sway and yaw direction. However, the result did not help in improving the station keeping performance. The DP system engineer then concluded that the spudcan will be modelled and gain factors including the special DP jack ups operational mode will be set in the revised software to meet the project requirement

The study conducted by us in chapter 4 shown to the DP vendor and advise him to consider modelling spudcan and consider the peculiar effect of spudcan top and bottom plate pressure response in up and down direction near to seabed when applying gain factors. After influence of seabed over on the leg and spudcan the drag force acting remain same.

5.7 MATHEMATICAL MODEL TRANSFER FUNCTION

It is evident from the offshore experiment the additional transfer function is required to correct the mathematical model to response to the near seabed effect. The gain factors in surge, sway and yaw as planned by the DP vendors may be one approach. However, this gain factors must be suitable for all environmental conditions.

The thought has been given to consider short time additional transfer function feature. The transfer functions can be activated when spudcan near to the seabed as observe in the CFD and tank experiment. Typically, the transfer functions should be engaged in the DP system, when leg spudcan is within 3~4 m from seabed. The peculiar response of the seabed observed both in leg lowering and lifting case. The drag forces observed highest near bed then they lower and increase again before lowering again to steady state value. The drag force response shown above in chapter 4 in figure below

- Drag force at distance from seabed in 2 knots current
- Drag force at distance from seabed in 1 knot current
- Drag force at distance from seabed in 0.5 knot current
- Drag coefficient jacking leg lowering from 5000mm to 50mm above seabed
- Drag coefficient jacking leg lifting from 50 mm to 5000 mm above seabed

The experiment data measured during the tank experiments to validate CFD prevails similar response. The response can be seen in the chapter 4 referred

- CFD results of lab experiment Test 2
- Comparison of CFD and Tank Experiment Results
- Tank experiment vs CFD results

It is decided to use CFD results to find the best transfer functions, which can be easily implemented in the DP control system. Currently, DP jack up vessel has jacking system leg interface. The vessel also has echosounder for seabed depth measurement. Since, the leg, spudcan information is known to the vessel. The transfer function can be integrated with DP control system for shorter time when near seabed. The transfer function will ensure the peculiar response of the drag forces to DP system, so that the DP system response rightly to the change in drag forces. The mathematical model then estimates in advance these forces and advise thrusters to compensate against this peculiar, expected behaviour.

The summary table used to collect data for transfer function as a function of distance is shown below in Table 5-3

Table 5-3 Distance Vs drag force response at different sea current

Distance	Drag Force 2kts	Drag Force 1kt	Drag Force 0.5kts
50	51498	12841	3190
1000	46721	11783	2952
1500	48137	12212	3071
1800	46848	11826	2980
2000	48481	12172	3018
2200	48085	12066	3007
3000	47094	11865	2971
5000	44467	11201	2842

The jack up legs transition has two typical modes, one lowering and other lifting. During this mode of transiting the leg also see, change in physics (fluid) surrounding his structural. The leg partially remains in air and based on the water depth of operation, when legs move the fluid environment changes to water. The drag forces can drastically affect, when fluid changes (i. e air to water or vice versa). The transit motion also changes the area. The dynamic changes of leg movement can bring massive changes. To simulate effects in mathematical calculation perform using formula of drag forces. The data inputs applied for the formulas are as follows in Table 5-4

Table 5-4 Data Input for drag force formula's

1.	Leg total length including spudcan	75 mtr
2.	Operational water depth	25 m

3.	spudcan height	4.25 mtr
4.	Spudcan area	31.7128 m2
5.	Leg handling speed	2 m/min
6.	Leg geometry and dia.	circular 4.5 mtr.
7.	Density of water	997.05 kg/m3
8.	Density of air	1.225 kg/m3
9.	Current	2 knots (1.028889 m/sec)
10.	Wind	25 knots (12.8611 m/s)
11.	Typically, hull and jack house	15 mtr

5.8 LEG LOWERING CALCULATIONS – DRAG FORCE BEHAVIOUR IN AIR AND WATER

The calculation is performed during leg lowering based on the Cd value indicated in chapter 4, the leg DN case result, when spudcan near 5 m from seabed are used. The variation among air and water drag force shown based on the leg in respective physics environment. The area changes in water and air area ultimately impacting the drag force. The fast leg speed means the variations seen by DP system faster and thruster response must be quick for this. Slower leg speed meaning the variation response is slow. The total force acting on the legs also shown, so the DP vendor understand the variation of leg force due to leg. The calculation below is for one leg and usually DP jack ups has 3, 4 to 6 legs. The Figure 5-23 below shows how the leg force variation occurs in air and leg for leg lowering condition. The calculation performed for fixed angle of attack (i.e. stern) for wind acting on the leg spudcan as a result the wind shape coefficient for cylindrical is consider as 1.0. The drag coefficient Cd of 0.7 and near seabed effect changes are used as estimated previously and indicated in the table below. Table 5-5 and Table 5-6. The blendermann's method is used for obtaining wind load coefficient for overall vessel used for industrial mission, while developing static DP capability plots.

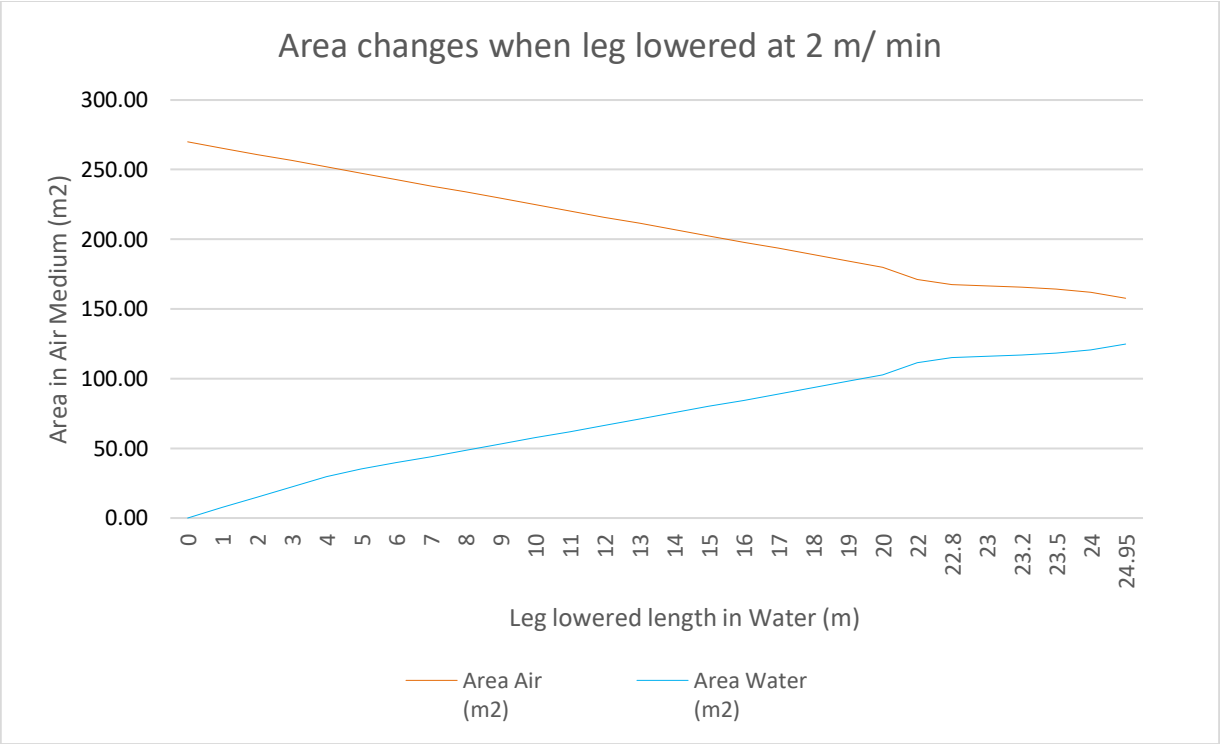

Figure 5-23 Area changes between air and water physics environment

The impact on the drag forces also plotted below in Figure 5-24, indicating overview drag force variation over leg length both in air and water physics environment. The domination of drag force due to sea current clearly visible

The environmental condition used for the drag force calculation stated in Table 5-4. The effect of wave acting on the leg & spudcan neglected for simplicity.

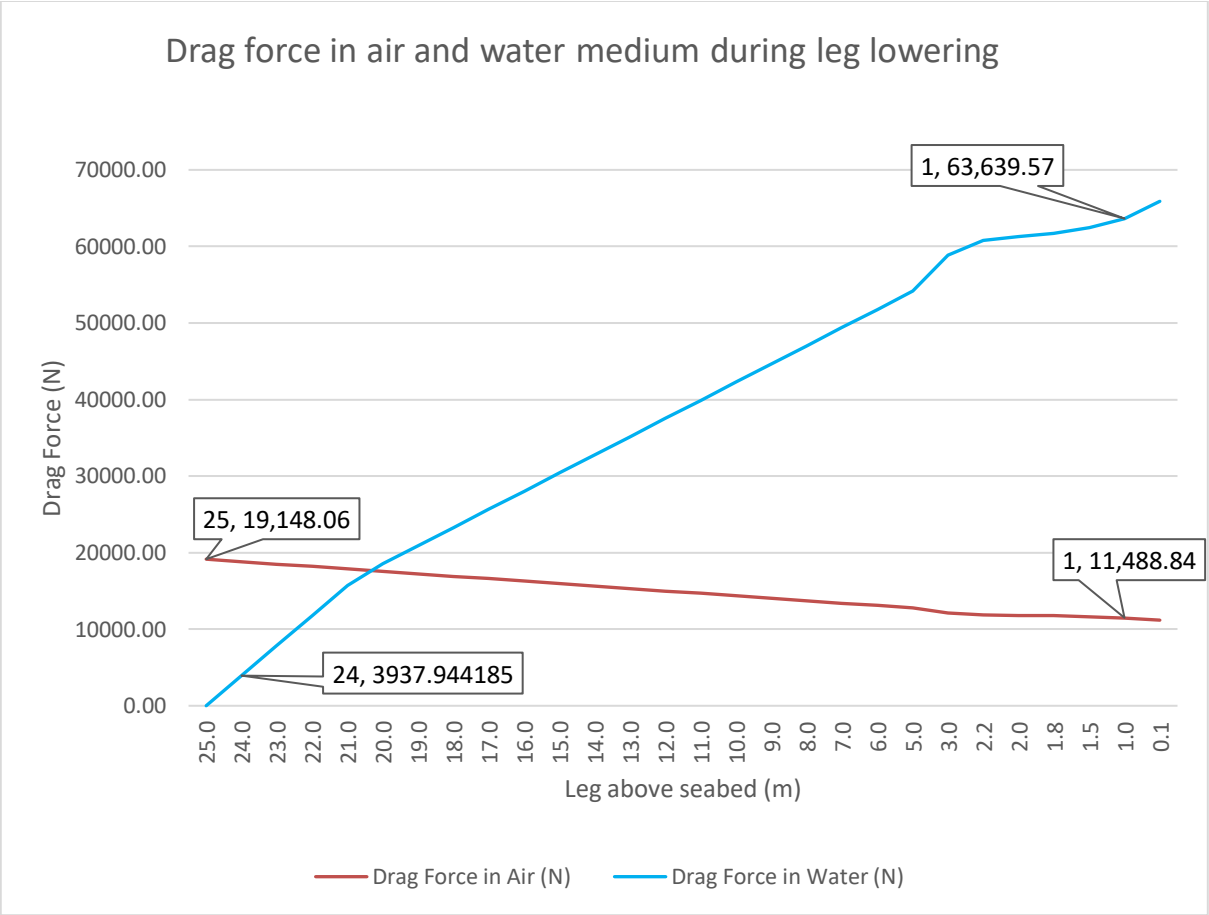

Figure 5-24 Drag Force Variation in Air and Water during Leg lowering case

The tabular information below in Table 5-5 provides complete overview of calculation plotted above. It is paramount important, the DP system designer must consider these forces, acting on the leg in DP mathematical model for better station keeping performance. The seabed effect is also important to consider as this is critical point. The DP system thrusters needs to respond correctly to this force variation to avoid drive on or drift off jack up vessel, when introducing special function in DP system for jack up vessel. The DP system designer required special function for short duration, when spudcan near seabed vicinity.

Table 5-5 Leg lowering – Drag force variations

Time Steps (Min)	Leg Length in Water (m)	Leg Length in Air (m)	Area Air (m2)	Area Water (m2)	Cd Air	Drag Force in Air (N)	Cd Water	Drag Force in Water (N)	Total Force Due to Leg (N)
0	0	60	270.00	0.00	0.7	19148.06	0.7	0.00	19148.06
0.5	1	59	265.50	7.46	0.7	18828.93	0.7	3937.94	22766.87
1	2	58	261.00	14.92	0.7	18509.80	0.7	7875.89	26385.68
1.5	3	57	256.50	22.39	0.7	18190.66	0.7	11813.83	30004.49
2	4	56	252.00	29.85	0.7	17871.53	0.7	15751.78	33623.30
2.5	5	55	247.50	35.09	0.7	17552.39	0.7	18517.40	36069.79
3	6	54	243.00	39.59	0.7	17233.26	0.7	20892.25	38125.51
3.5	7	53	238.50	44.09	0.7	16914.12	0.7	23267.10	40181.23
4	8	52	234.00	48.59	0.7	16594.99	0.7	25641.95	42236.94
4.5	9	51	229.50	53.09	0.7	16275.85	0.7	28016.81	44292.66

Time Steps (Min)	Leg Length in Water (m)	Leg Length in Air (m)	Area Air (m2)	Area Water (m2)	Cd Air	Drag Force in Air (N)	Cd Water	Drag Force in Water (N)	Total Force Due to Leg (N)
5	10	50	225.00	57.59	0.7	15956.72	0.7	30391.66	46348.38
5.5	11	49	220.50	62.09	0.7	15637.59	0.7	32766.51	48404.09
6	12	48	216.00	66.59	0.7	15318.45	0.7	35141.36	50459.81
6.5	13	47	211.50	71.09	0.7	14999.32	0.7	37516.21	52515.53
7	14	46	207.00	75.59	0.7	14680.18	0.7	39891.06	54571.25
7.5	15	45	202.50	80.09	0.7	14361.05	0.7	42265.91	56626.96
8	16	44	198.00	84.59	0.7	14041.91	0.7	44640.76	58682.68
8.5	17	43	193.50	89.09	0.7	13722.78	0.7	47015.62	60738.40
9	18	42	189.00	93.59	0.7	13403.65	0.7	49390.47	62794.11
9.5	19	41	184.50	98.09	0.7	13084.51	0.7	51765.32	64849.83
10	20	40	180.00	102.59	0.7	12765.38	0.7	54140.17	66905.55

Time Steps (Min)	Leg Length in Water (m)	Leg Length in Air (m)	Area Air (m2)	Area Water (m2)	Cd Air	Drag Force in Air (N)	Cd Water	Drag Force in Water (N)	Total Force Due to Leg (N)
11	22	38	171.00	111.59	0.7	12127.11	0.72295	58889.87	71016.98
11.4	22.8	37.2	167.40	115.19	0.7	11871.80	0.73817	60789.75	72661.55
11.5	23	37	166.50	116.09	0.7	11807.97	0.74424	61264.72	73072.70
11.6	23.2	36.8	165.60	116.99	0.7	11744.15	0.71917	61739.69	73483.84
11.75	23.5	36.5	164.25	118.34	0.7	11648.41	0.73896	62452.15	74100.56
12	24	36	162.00	120.59	0.7	11488.84	0.71723	63639.57	75128.41
12.475	24.95	35.05	157.73	124.86	0.7	11185.66	0.79055	65895.68	77081.34

Note: The drag coefficient changes when spudcan near to seabed. The effect of change in drag coefficient highlighted above.

5.9 LEG LIFTING CALCULATIONS – DRAG FORCE BEHAVIOUR IN AIR AND WATER

The variation of drag forces plotted below in Figure 5-25, showing complete overview of drag force variation over complete leg length in both in air and water physics medium. The environmental condition stated in Table 5-4.The domination of drag forces in water medium due to sea current clearly observed.

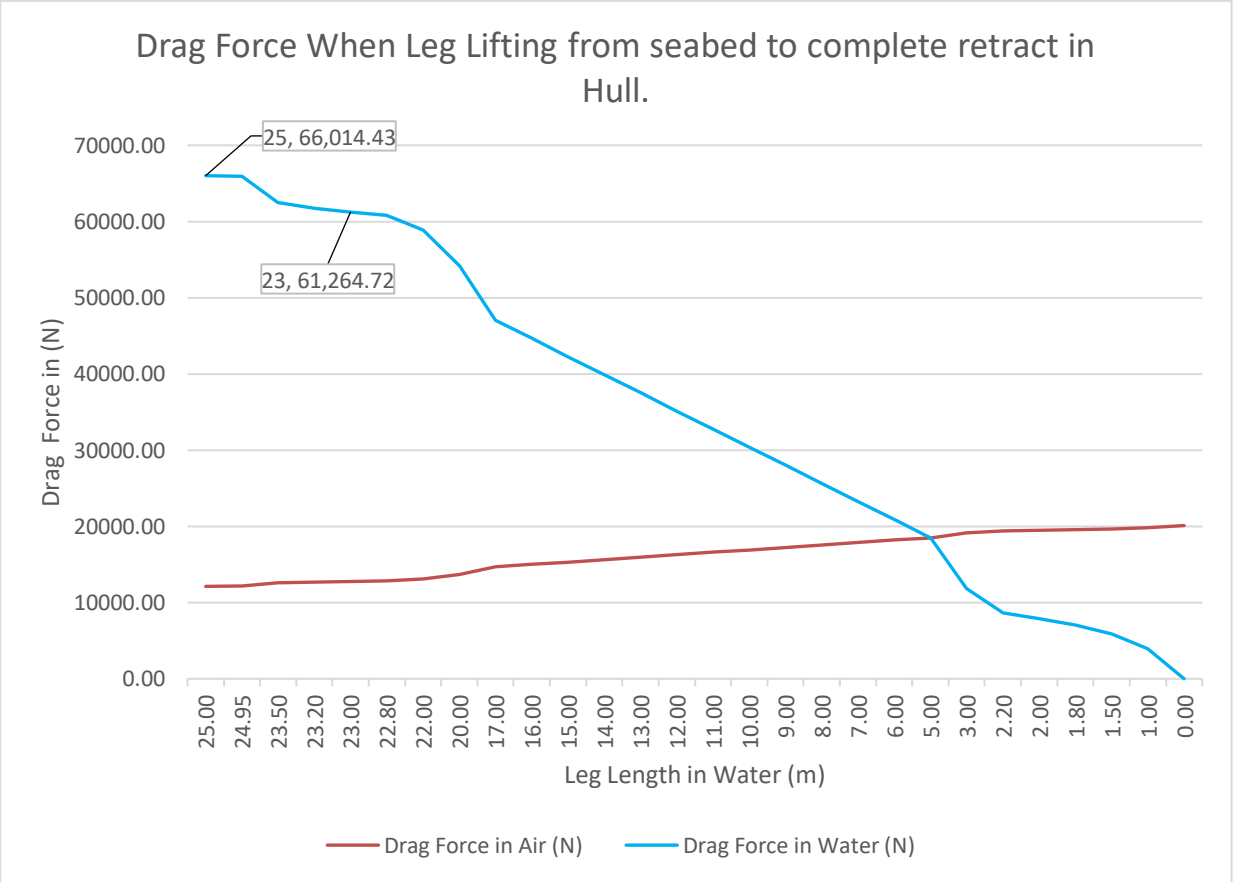

Figure 5-25 Drag Force Variation in Air and Water during Leg lifting case

The tabular information below in Table 5-6 provides complete overview of calculation plotted above. It is paramount important, the DP vendors must consider these forces, acting on the leg in the DP system for better station keeping. The seabed effects which are also important to consider as this is critical point, when DP thrusters needs to respond correctly, to the force variation to avoid drive off or drift off condition towards to the assets.

Table 5-6 Leg lifting– Drag force variations

Time Steps (Min)	Leg Length in Water (m)	Leg Length in Air (m)	Area Air (m2)	Area Water (m2)	Cd Air	Drag Force in Air (N)	Cd Water	Drag Force in Water (N)	Total Force Due to Leg (N)
0	25.00	38.00	171.00	125.09	0.70	12127.11	0.79354	66014.43	78141.53
0.025	24.95	38.05	171.23	124.86	0.70	12143.06	0.71988	65895.68	78038.75
0.75	23.50	39.50	177.75	118.34	0.70	12605.81	0.74993	62452.15	75057.96
0.9	23.20	39.80	179.10	116.99	0.70	12701.55	0.71880	61739.69	74441.24
1	23.00	40.00	180.00	116.09	0.70	12765.38	0.74235	61264.72	74030.10
1.1	22.80	40.20	180.90	115.19	0.70	12829.20	0.73031	60789.75	73618.96
1.5	22.00	41.00	184.50	111.59	0.70	13084.51	0.73060	58889.87	71974.38
2.5	20.00	43.00	193.50	102.59	0.70	13722.78	0.70	54140.17	67862.95
4	17.00	46.00	207.00	89.09	0.70	14680.18	0.70	47015.62	61695.80
4.5	16.00	47.00	211.50	84.59	0.70	14999.32	0.70	44640.76	59640.08

Time Steps (Min)	Leg Length in Water (m)	Leg Length in Air (m)	Area Air (m2)	Area Water (m2)	Cd Air	Drag Force in Air (N)	Cd Water	Drag Force in Water (N)	Total Force Due to Leg (N)
5	15.00	48.00	216.00	80.09	0.70	15318.45	0.70	42265.91	57584.37
5.5	14.00	49.00	220.50	75.59	0.70	15637.59	0.70	39891.06	55528.65
6	13.00	50.00	225.00	71.09	0.70	15956.72	0.70	37516.21	53472.93
6.5	12.00	51.00	229.50	66.59	0.70	16275.85	0.70	35141.36	51417.21
7	11.00	52.00	234.00	62.09	0.70	16594.99	0.70	32766.51	49361.50
7.5	10.00	53.00	238.50	57.59	0.70	16914.12	0.70	30391.66	47305.78
8	9.00	54.00	243.00	53.09	0.70	17233.26	0.70	28016.81	45250.06
8.5	8.00	55.00	247.50	48.59	0.70	17552.39	0.70	25641.95	43194.35
9	7.00	56.00	252.00	44.09	0.70	17871.53	0.70	23267.10	41138.63
9.5	6.00	57.00	256.50	39.59	0.70	18190.66	0.70	20892.25	39082.91
10	5.00	58.00	261.00	35.09	0.70	18509.80	0.70	18517.40	37027.20

Time Steps (Min)	Leg Length in Water (m)	Leg Length in Air (m)	Area Air (m2)	Area Water (m2)	Cd Air	Drag Force in Air (N)	Cd Water	Drag Force in Water (N)	Total Force Due to Leg (N)
11	3.00	60.00	270.00	22.39	0.70	19148.06	0.70	11813.83	30961.90
11.4	2.20	60.80	273.60	16.42	0.70	19403.37	0.70	8663.48	28066.85
11.5	2.00	61.00	274.50	14.92	0.70	19467.20	0.70	7875.89	27343.09
11.6	1.80	61.20	275.40	13.43	0.70	19531.03	0.70	7088.30	26619.33
11.75	1.50	61.50	276.75	11.19	0.70	19626.77	0.70	5906.92	25533.68
12	1.00	62.00	279.00	7.46	0.70	19786.33	0.70	3937.94	23724.28
12.5	0.00	63.00	283.50	0.00	0.70	20105.47	0.70	0.00	20105.47

5.10 MATHEMATICAL MODEL FOR LEG LOWERING OPERATION

The programme used for transfer function is MATLAB and Simulink. The data sets at sea current 0.5 kts, 1 kts and 2 kts were used. The input data characteristics of u1 (i.e., Distance) and output y1(Drag coefficient) use to evaluate the black box parameters (i.e., transfer function) outline is shown below in Figure 5-26

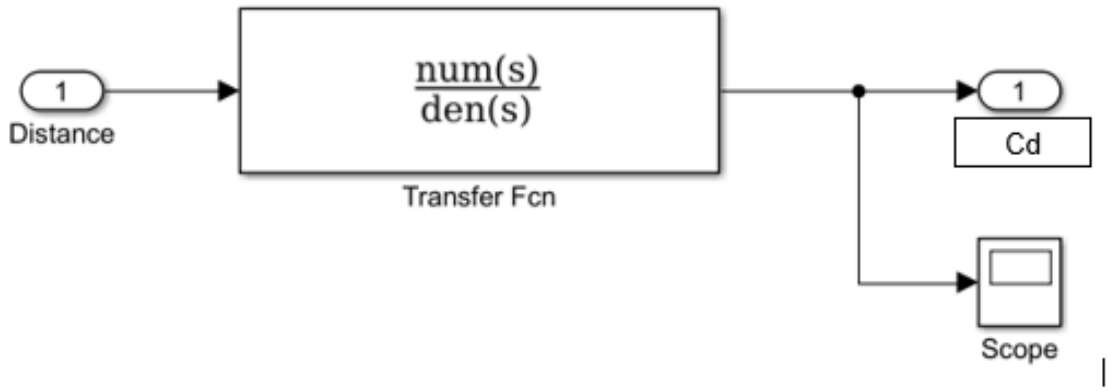

Figure 5-26 Transfer functions estimations

The input and output of the model is verified first for each data input sets; to evaluate the transfer function response during leg lowering shown in Figure 5-21. The y1 output represents drag coefficient, while u1 represents distance from seabed,

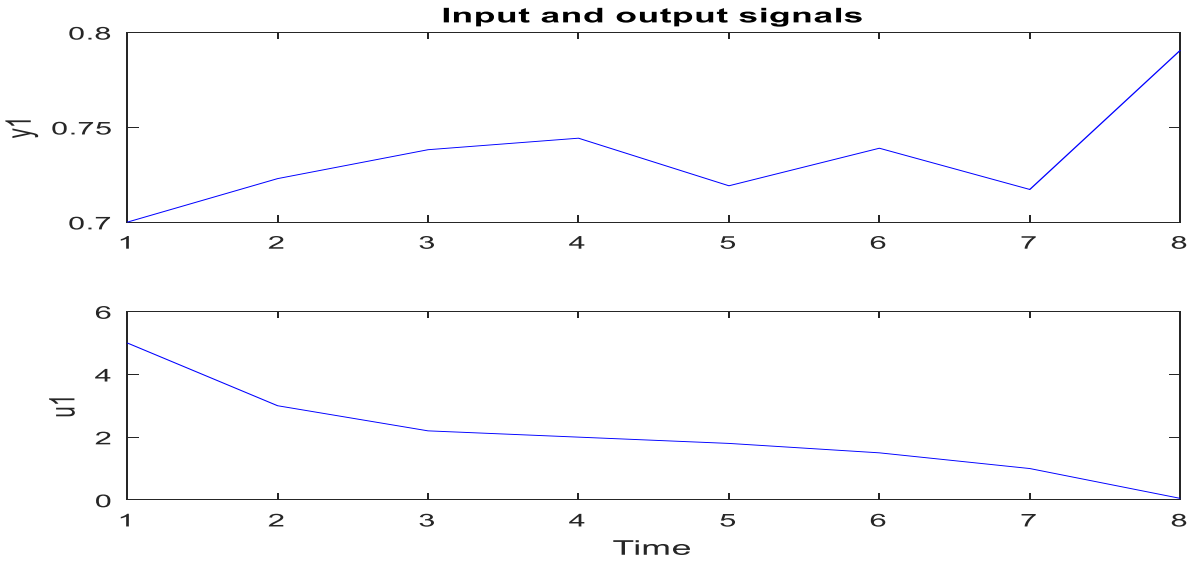

Figure 5-21 Data input distance Vs output drag coefficient for leg lowering condition

Based on the analysis, author have estimated 10 (options) of transfer function by defining various degrees of differential Laplace equations to satisfy input and output response as shown below in Figure 5-27 and the response of best fits shown below in Figure 5-28.

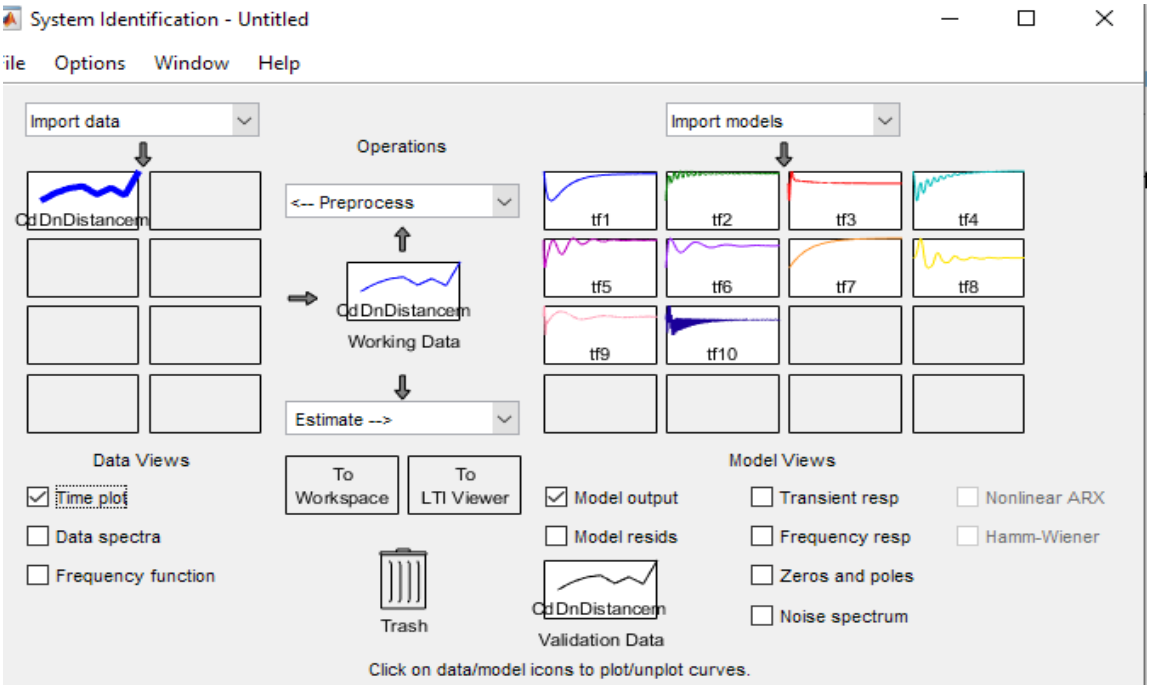

Figure 5-27 Transfer function estimation for leg lowering

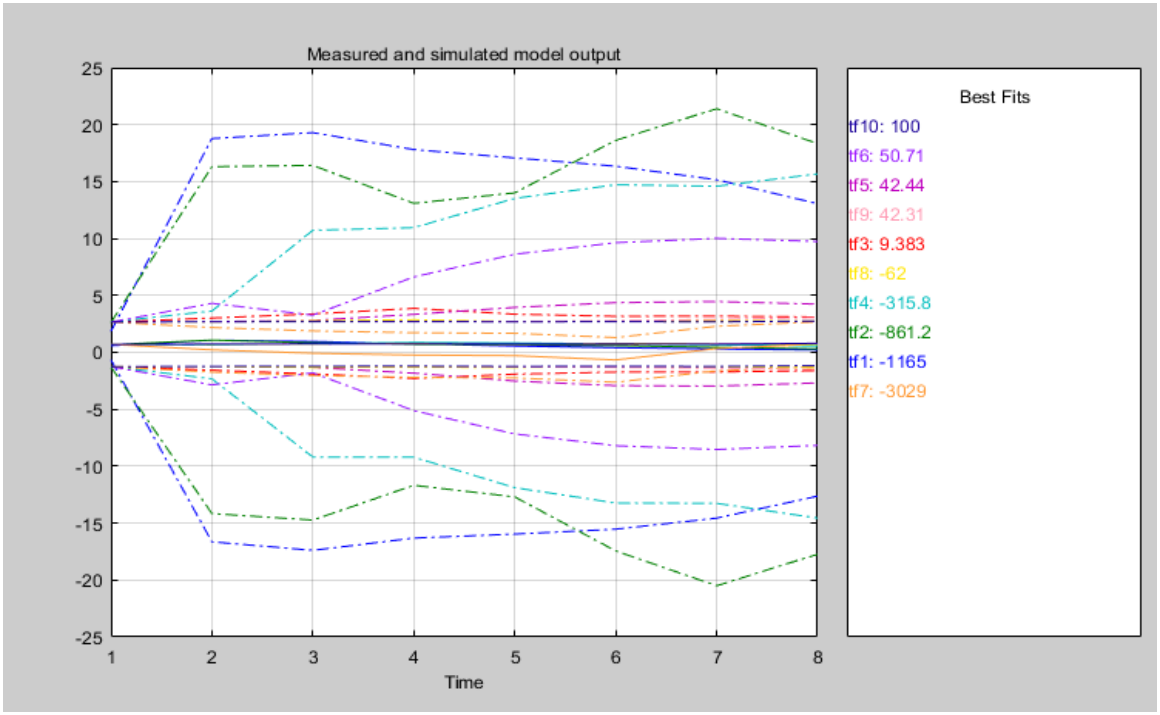

Figure 5-28 Transfer Function Fit Checks for Leg Lowering

The transfer function (TF10) shown below shows 100% fitting of the drag coefficient response with respect to system input output characteristics.

```
 From input "u1" to output "y1":
              0.7081 s^4 - 0.8885 s^3 + 0.264 s^2 + 0.2814 s - 0.0833
 ---------------------------------------------------------------------------------
 s^7 + 2.116 s^6 + 11.53 s^5 + 20.66 s^4 + 17.81 s^3 + 9.496 s^2 + 2.18 s + 0.07221
ame: tf10
ontinuous-time identified transfer function.
```

The non-linear model also shows 100%, fit to purpose.

nlarx1 =

Nonlinear ARX model with input1 Distance1 and output Drag coefficient Cd

Standard regressors corresponding to the orders

na = 2, nb = 2, nk = 1

Nonlinear regressors:

Cd(t-1)

Cd(t-2)

Distance(t-1)

Distance(t-2)

Nonlinearity: wave net with 1 unit

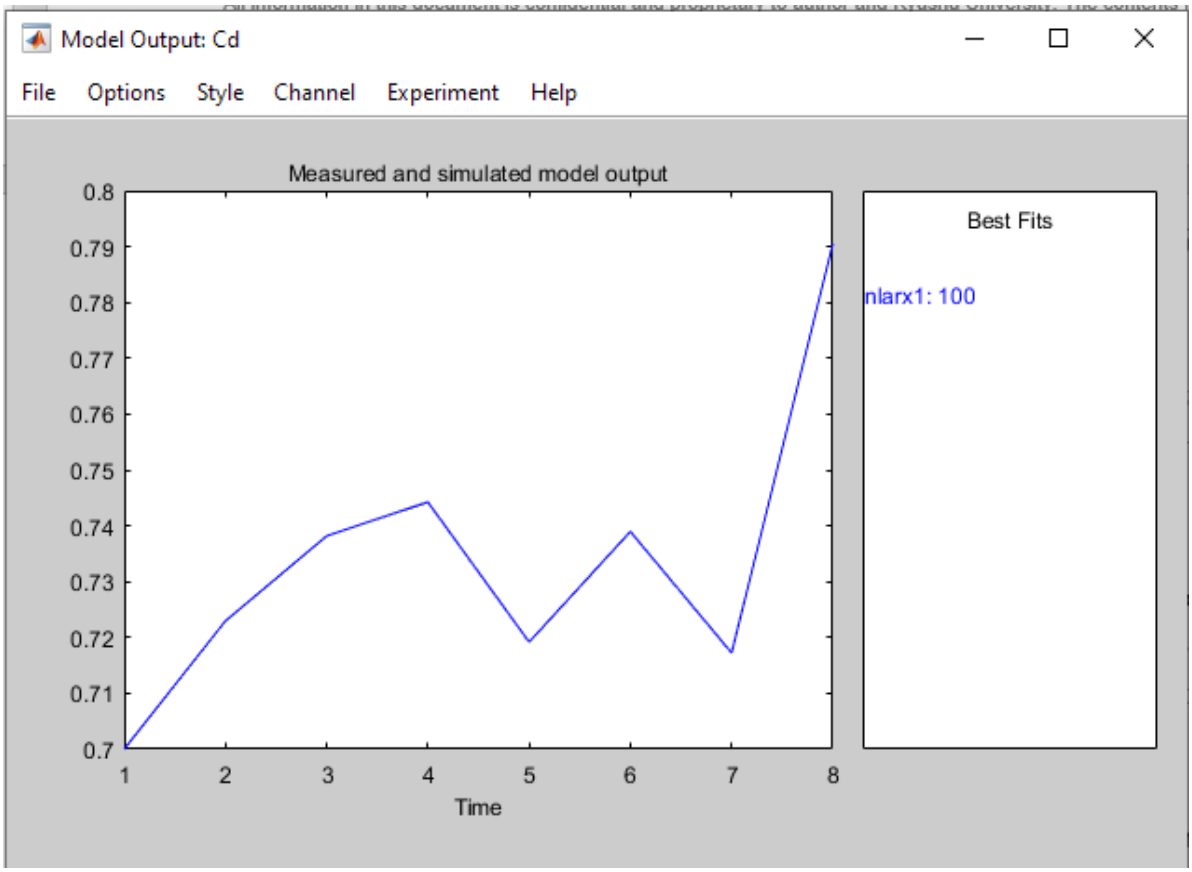

Figure 5-24 Non-linear model output for leg lowering condition

Regressors used in the nonlinear block of model (if any): CdUp(t-1), CdUp(t-2), DistanceUp(t-1), DistanceUp(t-2).

Final prediction error (FPE): Loss function: **8.217e-33**
Fit to working data: **100%**

5.11 MATHEMATICAL MODEL FOR LEG LIFTING OPERATION

During Leg Up condition, the mathematical model input supplied solver as shown below in Figure 5-29

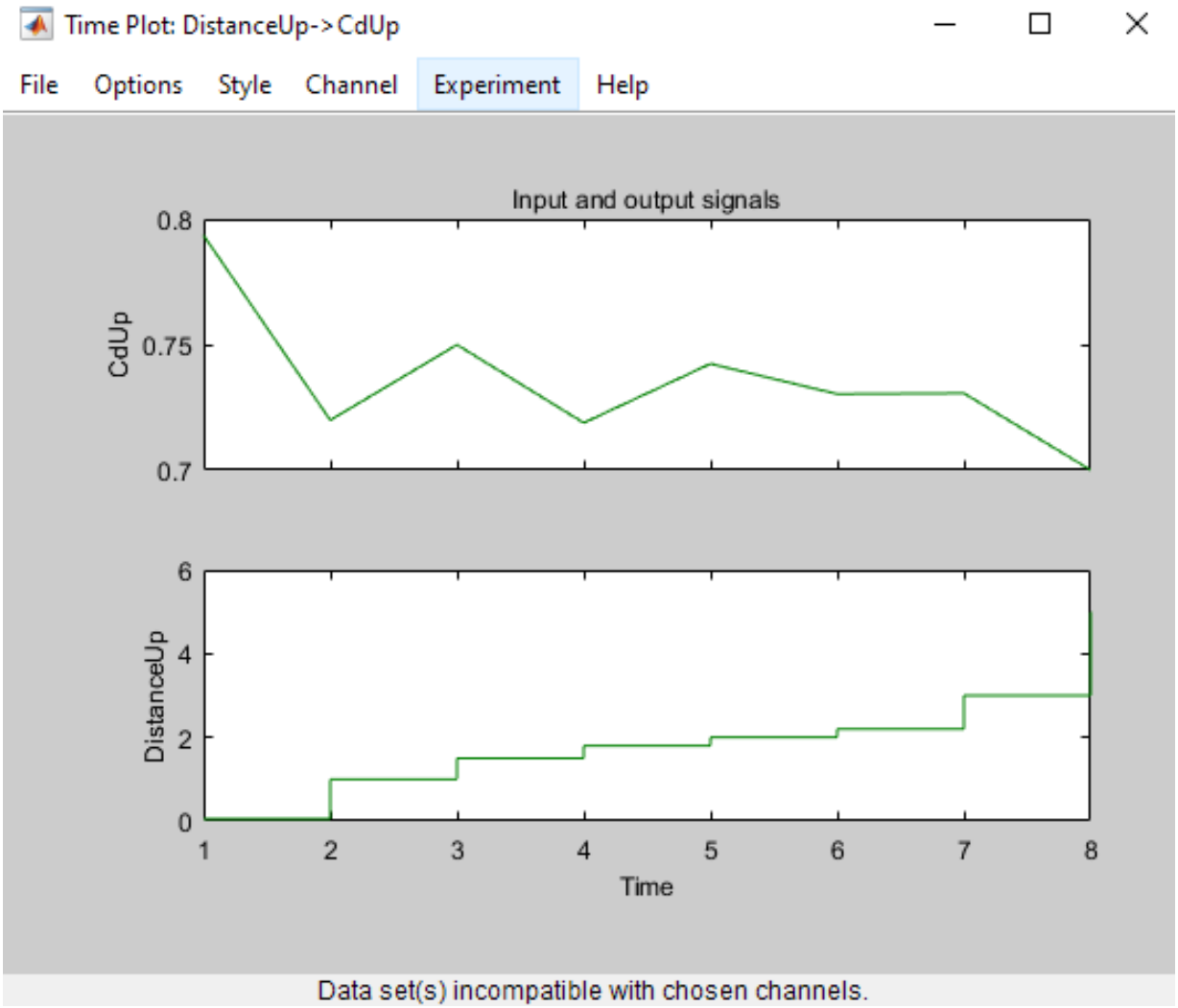

Figure 5-29 Data input distance Vs output drag coefficient for leg lowering condition

The output response then tested and found non-linear response 100% fitting and shown below in Figure 5-30

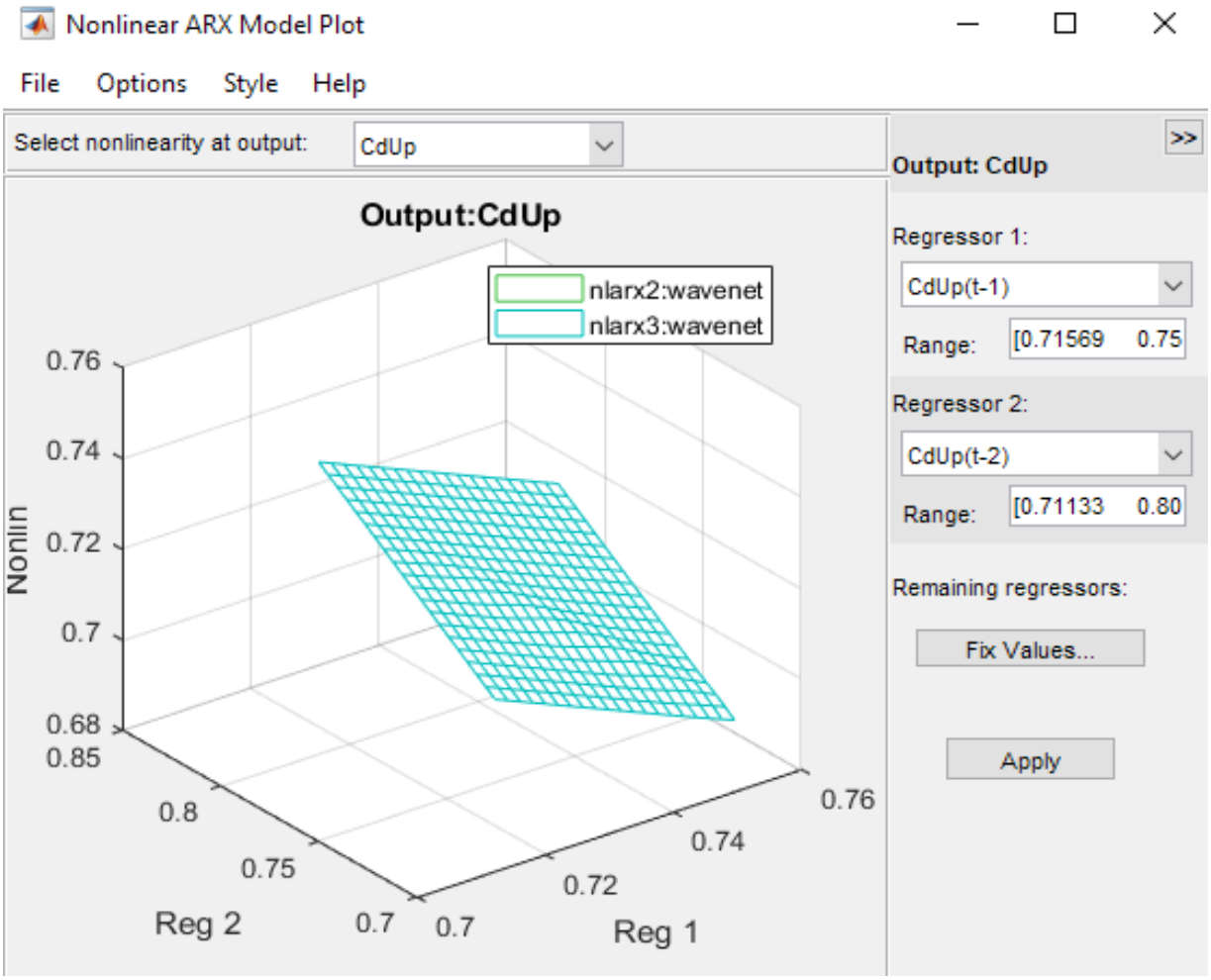

Figure 5-30 Non-linear model output for leg lifting

The DP vendor can take the approach by modelling near seabed variation to estimate drag force based on the steady state drag coefficient input. The variation in drag coefficient should be applied based on distance from seabed. Since, DP vendors has input of leg length, the additional echosounder depth measurement input should also be given to DP system to know seabed condition. Alternatively, load on the jacking system each leg must be provided to DP system to know soft pining during leg lowering and spudcan detach from seabed. The mathematical calculation can then be performed and applied in the DP system mathematical model to apply correct drag coefficient. The special mode definitely needed in the DP system of DP jack up vessels. The DP vendor or DPO needs to activate and deactivate this special mode during DP jack ups leg lowering and leg lifting from seabed in the SIMOPS operation. The hydrodynamic programmes should be used to established drag coefficient of steady conditions.

6 CONCLUSIONS

The CFD results show some interesting facts about the behaviour of the hydrodynamic forces (i.e., drag force Fx and lift force Fy) during the touchdown approach and lift off of a leg spudcan. In studying the effect of the sea bottom on the hydrodynamic forces, the author observed during careful evaluation drag force Fx increased when approaching to the seabed by approximately 12~16% for all cases. However, the lift force Fy increased sharply by approximately 300% for all the current cases during lowering. A peculiar behaviour of the drag coefficient was also observed when leg spudcan in the closed vicinity of seabed. The cyclic drag coefficient behaviour (i.e., increase, decrease, and then increase) due to seabed vicinity was visible.

The understand the peculiar behaviour, the top and bottom spudcan pressure monitored in the CFD analysis. The spudcan pressure result shows spudcan bottom plate pressure was higher than the top plate pressure when the spudcan was nearer to the seabed. However, when spudcan moved away from the seabed the bottom pressure change lower then top plate spudcan pressure. Direct measurement of both the lift force and the pressure difference between the top and bottom of the spudcan confirms the behaviour in line with the fundamental laws of physics.

The peculiar drag coefficient behaviour ultimately affects the drag force which will lead to position deviation if thruster fail to react to this peculiar behaviour.

When the jack up vessel's legs spudcan detach from the seabed, it was evident the vessel did not manage to maintain the position and heading during offshore experiments.

The CFD analysis, the tank experiments and offshore experiment provide interesting facts about hydrodynamic forces when leg spudcan operating near the seabed.

The drag force increased slightly during leg lowering, it showed a peculiar behaviour when the spudcan was at 1000 mm and 2000 mm above the seabed. The lift force direction changed at approximately 1800 mm during lowering. The CFD results show the hydrodynamic force during leg lowering and lifting reveal different behaviours. In view of this, industry should re-assess the DP control system associated with jack up vessels and the mathematical model approach should be carefully applied, capturing this peculiar behaviour of forces.

The offshore experiment showed the current DP system was not capable of maintaining the position required for the projects. The biggest threats observed when spudcan detached from the seabed, the vessel drifted beyond project acceptance level. DP system did not manage to control the position of the vessel soon after spudcan detached.

The DP system maker must update software especially when DP jack ups moves from the positions. It is paramount important, the active thrusters must be aligned with required thrust and direction such that soon after the spudcan detached the counter thrust generate by DP system to maintain position correctly apply by DP system.

The Figure 6-1 shows in green vessel original position, while the grey outline shows vessel position with deviation from the original position. During leg up and leg down shows position and heading difference during actual DP operation trials. The position deviation shows along the different corner of the vessel. The distance varies even when slight change in heading and position simulated.

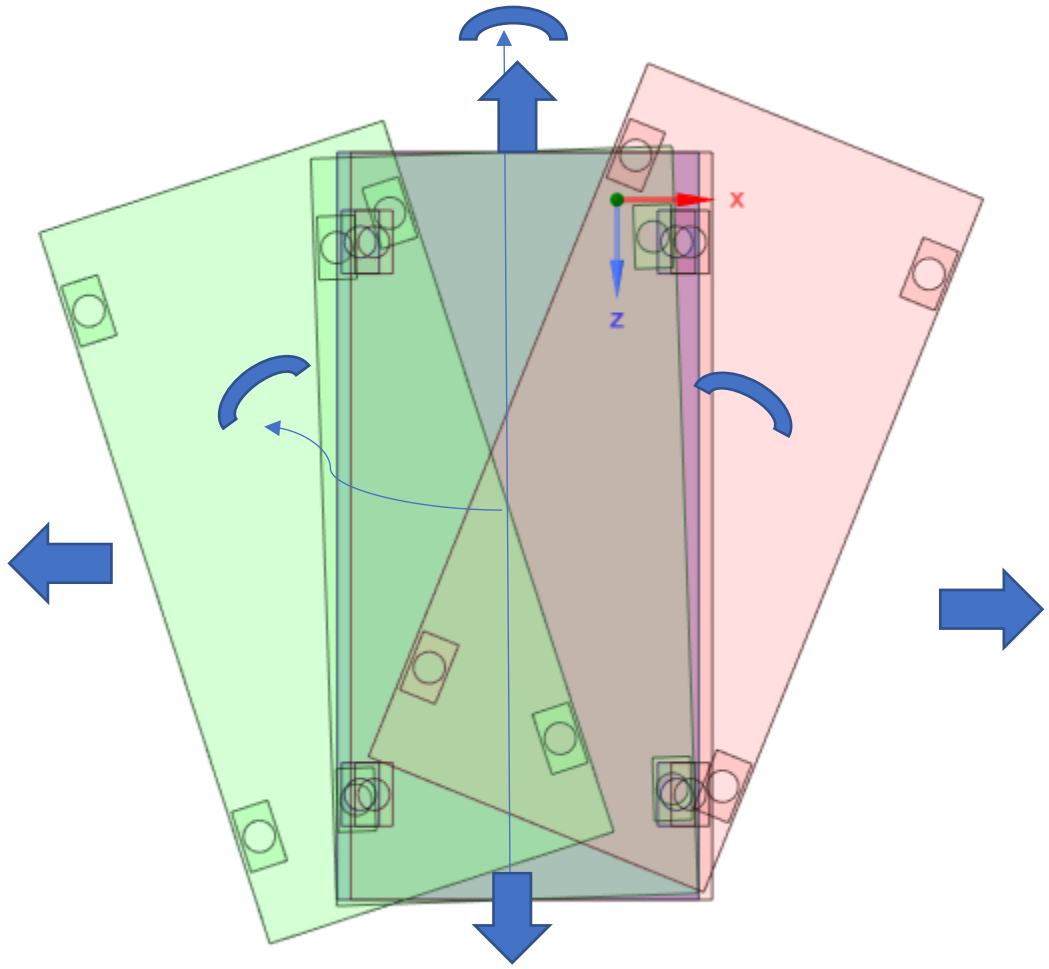

Figure 6-1 Position and heading deviation possible cause of collision in DP

The DP system designer for jack up vessel must consider a variable current from sea surface to seabed acting on the legs.

The oil majors, offshore wind industries and vessel owners need to know the maximum overshoot of position in real operating conditions for both lowering and lifting operations. Special emphasis must be given when the spudcan experiences bottom effects and spudcan removal from the seabed during a location move. The results evident in the CFD calculations, the tank experiments and offshore experiment prove that the jack up mathematical DP control approach (i.e., sensor-less) must be further evaluated case by case.

The offshore experiment provides evidence of vessel drifting soon after the spudcan is detached from the seabed. As a result, the author strongly recommends field trials to evaluate the bottom effect impact on the DP station keeping and to make a DP footprint during approach, entry and exit from the offshore installation.

The use of pressure sensors on the spudcan is recommended to interface with the DP system in addition to the leg length and leg load interface.

The CFD study reveals disturbed flow due to leg movement, leading to vortex effect and vibrations being observed on the leg and spudcan during the tank experiments. The fluid that enters through the holding pinhole in the leg also create flow turbulence. As a result, a programme of vortex measurements is recommended as future work along with estimation of vessel drag forces soon after spudcan detached from the seabed.

6.1 REFLECTION OF STUDY ON THE QUESTION RAISED IN CHAPTER 3

Q1. How is the current DP system of Jack ups taking into account jacking simultaneous operation?

The experiment conducted offshore has proved the DP software on board is not capable of maintaining the position, when moving from location despite sufficient time provided for learning to DP mathematical model.

Q2. What mathematical model DP Jack-ups vessel uses, in absence of sensors to account leg forces, while approaching and leaving the installation sites?

The DP mathematical model allocate gain factors in surge, saw and yaw direction to respond to additional drag force due to leg and spudcan. The boost mode gain factors are added, when leg near to seabed areas.

Q3. How variable leg speed lowering, and lifting are taken into account in hydrodynamic force calculation?

Currently leg speed interface is not available with DP system, however the leg length interface is given to DP system. The hydrodynamic forces calculations vary from different DP vendors. The Morrison equation approach taken by DP vendors. However, the large diameter of leg vs wavelength ratio does not satisfy Morrison equation criteria. If the diameter of the body is not small compared to the wavelength, diffraction effects have to be taken into account and this not taken by DP vendors in mathematical modelling. Also, DP system do not have current measurement input. It calculates current based on vessel response. The current system does not help during spudcan removal, while moving from the locations, as a result drift of vessel cannot be controlled soon after spudcan removal.

Q4. How DP system accounts, seabed effects which can affect hydrodynamic force?

The seabed effect not taken into consideration by DP vendors. Our study provided solution on how to tackle this issue. Now DP vendor is using CFD approach, model, leg spudcan in CFD and estimate hydrodynamic coefficient (i.e. Boost Gain Factors) especially during leg retracted position.

Q5. How DP model building process helps to account for hydrodynamic forces of jack ups when position, heading of the vessels remain the same till spudcan detach from the seabed?

DP system mathematical model will not update, when the spudcan in the seabed. The main outputs from the mathematical model are filtered estimates of the vessel's heading, position, and speed in each of the three degrees of freedom - surge, sway and yaw. The vessel's heading and position are measured using the gyrocompasses and position-reference systems and are used as the input data to the DP system. This data is compared to the predicted or estimated data produced by the mathematical model, and the differences are calculated. These differences are then used to update the mathematical model to the actual situation. The Kalman filtering technique continuously corrected model and help in accounting unmeasured forces.

Q6. How will thrusters align in the direction of demand thrust forces soon after spudcan detached from the seabed?

This was not thought earlier as allocation of thruster done by algorithm in the DP system based on the force calculation. Residual current help DP model to learn hydrodynamic behaviors and correct position by considering residual current. This is under

development; the plan is to modify algorithm in DP system of jack ups mathematical model and include auto position and boost functionality.

Q7. Do DP vendors know drifting distance and direction, soon after spudcan detach from the seabed?

No, this was never thought earlier. However, with modelling of leg spudcan and CFD analysis the current drag response estimation will be done and fitted in the algorithm based on sensor input.

Q8. Do DP mathematical models use an additional set of gain factors in surge, sway and yaw directions for tight position and heading controls? How do they calculate and apply?

This is a trade secret, and it will not be disclosed. However, of station keeping stability during lowering and retracting the leg will be demonstrated during offshore experiment The new software is ready with special feature of auto position and boost mode. The DPO needs to activate this when spudcan near seabed. The activation and deactivation of this demonstrated successfully recently.

Q9. How variable current acting on the leg at different depth level taken into accounts?

This is a trade secret, and it will not be disclosed. However, of station keeping stability during lowering and retracting the leg will be demonstrated during offshore experiment

Q10. How DP jack ups vessel different leg and spudcan design accounted in DP software?

Every vessel has dedicated mathematical model, so this will be taken into account by modelling leg and spudcan in hydrodynamic software and calculate the hydrodynamic gain coefficient for jack ups leg.

Q11. What best DP vendor can do to improve station keeping in SIMOPS operational mode?

Dedicated function for DP jackups will be added, which DPO requires to activate to enable auto position. The gain factors trends will be applied to suits both leg lowering and leg retracting operational condition.

6.2 OFFSHORE EXPERIMENT WITH UPDATED DP SOFTWARE TO LIMIT POSITION EXCURSION

The offshore DP trials caried out previous failed to prove the station keeping performance under various Jack up operational modes and discussed in chapter 5. The tank experiment and CFD has proved the transition phased required special attentions including spudcan near seabed effect. The DP vendor has carried out hydrodynamic analysis with modelled leg and spudcan to calculate hydrodynamic coefficient evaluation of vessel with leg and spudcan. The effect of near seabed communicated from our research to DP software vendor. The DP offshore trials then conducted to confirm new software response. To identify near seabed effect, the leg length interface to DP system from Jacking system, which is operating legs. To confirm detached of spudcan from the seabed, the load sensor of each leg spudcan also interface with DP System. The new DP Setup can be seen below in Figure 6-2

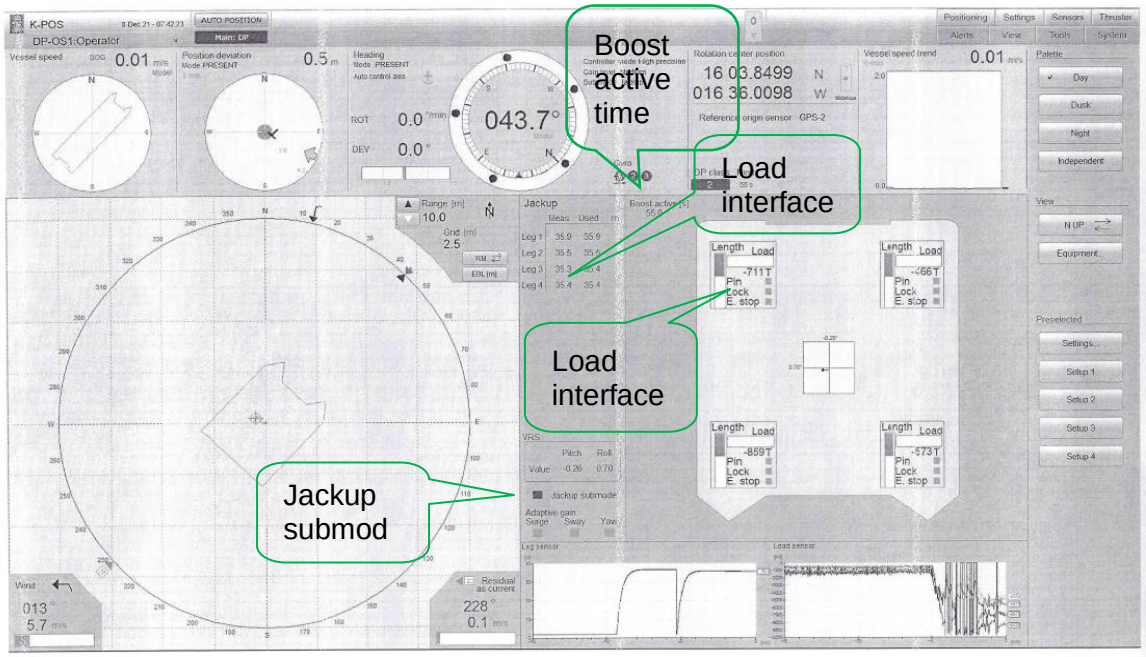

Figure 6-2 DP Jackup Legs Length and Load interface

The offshore experiment carried out at various water depth both for leg lowering and leg lifting cases under different environmental conditions.

The Figure 6-3 shows activation of boost mode during spudcan removal to limit the vessel excursion. The boost mode activated for short time of 55 sec and then removed. The residual current clearly shows change and leg removal from the seabed. The maximum excursion during this was noted 0.5m in surge and sway direction.

Figure 6-3 Marked up showing boost function activation and deactivation

The Figure 6-4 shows DP trials result of spudcan removal. The boost mode activated for short time and then removed. The load indicator clearly shows the spudcan detached condition from seabed. The maximum excursion during this was noted 0.3m from the set point. This proves the boost mode functionality set by DP vendor is working as desired to safely carry out work in DP for Jack up vessel.

The offshore experiment concluded; all DP jacks up must follow software amended for better station keeping stability.

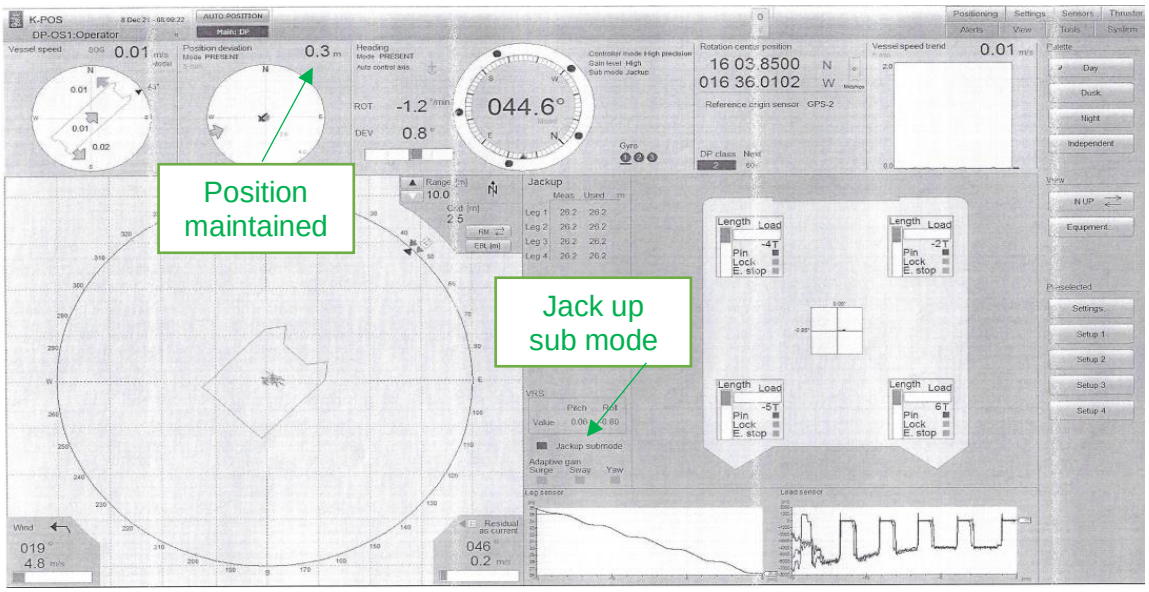

Figure 6-4 Jack up Position station keeping performance soon after leg removal

7 ACKNOWLEDGEMENT

The idea of research on this topic comes in the mind while working in industry as DP Surveyor and Jacking System health check-ups engineer. I am thankful to the nature for giving me an opportunity to work in this area and do something significant to identify the root cause of DP vessel station keeping issues of Jack up vessel during the Simultaneous Operation (SIMOPS). The journey of research in the area is complicated as both systems are highly sophisticated and difficult to approach to vendors of system designers. However, my current professional engagement has done this journey flawless. While researching, some projects on DP assurance work for Marine warranty projects. In this project DP Jack up, vessels will be used to complete the offshore industrial mission. My role in this project to assess the vessel suitability for operations. The gap discovered from the research applied and new offshore experiments proposed to the vessel owner and charter. The station keeping instability during 1st experiment echo the findings from experiment and CFD. The DP vendor agree current program needs modification to suit project needs of tight vessel position. The DP vendor then started implementing various solution to meet the project limits and define the operational limitation of DP Jack up vessel for the project.

I am thankful of my Prof Satoru Yamaguchi for his unconditional timely support and his systematic guiding helped me to complete my desired goal of bringing station keeping risk issue in front of the industry, I am also thankful to my wife and Son, who have supported me unconditionally and boosted my moral time to time, when went through difficult time due to poor job market, which impacted my company sponsorship. My wife supported and advised me to continue my research journey by self-funding through our savings. Lots of new learning and stressed period but one line keeps all of us keep going is **“Law of impermanence”.**

I am also very much thankful to the Mr.Ebihara Koki, Mr. Yoshitake and Mr. Ibaragi ,who has assisted me during marine tank experiments, Mr.Ole Lyngstadaas during offshore experiment and Kyushu Labs for providing their valuable time in supporting me during my research.

I am also very much thankful to Mr.Vijaya Bhaskarao M of Bureau Veritas for his guidance on CFD and Mr. Sen Abhayasinghe, Regional director, DP and critical system ABL group.

I must pay my sincere gratitude to my father, wife, son, brothers, friends and industrial experts for their unconditional love and moral support during this journey.

8 REFERENCES

[1.] Andries, h., Wallenberg, c., and Zana, s. 2017 Using CFD to assess the hydrodynamic loads on non-standard jack-up leg shape, Proceedings, The 27th International Offshore and Polar Eng. Conference, June 25–30, San Francisco, CA, ISOPE, 670–677.

[2.] Aguiar AP and Pascoal A. Dynamic positioning and way-point tracking of underactuated AUVs in the presence of ocean currents. Int J Control 2007; 80(7): 1092–1108.

[3.] Alfheim, H., Muggerud, K., 2016. Dynamic Positioning of the ReVolt Model-Scale Ship (Master's thesis). NTNU, https://ntnuopen.ntnu.no/ntnu-xmlui/handle/11250/ 2595418.

[4.] Bagnell, G.C., and P. Eng. "First Jackup Drilling Operation on Grand Banks of Newfoundland-Lessons Learned." Paper presented at the Offshore Technology Conference, Houston, Texas, U.S.A., April 2007. https://doi.org/10.4043/19077-MS.

[5.] Balchen, J., Jenssen, N., Eldar, M., Saelid, S., 1980. A dynamic positioning system based on Kalman filtering and optimal control. Model. Identif. Control 1 (3), 135–163. http://dx.doi.org/10.4173/mic.1980.3.1.

[6.] Bidikli B, Tatlicioglu E and Zergeroglu E.2013 Observer based output feedback tracking control of dynamically positioned surface vessels. In: Proceedings of the 2013 American control conference (ACC). Washington, DC, 17–19 June 2013. New York: IEEE.

[7.] Cadet O.,2003 "Introduction to Kalman Filter and its Use in Dynamic Positioning Systems", Dynamic Positioning Conference, Marine Technology Society, September 16-17, 2003.

[8.] Deghuee, B. 2012 Dynamics positioning control augmentation for jack-up vessels, Proceedings, MTS Dynamic Positioning Conference, October 9–10, Huston, TX, MTS.

[9.] Dillard S. Hammett, 1972, SEDCO - 445 Dynamic Stationed Drill Ship Paper presented at the Offshore Technology Conference, Houston, Texas, Paper Number: OTC-1626-MS.

[10.] DNV, 2019. The ReVolt - A new inspirational ship concept. https://www.dnvgl.com/ technology-innovation/revolt/index.html (visited on 2019/10/01).

[11.] DNVGL-RP-C205. 2010 Environmental Conditions and Environmental Loads, October.

[12.] Donha DC and Katebi MR. 2007, Automatic weight selection for H-infinity controller synthesis. Int J Syst Sci 2007; 38(8): 651–664.

[13.] Doyle J, Glover K and Francis F, 1989 State space solutions to standard H2 and HN control problems. IEEE T Automat Contr 1989; 34(1): 831–847.

[14.] Du, J., Xin, H., Krstic, M., Sun, Y., 2018. Dynamic positioning of ships with unknown parameters and disturbances. Control Eng. Pract. 76, 22–30. http://dx.doi.org/10.1016/j.conengprac.2018.03.015.

[15.] Elkadi, A. S. K., Van lottum, H., and Luger, H. J. 2014 A 3D coupled Eulerian-Lagrangian analysis of the dynamic interaction of jack-up legs with the Seabed, Delft, Netherlands: Delft University.

[16.] Evans, Aruther B 2005, Jules Verne's English Translations Science Fiction Studies XXXII (95): 80 -104. Retrieved 6 September 2012.

[17.] Fossen TI and Perez T. 2009, Kalman filtering for positioning and heading control of ships and offshore rigs. IEEE Contr Syst Mag 2009; 29(6): 32–46.

[18.] Fossen TI. 2011, Handbook of marine craft hydrodynamics and motion control. Chichester: John Wiley & Sons Ltd,.

[19.] Fossen, T. I. 2012 How to Incorporate Wind, Waves and Ocean Currents in the Marine Craft Equations of Motion. Proc. IFAC MCMC'12, 19-21 September, Arenzano, Italy 2012.

[20.] Ghezelbashan, A. and D'mello, C. 2018 Assessment of the hydrodynamic forces for equivalent modelling of jack-up legs, Proceedings, The 28th International Offshore and Polar Engineering Conference, ISOPE, June 10–15, Sapporo, Japan, 249–256.

[21.] Gimble MJ and Patton RJ.1980 The design of dynamic ship positioning control systems using stochastic optimal control theory. Optim Contr Appl Met 1980; 1(2): 167–202.

[22.] Glover K. 1984 All optimal Hankel-norm approximations of linear multivariable systems and their LN. error bounds. Int J Control 1984; 39(6): 1115–1193.

[23.] Hassani V, Sorensen AJ and Pascoal AM 2012. Robust dynamic positioning of offshore vessels using mixed-m synthesis Part I and II. In: Proceedings of 2012 IFAC workshop on automatic control in offshore oil and gas, Trondheim, Norway, 31 May 31–1 June 2012.

[24.] Hoes, R. S. 2012, Spudcan hydrodynamics: Analysis of hydrodynamic coefficient of Spudcan in proximity of seabed during Jack up installation, Netherland: Delf University of Technology.

[25.] Jensen, N.A., Realfsen, B., 2006. Power Optimal Thruster Allocation. Kongsberg Maritime https://pdfs.semanticscholar.org/064e/ 1b38204f5d855266a4eeb4af7b705a9bb2b9.pdf (visited on 2019/11/18).

[26.] Johannessen E and Egeland O. 1996, Robust performance in dynamic positioning systems. Model Ident Control 1996; 17(2): 75–86.

[27.] Katayama H. 2010, Design of reduced-order observer-based emulation controllers for dynamically positioned ships. In: Proceedings of the IEEE international conference on control applications (CCA 2010), Yokohama, Japan, 8– 10 September 2010. New York: IEEE.

[28.] Katebi, M., Yamamoto, I., Matsuura, M., Grimble, M., Hirayama, H., Okamoto, N., 2001. Robust dynamic ship positioning control system design and applications.

[29.] Kongsberg Maritime AS, 2008, "Kongsberg K-Pos DP (OS) Dynamic Positioning System Operator Manual", release 7.1, doc. No. 322281/A, Horten, October 2008.

[30.] Kreuzer, E., Solowjow, E., and Qiu, G. 2014 Leg-seabed interactions of jack-up vessels due to motions in irregular wave., Proceedings, ASME 2014 33rd International Conference on Ocean, Offshore and Arctic Engineering June 8–13, San Francisco,

[31.] Leavitt, J., 2008. Optimal thrust allocation in DP systems. In: Dynamic Positioning Committee, L-3 Communications DPCS, MTS. Dynamic Positioning Conference. https://dynamic-positioning.com/proceedings/dp2008/thrusters_leavitt_pp.pdf(visited on 2019/09/17).

[32.] Luman, Z., Roh, M.I., Hong, J.W., 2015. Optimal thrust allocation for dynamic positioning of deep-sea working vessel. J. Adv. Res. Ocean Eng. 1, 94–105.http://dx.doi.org/10.5574/JAROE.2015.1.2.094.

[33.] Mahjoob MJ, Poursina M and Nia AK 2006. Optimal H-infinity control of ship heading. In: Proceedings of the ASME 8th biennial conference on engineering systems design and analysis, vol. 3), Torino, 4–7 July 2006. New York: ASME.

[34.] Liebert Maximillian, 2019 Calculation of the dynamic positioning capability of an offshore wind farm vessel during the jack-up process in the early design stage, Proceedings, The ASME 2019 38th International Conference on Ocean, Offshore and Arctic Engineering OMAE2019 June 9-14, Glasgow, Scotland.

[35.] Morgan MJ.1978 Dynamic positioning of offshore vessels. Tulsa, OK: Petroleum Pub. Co, 1978.

[36.] Packard A and Doyle J. 1993, The complex structured singular value. Automatica 1993; 29(1): 71–109.

[37.] Pettersen KY and Fossen TI. 2000, Underactuated dynamic positioning of a ship—experimental results. IEEE T Contr Syst T 2000; 8(5): 856–863.

[38.] Saelid S, Jenssen NA and Balchen JG. 1983, Design and analysis of a dynamic positioning system based on Kalman filtering and optimal control. IEEE T Automat Contr 1983; 28(3): 331–339.

[39.] Samar R, Postlethwaite I and Gu D 1995, Model reduction with balanced realizations. Int J Control 1995; 62(1): 33–64.

[40.] Skjetne R, 2005, The maneuvering problem. PhD Thesis, Norwegian University of Science and Technology, Trondheim, 2005.

[41.] Sorensen AJ. 2011, A survey of dynamic positioning control systems. Annu Rev Control 2011; 35(1): 123–136.

[42.] Stephens, R. I., and Warwickshire, G. B. 2015 Method of estimating the environmental force acting on a supported Jack-up vessel, US Patent US 8,992,126 B2, March 31, 2015.

[43.] Thulkar, N., and Yamaguchi, S. 2018 Evaluation of Drag Coefficient Variation in Transit Mode on Leg & Spud Can of DP Jackups Vessel, Proceedings, The 28th International Ocean and Polar Engineering Conference, June 10–15, Sapporo, Japan, 1314–1321.

[44.] Yao, Z., Shen, Y., Gu, X., and Bu, L. 2015 Calculation and analysis of the wave load of jack-up offshore wind turbine installation vessel during dynamic positioning, Proceedings, First International Conference on Information Sciences, Machinery, Materials and Energy (ICISMME 2015), April 11–13, Chongqing, China.

[45.] Zheng J, Hossain MS and Wang D 2015 New Design Approach for Spudcan Penetration in Nonuniform Clay with an Interbedded Stiff Layer in Journal of Geotechnical and Geo-environmental Engineering.

[46.] H K Versteeg and W Malalasekera 2007 An Introduction to Computational Fluid Dynamics.